NOTICE

The quality of this microform is heavily dependent upon the quality of the original thesis submitted for microfilming. Every effort has been made to ensure the highest quality of reproduction possible.

If pages are missing, contact the university which granted the degree.

Some pages may have indistinct print especially if the original pages were typed with a poor typewriter ribbon or if the university sent us an inferior photocopy.

Reproduction in full or in part of this microform is governed by the Canadian Copyright Act, R.S.C. 1970, c. C-30, and subsequent amendments.

AVIS

La qualité de cette microforme dépend grandement de la qualité de la thèse soumise au microfilmage. Nous avons tout fait pour assurer une qualité supérieure de reproduction.

S'il manque des pages, veuillez communiquer avec l'université qui a conféré le grade.

La qualité d'impression de certaines pages peut laisser à désirer, surtout si les pages originales ont été dactylographiées à l'aide d'un ruban usé ou si l'université nous a fait parvenir une photocopie de qualité inférieure.

La reproduction, même partielle, de cette microforme est soumise à la Loi canadienne sur le droit d'auteur, SRC 1970, c. C-30, et ses amendements subséquents.

ISBN 0-315-56449-0

Open-Ended Waveguide Structures

by

Christopher L. Sibbald

A thesis
submitted to the School of Graduate Studies and Research
in partial fulfillment of the
requirements for the degree of
Master of Applied Science

Ottawa-Carleton Institute for Electrical Engineering
Department of Electrical Engineering
Faculty of Engineering
University of Ottawa

December 1988

UNIVERSITÉ D'OTTAWA
UNIVERSITY OF OTTAWA

I hereby declare that I am the sole author of this document. I authorize the University of Ottawa to lend this document to other institutions or individuals for the purpose of scholarly research.

Christopher L. Sibbald

I further authorize the University of Ottawa to reproduce this document by photocopying or by other means, in total or in part, at the request of other institutions or individuals for the purpose of scholarly research.

Christopher L. Sibbald

Abstract

Three numerical methods, the Finite-Element method, the Method of Moments, and the Mode Matching method have been applied to the analysis of open-ended waveguide structures. The objective of the study was to determine an aperture geometry which would minimize the uncertainty in the non-destructive measurement of material permittivity. Four aperture geometries were chosen for detailed study: the full aperture of the rectangular waveguide, and three reduced apertures. The reflection coefficient of the aperture in contact with known dielectrics was calculated in the frequency range 8.5-11.5 GHz. The theoretical results were validated by measurements performed on an HP8410 automatic network analyzer.

Acknowledgements

I would like to express my sincere gratitude to my co-supervisors, Dr. S. Stuchly and Dr. G. Costache, for their guidance and encouragement throughout this work. I would also like to thank the technical staff in the Department of Electrical Engineering (Mr. S. Symons, Mr. G. Hartsgrove, Mr. B. Carraro and Mr. M. Master) and in the Physics workshop for their contribution to this work. Finally, a heartfelt thanks is extended to all the graduate students with whom I had many stimulating discussions and to my wife Ann-Marie for her support and patience during this work.

The financial support of the Natural Science and Engineering Research Council of Cananda is gratefully acknowledged.

Table of Contents

Table of Figures

Table of Tables

Chapter 1:

Introduction

1.1 Motivation

The increasing use of microwaves and millimeter waves in such diverse fields as communications, radar, space technology, medicine, biology, agriculture and industrial processes demands accurate data on the dielectric properties of materials.

In the field of medicine, microwaves have found many therapeutic and diagnostic applications. Microwave induced hyperthermia [1], when used with conventional treatments such as chemotherapy and radiation therapy has increased the success rate of cancer treatments [2]. Microwave thermography [3] is often used in conjunction with hyperthermia in order to monitor the temperature within the tissues. Knowledge of the dielectric properties of tissues is essential in the design of the transducers and applicators used in both these methods. Furthermore, information on the differences between the permittivities of healthy and diseased tissues is needed in non-invasive diagnostics such as cancer detection [4].

Dielectric spectroscopy has also proven useful in the study of biochemical and biophysical processes [5]. For example, the dielectric relaxation of molecules provides information on their physical structure. In biology, changes in the permeability of artificial bilayer membranes (Liposomes) may be detected via permittivity measurements [6].

Microwaves are used in the field of agriculture for the drying of grain as well as for monitoring their moisture content [7]. These processes depend upon the dielectric properties of the grain as well as those of water. In industrial applications, microwaves have been used for on-line monitoring of moisture content as well as for dielectric and induction heating processes.

Microwave dosimetry requires information on the permittivity of human tissues and organs in order to assess possible health hazards associated with exposure to electromagnetic fields [8].

All of these methods require a non-destructive method for measuring permittivities. In many cases, such as in-vivo measurements, it is not possible to cut samples from the bulk. Coaxial line probes [9] have satisfied these requirements at lower frequencies, however, they are not suitable at the higher frequencies for which dielectric data is lacking. For this reason, a suitable sensor for dielectric measurements at low centimeter and millimeter wave frequencies is needed.

1.2 Objective

The objective of this work is to develop a sensor suitable for the non-destructive measurement of the permittivity of biological materials at low centimeter and millimeter wave frequencies. The proposed method uses a modified open-ended waveguide as a probe. The probe is placed in contact with the material under test, and the input reflection coefficient is measured. The permittivity of the material is then calculated from the measured quantity.

Several potential advantages of this technique over existing methods are:

1)No machining of the sample is required as is the case with infinite sample methods.

2)The sensor offers a relatively wide bandwidth as compared to resonant techniques.

3)The structure is compatible with standard measuring equipment. Network analyzers and calibration standards are available which enable fast and accurate measurement of the reflection coefficient.

4)Single-mode measurements are possible at much higher frequencies than with coaxial line probes.

The method, however, is not without difficulties. In the case of waveguides, one cannot make the static approximations used in the field analysis of TEM structures such as coaxial lines [10]. This results in complex field problems which must be solved in order to determine the relationship between the reflection coefficient and the material properties. Furthermore, in practice one is interested in the inverse problem. Given the value of the measured reflection, the objective is to determine the permittivity. Analytical solutions rarely exist for these inverse problems, and even if they do, uniqueness is always questionable.

Finally, it is apparent from previous studies [11], that the open-ended guide produces large uncertainties when measuring materials having a high dielectric constant (see Fig. 1.2). It is postulated that this difficulty may be overcome by modifying the aperture geometry. By terminating the guide in a capacitive iris, the radiation from the guide can be reduced. Simultaneously, the electrical energy storage in the vicinity of the aperture is increased. By analogy with the work done on the modified open-ended coaxial line probes [12], an optimum capacitance should exist which reduces the uncertainties [13].

In this thesis, the field analysis related to the determination of this optimum capacitance is presented. Three numerical methods are applied to solve this problem.

As for the inversion of the problem, several methods have been suggested by other investigators. Among these methods are: graphical interpolation from computed values [14], polynomial fitting

to computed values [11], and computer optimization loops [14]. Ideally however, an equivalent circuit whose elements are expressed explicitly in terms of the permittivity would allow analytical inversion of the solution.

1.3 Equivalent Circuit[15]

The input impedance of the modified open-ended guide depends on two factors:

1) the amount of energy radiated into the half-space, and
2) the energy storage in the vicinity of the aperture.

These two effects are best represented by an equivalent circuit consisting of shunt elements connected across the waveguide in the plane of the aperture. This equivalent circuit is shown in Fig. 1.1.

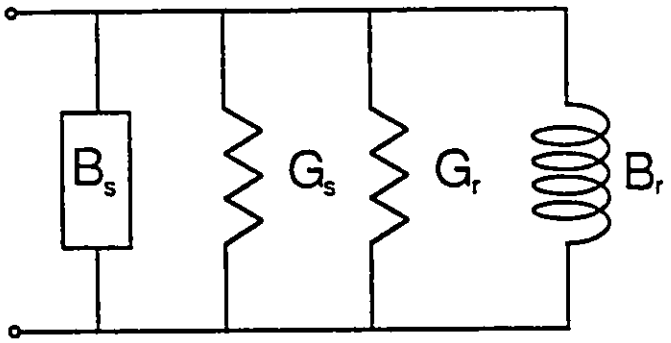

Fig. 1.1: Generalized Equivalent of an Open-Ended Waveguide

It should be noted that this equivalent circuit applies only to the dominant mode. When measurements are made, a reference plane must be chosen far enough from the aperture to ensure that the evanescent modes are negligible. A convenient choice for this reference plane is a distance $n\lambda_g/2$ from the aperture. In this plane the reflection coefficient of the propagating mode is the same as at the aperture itself.

The elements depicted in Fig. 1.1 may be related to physical phenomena as follows: The shunt conductance G_r represents the portion of energy lost due to radiation into the half space. Although this energy is not actually dissipated, it vanishes as far as the waveguide is concerned. Energy storage in the reactive field in the vicinity of the aperture is modelled by the shunt susceptance B_s. The nature of this susceptance is determined by the evanescent modes required to satisfy the boundary conditions in the plane of the aperture. Evanescent TE modes store predominantly magnetic energy and are best represented by a shunt inductance. On the other hand, evanescent TM modes store predominantly electric energy and, hence, contribute a shunt capacitance to the equivalent circuit. The continuity of the tangential fields across the aperture leads one to believe that the same type of energy is stored in the region $z > 0$.

When the dielectric filling the half-space is lossy, two more elements are required in the equivalent circuit. Power dissipated in the near field due to dielectric losses appears as a shunt conductance G_s, while radiation into a lossy dielectric produces an inductive susceptance B_r [15].

All four elements of the equivalent circuit depend upon the near field distribution. Hence, these elements are functions of the geometry of the aperture as well as the properties of the material. This makes it virtually impossible to write explicit expressions for the individual elements. Once the aperture geometry is chosen, however, suitable approximations might be possible which would allow one to write expressions for the elements, in terms of the permittivity and some other unknown parameters. These parameters may then be determined by curve fitting to the results obtained from the field analysis.

1.4 Present State of Knowledge

A large number of papers have been published describing various studies of open-ended guides. Earlier works [16] considered only the far field radiation patterns in free space. In these studies, the aperture field distribution was assumed to be that of the TE_{10} mode. The reflection coefficient inside the guide was not calculated. Lewin [17] was the first to consider the internal problem. He derived a stationary expression for the input admittance of a rectangular guide radiating into air. However, the higher order modes were neglected.

One of the methods used in the present study is based on the work of Mautz and Harrington [18]. An integral equation, in terms of an equivalent magnetic current on the aperture, is derived and solved by the method of moments. This analysis considers higher order modes and yields the input admittance, the reflection coefficient, the tangential electric field in the aperture and the radiation pattern.

Cross polarization in rectangular apertures was considered by Jamieson and Rozzi [19], while an exact solution by the correlation matrix method was proposed by MacPhie and Zaghloul [20].

In all these papers, the guide has been radiating into free space. When a dielectric is placed in contact with the aperture the input admittance and radiation pattern change. Compton [21] was the first to analyze this problem. Considering the aperture field to be composed of the TE_{10} and TE_{30} modes, he obtained input admittance values for the case of an infinite lossy medium and a finite lossy slab.

The advent of space-borne antennas stimulated much more work in this area. When a space vehicle re-enters the earths atmosphere, a layer of charged particles forms over the antennas.

Among those who studied this problem are: Villeneuve [22], who used a variational method to analyze the problem of radiation into a homogeneous, lossless plasma; Galejs [23], who solved the more complex problem involving a stratified, lossy plasma; and Croswell [24], who applied the method of Compton [21] to the case of an inhomogeneous, lossy plasma.

More recently, the model used by Galejs [23] has been applied in the analysis of radiation into lossy dielectrics [25,26]. In this method, which is described in more detail in Chapter 3, the half-space is replaced by an imaginary waveguide whose cross-sectional dimensions are very large. When the dielectric is lossy and the dimensions of the second guide are chosen large enough, this waveguide discontinuity problem adequately simulates the unbounded problem.

The first application of open-ended guides to permittivity measurements was proposed by Decreton *et. al.* [14]. The input reflection coefficient of the guide as a function of the permittivity of the sample was calculated using a variational approach. Computer generated charts relating the VSWR and phase shift to the complex permittivity were presented allowing graphical inversion of the problem. In addition, a computer program was suggested, which used an optimization algorithm to invert the problem. This analysis, however, was restricted to relatively low dielectric constants. ($\varepsilon' < 15$, $\varepsilon'' < 10$)

More extensive data was presented in [11]. The method of characteristic modes was used and a polar plot (Smith Chart) was presented showing the complex reflection coefficient in X-band waveguide at 10 GHz, with the dielectric constant and loss factor as parameters. From this plot, which is reproduced in Fig. 1.2, it is evident that large uncertainties in the measurement of permittivity exist for materials having high dielectric constants.

None of the above publications considered the modified aperture problem. Although the method used in [18] is quite general with respect to the aperture geometry, it was used to analyse radiation into free-space only.

In conclusion, it has been demonstrated that the open-ended guide has the potential of providing a fast and accurate means of making non-destructive permittivity measurements. The structure, however, exhibits large uncertainties for materials having high dielectric constants. Until now, no attempt has been made to reduce these uncertainties.

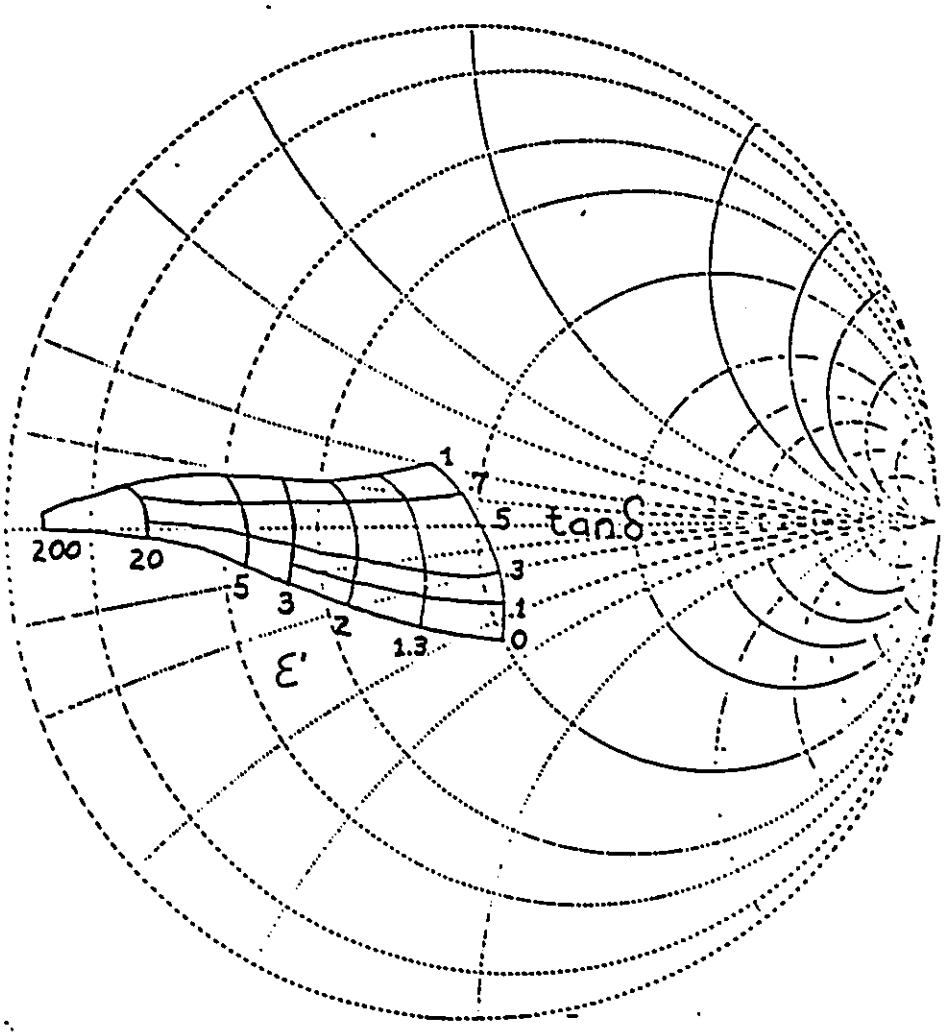

Fig. 1.2: Reflection Coefficient in Open Guide at 10 GHz

Chapter 2:

Application of the Finite Element Method to Open-Ended Waveguide Problems

2.1 Introduction

This chapter presents a novel approach to determining the input reflection coefficient of a modified open-ended waveguide structure in contact with a lossy dielectric. The structure consists of a rectangular waveguide, assumed to extend from $z = -\infty$ to $z = d$, terminated in the plane $z = d$ by a metal screen containing one or more apertures. The half space $z > d$ is filled with a homogeneous, lossy dielectric. The guide is excited by the dominant TE_{10} mode and the frequency of operation is low enough to ensure mono-mode operation of the guide.

An electromagnetic boundary value problem is formulated in terms of the magnetic Hertzian potential. Although the problem is theoretically unbounded, an approximate boundary condition is imposed on the aperture. It has been shown [27,28] that the exact electromagnetic boundary conditions at the surface of a lossy dielectric may be approximated by the Leontovich condition [29]. This condition relates the tangential components of the electric and magnetic fields at the dielectric interface through a surface impedance which is a function of the electromagnetic properties of the material.

The boundary condition at $z = 0$ is obtained by assuming the field distribution in this plane to be a sum of the incident and reflected waves of the TE_{10} mode. This assumption is justified by chosing the distance d large enough to ensure that the evanescent higher order modes excited at the aperture have decayed to amplitudes small enough to be neglected.

The Finite Element Method (FEM) is then used to reduce this boundary value problem to a system of linear algebraic equations. The interior of the waveguide, $0 \leq z \leq d$, is subdivided into rectangular "brick" elements having 27 nodes. The potential in each element is written in terms of the 27 node potentials via 2nd order Lagrangian interpolatory functions. Galerkin's method of weighted residuals is then used to find an approximate solution in each region, taking care that this solution is continuous across inter-element boundaries. The resulting solution is the union of the solutions for each sub-region. Once the magnetic Hertzian potential is determined, the input reflection coefficient may be calculated from the potentials at $z = 0$.

2.2 Geometry and Assumptions

The geometry of the problem is shown in Fig. 2.1. An air-filled rectangular waveguide of cross sectional dimensions a × b extends from $z = -\infty$ to $z = d$. The guide is terminated in the plane $z = d$ by a conducting screen which contains one or more apertures. The half space $z > d$ is filled with a homogeneous, linear, isotropic, dielectric having a relative permittivity $\hat{\varepsilon}_r = \varepsilon' - j\varepsilon''$. The volume contained by the waveguide walls and the planes $z = 0$ and $z = d$ is denoted R while the boundary of this region is denoted S. The following assumptions have been made:

1) The incident wave is in the dominant TE_{10} mode
2) The frequency of operation is low enough and the distance d is large enough to ensure mono-mode operation at z=0
3) All metal is perfectly conducting.
4) The dielectric fills the entire half-space z > d
5) The dielectric has a large relative permittivity. (i.e. $|\hat{\varepsilon}_r| \gg 1$)
6) Cross polarization is negligible. (i.e. $E_x = 0$)

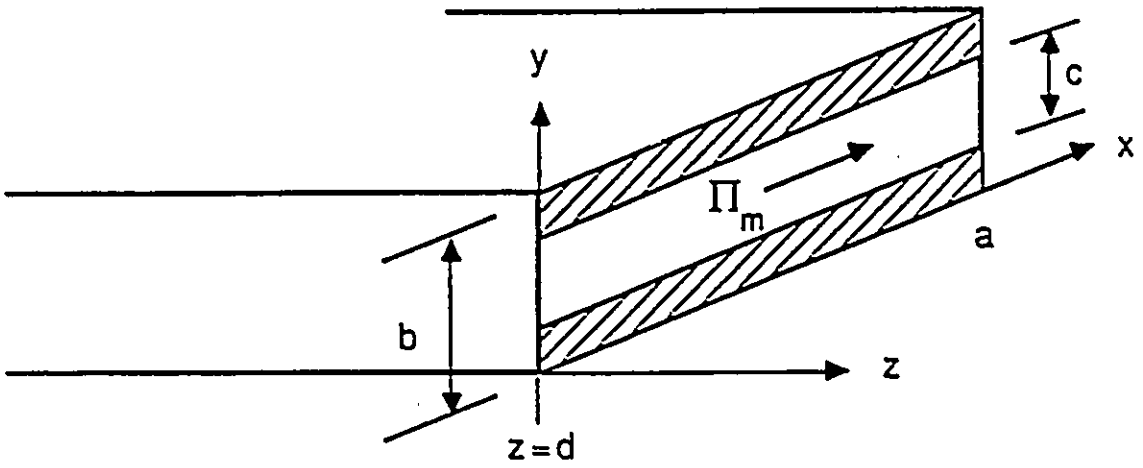

Fig. 2.1: Geometry used in the Finite-Element Analysis

2.3 Mathematical Formulation

2.3.1 The Differential Equation

In the region R, where the TE_{10} mode is assumed incident, the discontinuity caused by the aperture and the change in dielectric produces a reflected TE_{10} as well as evanescent higher order modes. Neglecting cross polarization, these modes will be of the LSE_{mn} (TE^x) mode set, having no E_x component. For this reason, the problem is conveniently formulated in terms of an x-directed magnetic Hertzian potential of the form:

$$\underline{\vec{\Pi}}_m = \underline{\psi}(x,y,z)\vec{x} \tag{2.1}$$

All components of the fields may be derived from $\underline{\vec{\Pi}}_m$ according to the following equations.

$$\underline{\vec{E}} = \nabla \times \underline{\vec{\Pi}}_m \tag{2.2}$$

$$\underline{\vec{H}} = \frac{j}{\omega\mu}\left\{\nabla\nabla \cdot \underline{\vec{\Pi}}_m + k_0^2 \underline{\vec{\Pi}}_m\right\} \tag{2.3}$$

In order to satisfy Maxwell's equations inside the guide, the magnetic Hertzian potential must be a solution of the vector Helmholtz equation. In particular, for the potential defined by equation (2.1), ψ must be a solution of,

$$\nabla^2 \underline{\psi} + k_0^2 \underline{\psi} = 0 \tag{2.4}$$

2.3.2 Boundary Conditions

Imposing the condition of zero tangential electric field on the metallic walls of the waveguide, leads to the following boundary conditions in terms of $\underline{\Psi}$,

$$\underline{\Psi} = 0 \qquad @\, x = 0, \quad x = a \tag{2.5}$$

$$\frac{\partial \underline{\Psi}}{\partial \vec{n}} \qquad @\, y = 0, \quad y = b \tag{2.6}$$

where $\vec{n}$ denotes an outward-directed normal vector to S.

The sending end boundary condition (z = 0) is obtained by neglecting the higher order modes. Therefore, the potential at this point will be composed of the incident TE_{10} mode and a reflected TE_{10} mode. In terms of $\underline{\Psi}$,

$$\underline{\Psi}(x, y, 0) = \frac{1}{jk_1}\{1 - \underline{\Gamma}_1\} \sin\frac{\pi x}{a} \tag{2.7}$$

Here, k_1 is the z-component of the dominant mode propagation constant and $\underline{\Gamma}_1$ is the unknown reflection coefficient of this mode. Similarly, expanding (2.2) under the assumption that only the dominant mode is non-zero, yields,

$$\underline{E}_y(x, y, 0) = -\{1 + \underline{\Gamma}_1\} \sin\frac{\pi x}{a} = \left.\frac{\partial \underline{\Psi}}{\partial z}\right|_{z=0} \tag{2.8}$$

Combining (2.8) and (2.7), one obtains the following inhomogeneous Cauchy boundary condition,

$$-\left.\frac{\partial \underline{\Psi}}{\partial \vec{n}}\right|_{z=0} = jk_1 \underline{\Psi}(x, y, 0) - 2\sin\frac{\pi x}{a} \tag{2.9}$$

For the other boundary, at z = d, the Leontovich condition [27], may be written as,

$$\underline{E}_y = -\underline{\eta}\,\underline{H}_x \tag{2.10}$$

with the "surface impedance" $\underline{\eta}$ being defined as,

$$\underline{\eta} = \sqrt{\frac{\mu_0 \tilde{\mu}_r}{\varepsilon_0 \hat{\varepsilon}_r}} \tag{2.11}$$

In terms of $\underline{\Psi}$, (2.10) may be written as,

$$\frac{\partial \underline{\Psi}}{\partial n} = -\frac{j\underline{\eta}}{\omega\mu_0}\left\{\frac{\partial^2 \underline{\Psi}}{\partial x^2} + k_0^2 \underline{\Psi}\right\} \tag{2.12}$$

The boundary at z = d is in fact a composite boundary, made up of a perfectly conducting part (metal screen) and a dielectric part (apertures). It can be seen from (2.11) that for the metal regions $\underline{\eta} \to 0$ and , hence , (2.12) goes smoothly over to the homogeneous Neumann boundary one would expect at the surface of a perfect conductor.

2.3.3 The Finite Element Method

The finite element method used is based on Galerkin's method of weighted residuals [30]. The region R is subdivided into rectangular brick elements similar to the one shown in Fig. 2.2. Each element has 27 nodes and encloses a volume R_b. The surface of this generic brick is denoted S_b. The potential everywhere in the region R_b and on the surface S_b is expressed in terms of the 27 node potentials, $\underline{\phi}_{ib}$, via 2nd order Lagrangian interpolatory functions.

$$\underline{\Psi}_b = \sum_{i=1}^{27} N_{ib}\,\underline{\phi}_{ib} \tag{2.13}$$

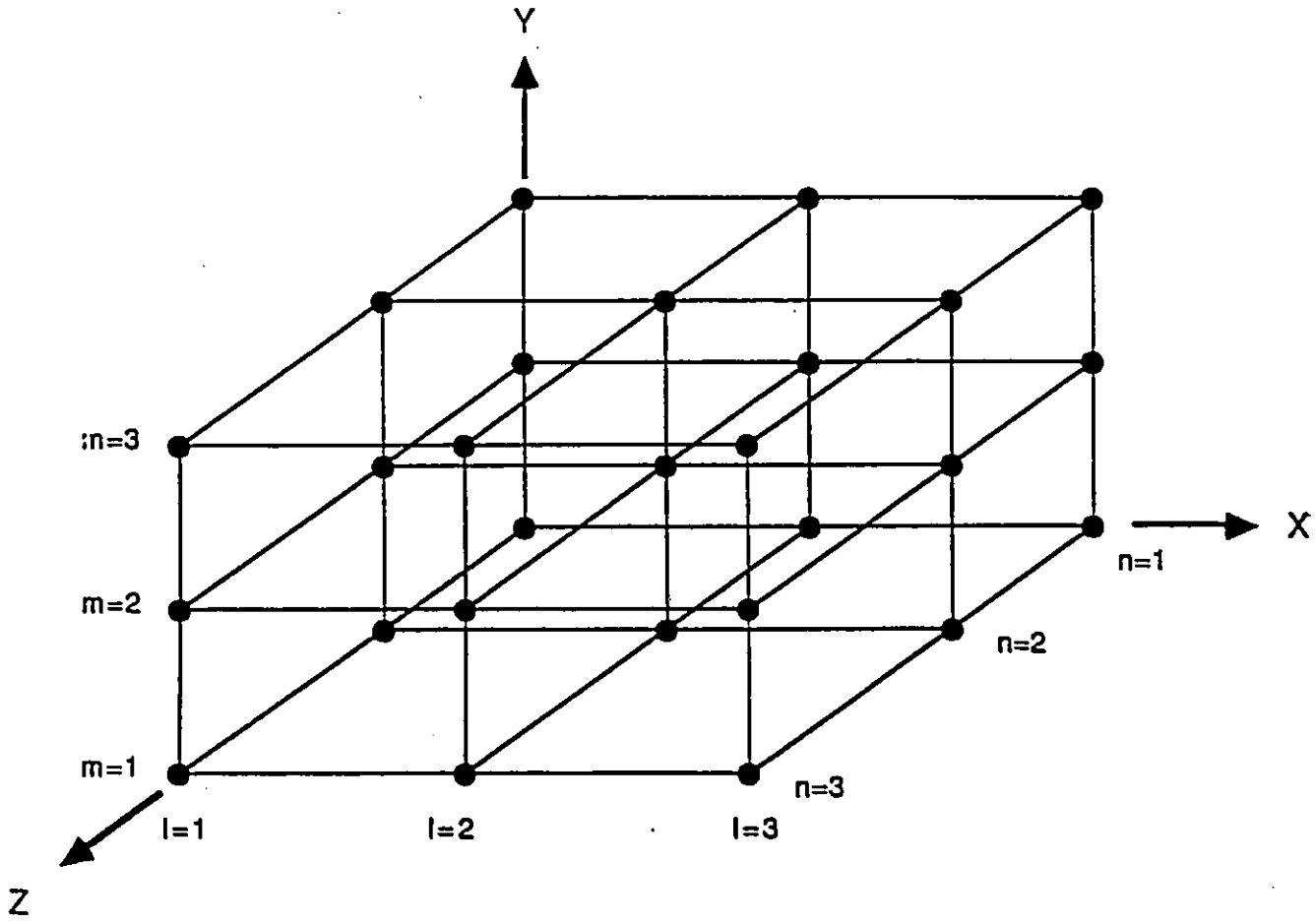

Fig. 2.2: A Typical 27 Node Brick Element

The interpolatory functions, also called shape functions, are defined as follows,

$$N_{ib} = \begin{cases} L_l(x)L_m(y)L_n(z) & (x,y,z) \in R_b \\ 0 & (x,y,z) \notin R_b \end{cases} \tag{2.14}$$

where the Lagrange polynomials are given by

$$L_l(x) = \prod_{\substack{k=1 \\ k \neq l}}^{3} \left\{ \frac{x - x_k}{x_l - x_k} \right\} \tag{2.15}$$

$$L_m(y) = \prod_{\substack{k=1 \\ k \neq m}}^{3} \left\{ \frac{y - y_k}{y_m - y_k} \right\} \tag{2.16}$$

$$L_n(z) = \prod_{\substack{k=1 \\ k \neq n}}^{3} \left\{ \frac{z - z_k}{z_n - z_k} \right\} \tag{2.17}$$

The mapping of the l, m, n indices to the local node index i is summarized in Table 2.1.

Table 2.1: Mapping of Coordinate Indices to Local Node Index

Local Node Index	Coordinate Indices		
i	l	m	n
1	1	1	1
2	2	1	1
3	3	1	1
4	1	2	1
5	2	2	1
⋮	⋮	⋮	⋮
27	3	3	3

It is more convenient at this point to express equation (2.13) in the matrix form,

$$\underline{\Psi}_b = \overline{N}_b \underline{\overline{\phi}}_b^T \tag{2.18}$$

where the bar denotes a row vector and the ^{T} denotes matrix transposition. In this notation, the potential everywhere in the region R is,

$$\underline{\tilde{\Psi}} = \sum_{b=1}^{\#\,of\,bricks} \overline{N}_b \underline{\overline{\phi}}_b^T \tag{2.19}$$

The finite element discretization is now complete and one may apply the method of weighted residuals to determine the node potentials, $\underline{\phi}_{ib}$, such that $\underline{\tilde{\Psi}}$ is an approximate solution to the boundary value problem at hand.

Substituting (2.19) into (2.4) yields,

$$\nabla^2 \underline{\tilde{\Psi}} + k_0^2 \underline{\tilde{\Psi}} = \delta(x,y,z) \tag{2.20}$$

The term $\underline{\delta}$ in (2.20) is referred to as the residual. Clearly, at the solution point the residual must vanish and $\underline{\tilde{\Psi}}$ must satisfy the boundary conditions on S. One can obtain an approximate solution in the following manner.

Define weighting functions,

$$W_r = \overline{N}_r \qquad r = 1,2,3,\ldots,NB \tag{2.21}$$

where NB represents the number of bricks.

Next, pre-multiply (2.20) by the weighting functions and integrate over the region R.

$$\int_R \sum_{r=1}^{NB} \overline{N}_r^T \sum_{b=1}^{NB} \left(\nabla^2 \overline{N}_b \underline{\overline{\phi}}_b^T + k_0^2 \overline{N}_b \underline{\overline{\phi}}_b^T \right) dR = 0 \tag{2.22}$$

In (2.22) the residual has been forced to zero. The orthogonality of the shape functions and the linearity of the integration may be exploited to reduce (2.22) to,

$$\sum_{b=1}^{NB} \int_{R_b} \overline{N}_b^T \nabla^2 \overline{N}_b \underline{\overline{\phi}}_b^T + k_0^2 \overline{N}_b^T \overline{N}_b \underline{\overline{\phi}}_b^T dR = 0 \tag{2.23}$$

Finally, the boundary conditions may be included by applying Green's identity to the first term of (2.23).

$$\sum_{b=1}^{NB} \left\{ \int_{S_b} \overline{N}_b^T \frac{\partial \overline{N}_b}{\partial \overline{n}} \underline{\overline{\phi}}_b^T dS - \int_{R_b} \nabla \overline{N}_b^T \cdot \nabla \overline{N}_b \underline{\overline{\phi}}_b^T + k_0^2 \overline{N}_b^T \overline{N}_b \underline{\overline{\phi}}_b^T dR \right\} = 0 \tag{2.24}$$

where $\overline{n}$ is the outward directed normal to S_b.

At the inter-element boundaries, the tangential components of the electric field must be continuous. This condition places the following constraint on the potential at the boundary between elements i and j,

$$\frac{\partial \underline{\Psi}_i}{\partial \overline{n}_i} - \frac{\partial \underline{\Psi}_j}{\partial \overline{n}_j} = 0$$

Hence, the contribution of the surface integral on the inter-element boundaries will sum to zero, and one needs only to consider those surfaces S_b which lie on the external surface S. Furthermore, homogeneous Neumann boundaries give no contribution while Dirichlet boundaries are forced. This leaves only the boundaries at z = 0 and on the aperture(s).

For bricks having a face in the z = 0 plane, one obtains the following contribution,

$$\int_{S_{z=0}} \overline{N}_b^T \frac{\partial \overline{N}_b}{\partial \overline{n}} \underline{\overline{\phi}}_b^T dS = 2 \int_{S_{z=0}} \overline{N}_b^T \sin\frac{\pi x}{a} dS - jk_1 \int_{S_{z=0}} \overline{N}_b^T \overline{N}_b \underline{\overline{\phi}}_b^T dS \tag{2.25}$$

Where use has been made of (2.9).

Similarly, applying the boundary condition on the aperture, one obtains,

$$\int_{Ap} \overline{N}_b^T \frac{\partial \overline{N}_b}{\partial \overline{n}} \underline{\overline{\phi}}_b^T dS = -\frac{j\underline{\eta}}{\omega\mu_0} \int_{Ap} \overline{N}_b^T \frac{\partial^2 \overline{N}_b}{\partial x^2} \underline{\overline{\phi}}_b^T + k_0^2 \overline{N}_b^T \overline{N}_b \underline{\overline{\phi}}_b^T dS \tag{2.26}$$

Substitution of (2.26) and (2.25) into (2.24) yields the final form of the Galerkin integral,

$$\begin{aligned} \sum_{b=1}^{NB} \{ & \int_{R_b} \nabla \overline{N}_b^T \cdot \nabla \overline{N}_b \underline{\overline{\phi}}_b^T dR - k_0^2 \int_{R_b} \overline{N}_b^T \overline{N}_b \underline{\overline{\phi}}_b^T dR \\ & + jk_1 \int_{S_{z=0}} \overline{N}_b^T \overline{N}_b \underline{\overline{\phi}}_b^T dS + \frac{j\underline{\eta}}{\omega\mu_0} \int_{Ap} \overline{N}_b^T \frac{\partial \overline{N}_b}{\partial x^2} \underline{\overline{\phi}}_b^T + k_0^2 \overline{N}_b^T \overline{N}_b \underline{\overline{\phi}}_b^T dS \} \\ & = 2 \sum_{b=1}^{NB} \int_{S_{z=0}} \overline{N}_b^T \sin\frac{\pi x}{a} dS \end{aligned} \tag{2.27}$$

Equation (2.27) can be written in the matrix notation as,

$$[\underline{A}] \cdot [\underline{\phi}] = [\underline{b}] \tag{2.28}$$

This last equation may be solved by standard methods, yielding the node potentials of the finite element mesh,

$$[\underline{\phi}] = [\underline{A}]^{-1} \cdot [\underline{b}] \tag{2.29}$$

2.3.4 Calculation of $\underline{\Gamma}_1$

The final step in the analysis is the determination of the dominant mode reflection coefficient. This quantity is easily calculated from the node potentials in the plane $z = 0$. In this plane the magnetic Hertzian potential is related to the reflection coefficient by equation (2.7). Solving this equation for $\underline{\Gamma}_1$ we obtain,

$$\underline{\Gamma}_1 = 1 - \frac{jk_1\underline{\phi}_n|_{z=0}}{\sin\frac{\pi x}{a}} \tag{2.30}$$

where any node potential in the plane $z = 0$ may be used. However, due to the various approximations involved as well as round-off error, the value of $\underline{\Gamma}_1$ calculated according to (2.30) depends on the choice of node. For this reason, an average $\underline{\Gamma}_1$ is calculated.

$$\underline{\Gamma}_1 = \frac{1}{NN}\sum_{n=1}^{NN}\left\{1 - \frac{jk_1\underline{\phi}_n}{\sin\frac{\pi x}{a}}\right\} \tag{2.31}$$

Where NN is the number of nodes in the plane $z = 0$. (nodes at $x = 0, a$ excluded)

Finally, by chosing the reference plane $z = 0$ a distance $n\lambda_g/2$ from the aperture, the reflection coefficient calculated by (2.31) is the same as at the aperture itself.

2.4 Description of the Computer Program

A three dimensional Finite-element program has been developed based on the theory presented in this chapter. The program has been written specifically for apertures which possess axial symmetry. This allows one to place magnetic walls at x=a/2 and y=b/2, hence, reducing the region to be discretized four-fold. A FORTRAN listing of the program may be found in Appendix B.

The program may be divided into three major sections: the mesh generation, the assembly of the finite-element matrices, and the solution of the system of equations. The mesh generation routine, GRID, is an interactive subprogram which prompts for the information necessary to define the problem geometry. Based on this input data, the finite-element mesh is automatically generated. A uniform grid in the z-direction and piecewise uniform grids in the x- and y-directions are used in the discretization. Following this initialization, the finite-element matrices are assembled and the resulting system of equations is solved, using Gaussian elimination, by the LINPACK [31] subroutine ZGECO.

The program outputs are the nodal potentials and the corresponding nodal coordinates as well as the computed reflection coefficient in the plane z=0.

2.5 Convergence of the Method

Because the Helmholtz operator is not self-adjoint, convergence of the finite-element method is not guaranteed [32]. For this reason, a convergence study was performed. The mesh was successively refined and the behavior of the computed reflection coefficient was observed. The results of this study showed:

1) Increasing the number of grid lines in the y-direction beyond 5 had no effect on the computed reflection coefficient.
2) Refinement of the mesh in the x- and z-directions lead to convergence.
3) Convergence was dominated by the number of grid lines in the x-direction

Therefore, one concludes that the total number of nodes (unknowns) is not as critical for convergence as the placement of the nodes.

Figures 2.3 and 2.4 show the convergence of $|\underline{\Gamma}|$ at 10 GHz for two representative cases: transmission through the full aperture (10.16 x 22.86 mm) into water, and transmission through a 2 mm aperture (2 x 22.86 mm) into water. There are four curves per plot, each corresponding to a fixed number of grid lines in the x-direction. In all cases five grid lines were used in the y-direction and the number of z-grid lines varied from 7 to 15.

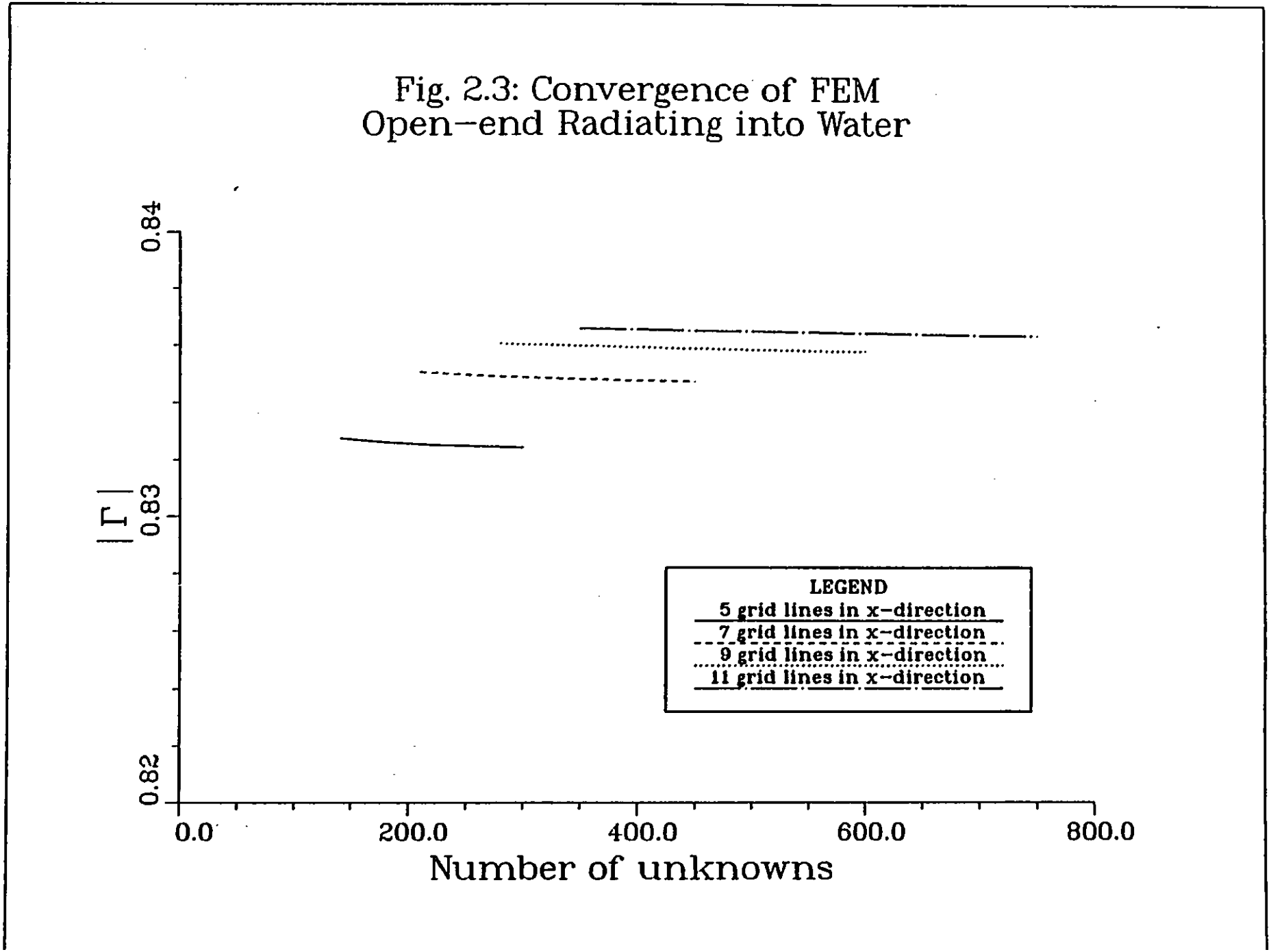
Fig. 2.3: Convergence of FEM
Open–end Radiating into Water
0.84
0.83
0.82
|Γ|
0.0
200.0
400.0
600.0
800.0
Number of unknowns
LEGEND
5 grid lines in x–direction
7 grid lines in x–direction
9 grid lines in x–direction
11 grid lines in x–direction

Fig. 2.4: Convergence of FEM
2 mm Aperture Radiating into Water

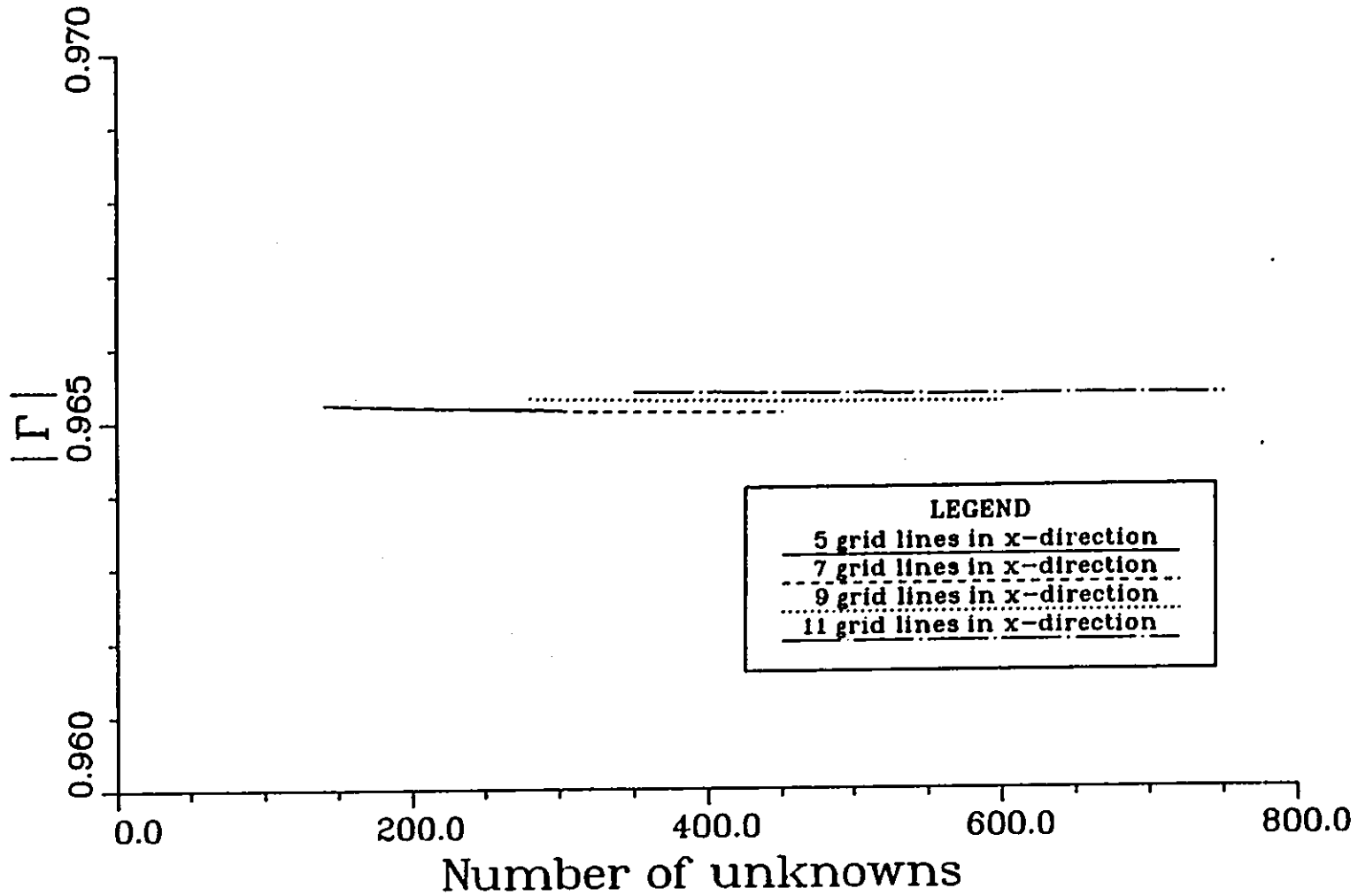

Chapter 3:

Application of the Mode Matching Method to Open-Ended Waveguide Problems

3.1 Introduction

This chapter describes another numerical method which has been successfully applied to solve open-ended waveguide problems, namely, the mode matching method. Several investigators [25,26] have shown that, when the dielectric in contact with the open end of a waveguide is lossy, the half-space region may be modeled by an oversized waveguide. If the cross sectional dimensions of this second guide are chosen large enough and the dielectric is sufficiently lossy, the presence of the metal walls of the second guide have a negligible effect on the dominant mode reflection coefficient in the smaller input guide. Using the well known technique of mode matching to solve this discontinuity problem one can obtain the reflection coefficient of the modified open-ended waveguide. This present case differs from those in [25,26] in that the aperture at the junction between the two guides is modified.

3.2 Geometry and Assumptions

The geometry of the problem is shown in Fig. 3.1. The input guide and the output guide have dimensions $a_1 \times b_1$ and $a_3 \times b_3$ respectively and are coaxial. The junction is located at z = 0 and a metal screen containing a rectangular aperture is placed in this plane. The input guide is air filled and the output guide is filled with a homogeneous, linear, isotropic, non-magnetic dielectric whose relative permittivity is $\hat{\varepsilon}_r = \varepsilon' - j\varepsilon''$

The following simplifying assumptions have been made:

(1) All metal is considered perfectly conducting.
(2) The iris is considered to have zero thickness.
(3) The incident field in the input guide is the dominant TE_{10} mode.
(4) The frequency is low enough to ensure mono-mode propagation in the input guide.
(5) The output guide is matched.
(6) Cross polarization is negligible.
(7) The edges of the aperture are parallel to the walls of the waveguide.
(8) The dielectric is lossy.

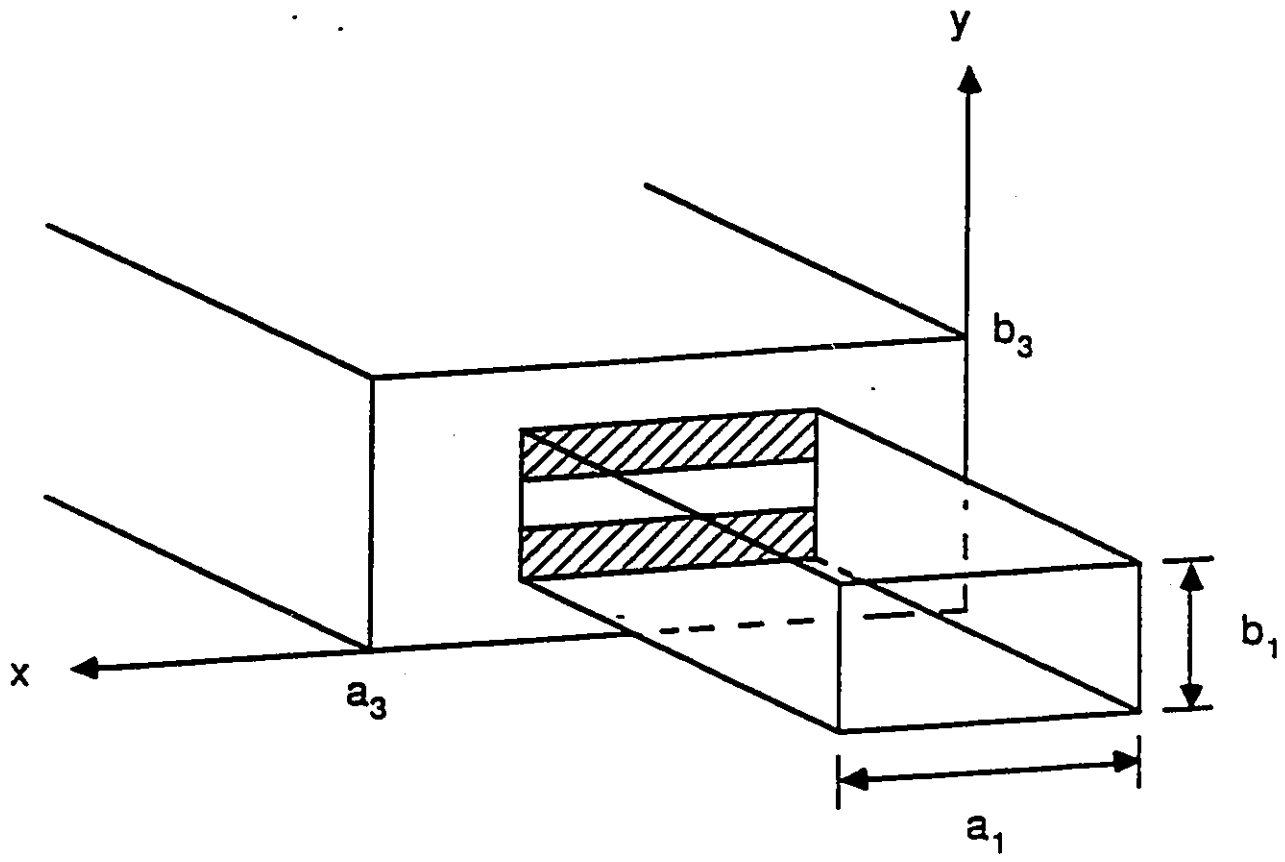

Fig. 3.1: Geometry used in Mode Matching

3.3 Mathematical Development

3.3.1 The Mode Matching Method

The structure of Fig. 3.1 may be divided into three regions as shown in Fig. 3.2. These regions are:

Region 1:	input guide (or guide 1)	$z<0$
Region 2:	aperture (guide 2)	$z=0$
Region 3:	output guide (guide 3)	$z>0$

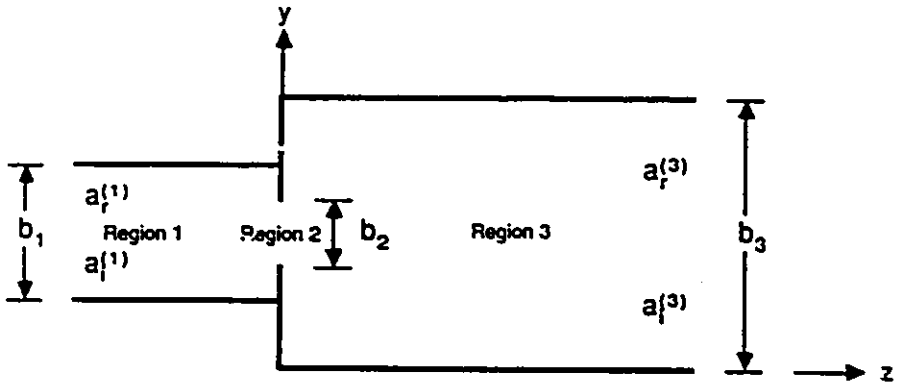

Fig. 3.2: The Three Regions used for Mode Matching

The transverse components, (x and y), of the electric and magnetic fields in each region are expanded in a series of waveguide modes (eigenmodes). The transverse fields of each mode may be written as:

$$\vec{E}_{ti}(x,y,z)=\underline{A}\,\vec{e}_i(x,y)e^{(\pm\gamma_i z)} \tag{3.1}$$

$$\vec{H}_{ti}(x,y,z)=\mp\underline{A}\,\vec{h}_i(x,y)e^{(\pm\gamma_i z)} \tag{3.2}$$

Where $\vec{e}_i$, $\vec{h}_i$ and $\underline{\gamma}_i$ are the transverse vector functions and propagation constant of the ith eigenmode, respectively, and $\underline{A}$ is a complex amplitude factor. In equation (3.2) the negative sign is chosen for waves propagating in the negative z direction and the positive sign is

chosen for waves propagating in the positive z direction. In addition, for any closed guiding structure with perfectly conducting walls, the transverse mode functions have the following orthogonality property [33],

$$\int_A \vec{\underline{e}}_i \times \vec{\underline{h}}_j \cdot \vec{z}\, ds = 0 \qquad if \quad i \neq j \tag{3.3}$$

Where the integration is performed over the waveguide cross section.

Using this notation, the total transverse fields in region 1, written for z = 0, are:

$$\vec{\underline{E}}_t^{(1)} = \sum_{p=1}^{\infty} (\underline{a}_{ip}^{(1)} + \underline{a}_{rp}^{(1)}) \vec{\underline{e}}_p^{(1)} \tag{3.4}$$

$$\vec{\underline{H}}_t^{(1)} = \sum_{p=1}^{\infty} (\underline{a}_{ip}^{(1)} - \underline{a}_{rp}^{(1)}) \vec{\underline{h}}_p^{(1)} \tag{3.5}$$

where $\underline{a}_{ip}^{(1)}$ is the amplitude coefficient for the mth mode incident on the aperture in guide 1 and

$\underline{a}_{rp}^{(1)}$ is the amplitude coefficient for the mth mode propagating away from the aperture in guide 1.

Similarly, the transverse fields in region 3, for z = 0 are:

$$\vec{\underline{E}}_t^{(3)} = \sum_{q=1}^{\infty} (\underline{a}_{iq}^{(3)} + \underline{a}_{rq}^{(3)}) \vec{\underline{e}}_q^{(3)} \tag{3.6}$$

$$\vec{\underline{H}}_t^{(3)} = \sum_{q=1}^{\infty} (\underline{a}_{rq}^{(3)} - \underline{a}_{iq}^{(3)}) \vec{\underline{h}}_q^{(3)} \tag{3.7}$$

where $\underline{a}_{iq}^{(3)}$ is the amplitude coefficient for the nth mode incident on the aperture in guide 3 and

$\underline{a}_{rq}^{(3)}$ is the amplitude coefficient for the nth mode propagating away from the aperture in guide 3.

Finally, in order to apply mode matching, it is necessary to express the fields in the aperture as a series of vector functions. The transverse fields of the eigenmodes for a homogeneous waveguide with the same cross sectional dimensions of the aperture may be used for this purpose. Denoting these eigenmodes by $\underline{\vec{e}}_u^{(2)}$ and $\underline{\vec{h}}_u^{(2)}$ one may write,

$$\underline{\vec{E}}_t^{(2)} = \sum_{u=1}^{\infty} \underline{b}_u \underline{\vec{e}}_u^{(2)} \tag{3.8}$$

$$\underline{\vec{H}}_t^{(2)} = \sum_{i=1}^{\infty} \underline{c}_u \underline{\vec{h}}_u^{(2)} \tag{3.9}$$

It should be noted that, although (3.8) and (3.9) are derived from waveguide modes they are not related through a wave impedance. This fact allows a more general solution to Maxwell's equations in the aperture region. For example, the longitudinal component of the electric field need not vanish at the edges of the aperture as would be the case for a true waveguide mode.

Now, the tangential components of the fields must be continuous at the aperture. Therefore, equations (3.4) to (3.9) may be used to obtain:

$$\sum_{p=1}^{\infty} (\underline{a}_{ip}^{(1)} + \underline{a}_{rp}^{(1)}) \underline{\vec{e}}_p^{(1)} = \sum_{u=1}^{\infty} \underline{b}_u \underline{\vec{e}}_u^{(2)} \tag{3.10}$$

$$\sum_{u=1}^{\infty} \underline{b}_u \underline{\vec{e}}_u^{(2)} = \sum_{q=1}^{\infty} (\underline{a}_{iq}^{(3)} + \underline{a}_{rq}^{(3)}) \underline{\vec{e}}_q^{(3)} \tag{3.11}$$

$$\sum_{p=1}^{\infty} (\underline{a}_{ip}^{(1)} - \underline{a}_{rp}^{(1)}) \underline{\vec{h}}_p^{(1)} = \sum_{u=1}^{\infty} \underline{c}_u \underline{\vec{h}}_u^{(2)} \tag{3.12}$$

$$\sum_{u=1}^{\infty} \underline{c}_u \underline{\vec{h}}_u^{(2)} = \sum_{q=1}^{\infty} (\underline{a}_{rq}^{(3)} - \underline{a}_{iq}^{(3)}) \underline{\vec{h}}_q^{(3)} \tag{3.13}$$

If one post multiplies equation (3.10) by $\underline{\vec{h}}_P^{(1)}$, where P is any positive integer, and integrates over the aperture area, A_2, one obtains:

$$\sum_{p=1}^{\infty}(\underline{a}_{ip}^{(1)}+\underline{a}_{rp}^{(1)})\int_{A_2}\underline{\vec{e}}_p^{(1)}\times\underline{\vec{h}}_P^{(1)}\cdot\vec{z}ds=\sum_{u=1}^{\infty}\underline{b}_u\int_{A_2}\underline{\vec{e}}_u^{(2)}\times\underline{\vec{h}}_P^{(1)}\cdot\vec{z}ds \qquad P=1,2,\ldots,\infty \quad (3.14)$$

However, the total transverse electric field in guide 1 must vanish on the metal screen, and hence:

$$\sum_{p=1}^{\infty}(\underline{a}_{ip}^{(1)}+\underline{a}_{rp}^{(1)})\int_{A_0}\underline{\vec{e}}_p^{(1)}\times\underline{\vec{h}}_P^{(1)}\cdot\vec{z}ds=0 \qquad (3.15)$$

for any P. Here the integration over the metal screen is denoted A_0.

Using this fact, the integration on the left hand side of (3.14) may be extended to the entire cross section of guide 1,

$$\sum_{p=1}^{\infty}(\underline{a}_{ip}^{(1)}+\underline{a}_{rp}^{(1)})\int_{A_1}\underline{\vec{e}}_p^{(1)}\times\underline{\vec{h}}_P^{(1)}\cdot\vec{z}ds=\sum_{u=1}^{\infty}\underline{b}_u\int_{A_2}\underline{\vec{e}}_u^{(2)}\times\underline{\vec{h}}_P^{(1)}\cdot\vec{z}ds \qquad P=1,2,\ldots,\infty \quad (3.16)$$

Due to the orthogonality property of the modes, (3.3), all of the terms of the summation vanish except the term p=P. This simplifies (3.16) so that,

$$(\underline{a}_{iP}^{(1)}+\underline{a}_{rP}^{(1)})=\frac{\sum_{u=1}^{\infty}\underline{b}_u\int_{A_2}\underline{\vec{e}}_u^{(2)}\times\underline{\vec{h}}_P^{(1)}\cdot\vec{z}ds}{\int_{A_1}\underline{\vec{e}}_P^{(1)}\times\underline{\vec{h}}_P^{(1)}\cdot\vec{z}ds} \quad ; \qquad P=1,2,\ldots,\infty \qquad (3.17)$$

Finally, the denominator in (3.17) may be set to unity by properly normalizing the mode functions.

Similar manipulations on equations (3.11) to (3.13) yield:

$$(\underline{a}_{iQ}^{(3)} + \underline{a}_{rQ}^{(3)}) = \sum_{u=1}^{\infty} \underline{b}_u \int_{A_2} \vec{\underline{e}}_u^{(2)} \times \vec{\underline{h}}_Q^{(3)} \cdot \vec{z}\, ds \quad ; \qquad Q = 1,2,\ldots,\infty \tag{3.18}$$

$$\underline{c}_U = \sum_{p=1}^{\infty} (\underline{a}_{ip}^{(1)} - \underline{a}_{rp}^{(1)}) \int_{A_2} \vec{\underline{e}}_U^{(2)} \times \vec{\underline{h}}_p^{(1)} \cdot \vec{z}\, ds \quad ; \qquad U = 1,2,\ldots,\infty \tag{3.19}$$

$$\underline{c}_U = \sum_{q=1}^{\infty} (\underline{a}_{rq}^{(3)} - \underline{a}_{iq}^{(3)}) \int_{A_2} \vec{\underline{e}}_U^{(2)} \times \vec{\underline{h}}_q^{(3)} \cdot \vec{z}\, ds \quad ; \qquad U = 1,2,\ldots,\infty \tag{3.20}$$

In order to solve equations (3.17) to (3.20) for the unknown amplitude coefficients, one must truncate the series using:

p_1 modes in input guide.	(i.e. P, p = 1,2, . . ., p_1)
p_2 modes in aperture.	(i.e. U, u = 1,2, . . ., p_2)
p_3 modes in output guide.	(i.e. Q, q = 1,2, . . ., p_3)

Following truncation, equations (3.17) to (3.20) yield the following systems of equations:

$$\begin{bmatrix} \underline{a}_{i1}^{(1)} + \underline{a}_{r1}^{(1)} \\ \underline{a}_{i2}^{(1)} + \underline{a}_{r2}^{(1)} \\ \cdot \\ \cdot \\ \underline{a}_{ip_1}^{(1)} + \underline{a}_{rp_1}^{(1)} \end{bmatrix} = \begin{bmatrix} \underline{R}_{11} & \underline{R}_{12} & \cdots & \underline{R}_{1p_2} \\ \underline{R}_{21} & \underline{R}_{22} & \cdots & \underline{R}_{2p_2} \\ \cdot & \cdot & \cdots & \cdot \\ \cdot & \cdot & \cdots & \cdot \\ \underline{R}_{p_1 1} & \underline{R}_{p_1 2} & \cdots & \underline{R}_{p_1 p_2} \end{bmatrix} \cdot \begin{bmatrix} \underline{b}_1 \\ \underline{b}_2 \\ \cdot \\ \cdot \\ \underline{b}_{p_1} \end{bmatrix} \tag{3.21}$$

$$\textit{where:} \quad \underline{R}_{pu} = \int_{A_2} \vec{\underline{e}}_u^{(2)} \times \vec{\underline{h}}_p^{(1)} \cdot \vec{z} ds \tag{3.22}$$

$$\begin{bmatrix} \underline{a}_{i1}^{(3)} + \underline{a}_{r1}^{(3)} \\ \underline{a}_{i2}^{(3)} + \underline{a}_{r2}^{(3)} \\ \cdot \\ \cdot \\ \underline{a}_{ip_3}^{(3)} + \underline{a}_{rp_3}^{(3)} \end{bmatrix} = \begin{bmatrix} \underline{R}'_{11} & \underline{R}'_{12} & \cdots & \underline{R}'_{1p_2} \\ \underline{R}'_{21} & \underline{R}'_{22} & \cdots & \underline{R}'_{2p_2} \\ \cdot & \cdot & \cdots & \cdot \\ \cdot & \cdot & \cdots & \cdot \\ \underline{R}'_{p_3 1} & \underline{R}'_{p_3 2} & \cdots & \underline{R}'_{p_3 p_2} \end{bmatrix} \cdot \begin{bmatrix} \underline{b}_1 \\ \underline{b}_2 \\ \cdot \\ \cdot \\ \underline{b}_{p_2} \end{bmatrix} \tag{3.23}$$

$$\textit{where:} \quad \underline{R}'_{qu} = \int_{A_2} \vec{\underline{e}}_u^{(2)} \times \vec{\underline{h}}_q^{(3)} \cdot \vec{z} ds \tag{3.24}$$

$$\begin{bmatrix} \underline{c}_1 \\ \underline{c}_2 \\ \cdot \\ \cdot \\ \underline{c}_{p_2} \end{bmatrix} = \begin{bmatrix} \underline{S}_{11} & \underline{S}_{12} & \cdots & \underline{S}_{1p_1} \\ \underline{S}_{21} & \underline{S}_{22} & \cdots & \underline{S}_{2p_1} \\ \cdot & \cdot & \cdots & \cdot \\ \cdot & \cdot & \cdots & \cdot \\ \underline{S}_{p_2 1} & \underline{S}_{p_2 2} & \cdots & \underline{S}_{p_2 p_1} \end{bmatrix} \cdot \begin{bmatrix} \underline{a}_{i1}^{(1)} - \underline{a}_{r1}^{(1)} \\ \underline{a}_{i2}^{(1)} - \underline{a}_{r2}^{(1)} \\ \cdot \\ \cdot \\ \underline{a}_{ip_1}^{(1)} - \underline{a}_{rp_1}^{(1)} \end{bmatrix} \tag{3.25}$$

$$\textit{where:} \quad \underline{S}_{up} = \int_{A_2} \vec{\underline{e}}_u^{(2)} \times \vec{\underline{h}}_p^{(1)} \cdot \vec{z} ds \tag{3.26}$$

$$\begin{bmatrix} \underline{c}_1 \\ \underline{c}_2 \\ \cdot \\ \cdot \\ \underline{c}_{p_2} \end{bmatrix} = \begin{bmatrix} \underline{S}'_{11} & \underline{S}'_{12} & \cdots & \underline{S}'_{1p_3} \\ \underline{S}'_{21} & \underline{S}'_{22} & \cdots & \underline{S}'_{2p_3} \\ \cdot & \cdot & \cdots & \cdot \\ \cdot & \cdot & \cdots & \cdot \\ \underline{S}'_{p_2 1} & \underline{S}'_{p_2 2} & \cdots & \underline{S}'_{p_2 p_3} \end{bmatrix} \cdot \begin{bmatrix} \underline{a}_{r1}^{(3)} - \underline{a}_{i1}^{(3)} \\ \underline{a}_{r2}^{(3)} - \underline{a}_{i2}^{(3)} \\ \cdot \\ \cdot \\ \underline{a}_{rp_3}^{(3)} - \underline{a}_{ip_3}^{(3)} \end{bmatrix} \tag{3.27}$$

$$\textit{where:} \quad \underline{S}'_{uq} = \int_{A_2} \vec{\underline{e}}_u^{(2)} \times \vec{\underline{h}}_q^{(3)} \cdot \vec{z} ds \tag{3.28}$$

Using matrix notation, equations (3.21) to (3.27) can be written in a more compact format:

$$[\underline{a}_i^{(1)}] + [\underline{a}_r^{(1)}] = [\underline{R}] \cdot [\underline{b}] \tag{3.29}$$

$$[\underline{a}_i^{(3)}] + [\underline{a}_r^{(3)}] = [\underline{R}'] \cdot [\underline{b}] \tag{3.30}$$

$$[\underline{c}] = [\underline{S}] \cdot [\underline{a}_i^{(1)}] - [\underline{S}] \cdot [\underline{a}_r^{(1)}] \tag{3.31}$$

$$[\underline{c}] = [\underline{S}'] \cdot [\underline{a}_r^{(3)}] - [\underline{S}'] \cdot [\underline{a}_i^{(3)}] \tag{3.32}$$

Pre-multiplying (3.29) by $[\underline{S}]$ and substituting into (3.31) yields:

$$[\underline{c}] = 2 \cdot [\underline{S}] \cdot [\underline{a}_i^{(1)}] - [\underline{S}] \cdot [\underline{R}] \cdot [\underline{b}] \tag{3.33}$$

Similarly, combining (3.30) and (3.32) gives:

$$[\underline{c}] = [\underline{S}'] \cdot [\underline{R}'] \cdot [\underline{b}] - 2 \cdot [\underline{S}'] \cdot [\underline{a}_i^{(3)}] \tag{3.34}$$

Finally, equating (3.33) and (3.34) one obtains a system of equations in terms of the unknown electric field amplitudes in the aperture and the incident field amplitudes.

$$[\underline{S}\underline{R} + \underline{S}'\underline{R}'] \cdot [\underline{b}] = 2 \cdot [\underline{S}\,\underline{a}_i^{(1)} + \underline{S}'\underline{a}_i^{(3)}] \tag{3.35}$$

According to assumption (5), $[\underline{a}_i^{(3)}] = [0]$, while assumption (2) states that

$$\underline{a}_{ip}^{(1)} = 0 \quad \forall p \neq 1$$

so that in the case at hand the final system of equations can be simplified to:

$$[\underline{S}\underline{R} + \underline{S}'\underline{R}'] \cdot [\underline{b}] = 2 \cdot [\underline{S}] \cdot [\underline{a}_i^{(1)}] \tag{3.36}$$

3.3.2 Eigenmodes

Since the incident field in guide 1 (TE_{10}) has no x-component of the electric field, the discontinuity will excite TE_{mn} and TM_{mn} modes such that the resultant electric field has no x-component. This set of modes is conveniently represented by the LSE_{mn} modes. Hence we will use the LSE modes as basis functions in the input and output guide [33].

In the aperture region another mode set must be used in general, depending on the cross sectional geometry of the aperture. However, in the present case the aperture is restricted to having a rectangular cross section, and hence, the LSE modes are suitable here as well.

The transverse mode functions of the LSE modes may be derived by solving the scalar Helmholtz equation for the x-directed magnetic Hertzian potential [33]. In a homogeneous guide, having perfectly conducting walls, these modes satisfy the orthogonality condition given in equation (3.3). Furthermore, it may be shown that,

$$\int_A \underline{\vec{e}}_i \times \underline{\vec{h}}_i \cdot \vec{z}\, ds = \underline{Y}_i \tag{3.37}$$

Where the integration is performed over the cross section of the guide and $\underline{Y}_i$ is the z-directed wave admittance of the ith mode, given by,

$$\underline{Y}_i = \frac{\left(\frac{m\pi}{a}\right)^2 - \hat{\varepsilon}_r k_0^2}{j\omega\mu\underline{\gamma}_i} \tag{3.38}$$

In equation (3.38), $\hat{\varepsilon}_r$ is the relative permittivity of the material filling the guide and $\underline{\gamma}_i$ is the propagation constant of the ith mode.

Therefore, the normalization required to set the denominator of (3.17)-(3.20) to unity may be obtained from (3.37) and the condition that,

$$-\frac{\underline{h}_x}{\underline{e}_y} = \underline{Y}_i$$

The resulting normalized mode functions are,

$$\vec{\underline{e}}_i = \vec{y}\sqrt{\frac{2\varepsilon_{n_i}}{ab\underline{Y}_i}}\sin k_{xi}x\cos k_{yi}y \tag{3.39}$$

$$\vec{\underline{h}}_i = -\sqrt{\frac{2\varepsilon_{n_i}\underline{Y}_i}{ab}}\left\{\vec{x}\sin k_{xi}x\cos k_{yi}y + \vec{y}\left(\frac{k_{xi}k_{yi}}{j\omega\mu\underline{\gamma}_i\sqrt{\underline{Y}_i}}\right)\cos k_{xi}x\sin k_{yi}y\right\} \tag{3.40}$$

where,

$$k_{xi} = \frac{m_i\pi}{a} \tag{3.41}$$

$$k_{yi} = \frac{n_i\pi}{b} \tag{3.42}$$

$$\underline{\gamma}_i = \sqrt{k_{xi}^2 + k_{yi}^2 - \varepsilon_r k_0^2} \tag{3.43}$$

$$\varepsilon_{n_i} = \begin{cases} 1 & n_i = 0 \\ 2 & n_i > 0 \end{cases} \tag{3.44}$$

These mode functions are valid in all three regions providing the appropriate dimensions, transformation of coordinates and permittivity are used.

3.3.3 Calculation of Matrix Elements

The solution of the problem requires the assembly of four matrices. These matrices, $[\underline{R}]$, $[\underline{R'}]$, $[\underline{S}]$ and $[\underline{S'}]$ are defined by equations (3.21) through (3.28). Examining these definitions one realizes that,

$$[\underline{S}] = [\underline{R}]^T \tag{3.45}$$

$$[\underline{S'}] = [\underline{R'}]^T \tag{3.46}$$

where the ^{T} denotes matrix transposition. Hence, it is only necessary to construct the $[\underline{R}]$ and $[\underline{R'}]$ matrices.

Figure 3.3 illustrates the coordinates used in the derivation.

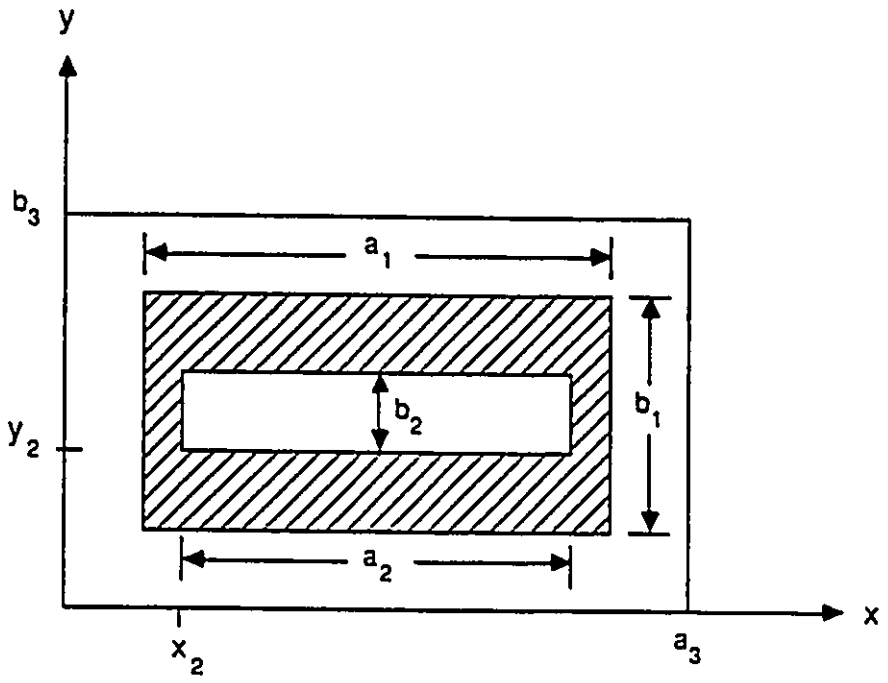

Fig. 3.3: Coordinates used in the Calculation of Matrix Elements

Using the coordinates defined in Fig. 3.3 and the eigenmodes developed in the previous section, the following expressions are obtained for the matrix elements.

$$\underline{R}_{pu} = 2\sqrt{\frac{\varepsilon_{n_u}\varepsilon_{n_p}\underline{Y}_p^{(1)}}{a_1 b_1 a_2 b_2 \underline{Y}_u^{(2)}}} \int_{x_2}^{x_2+a_2} \sin\{k_{xu}^{(2)}(x-x_2)\}\sin\{k_{xp}^{(1)}(x-x_1)\}\,dx \cdot \int_{y_2}^{y_2+b_2} \cos\{k_{yu}^{(2)}(y-y_2)\}\cos\{k_{yp}^{(1)}(y-y_1)\}\,dy \qquad (3.47)$$

$$\underline{R'}_{qu} = 2\sqrt{\frac{\varepsilon_{n_u}\varepsilon_{n_q}\underline{Y}_q^{(3)}}{a_3 b_3 a_2 b_2 \underline{Y}_u^{(2)}}} \int_{x_2}^{x_2+a_2} \sin\{k_{xu}^{(2)}(x-x_2)\}\sin\{k_{xq}^{(3)}x\}\,dx \cdot \int_{y_2}^{y_2+b_2} \cos\{k_{yu}^{(2)}(y-y_2)\}\cos\{k_{yq}^{(3)}y\}\,dy \qquad (3.48)$$

These integrals have simple analytical solutions and two FORTRAN functions are included in the computer progam for their evaluation.

3.3.4 Calculation of $\underline{\Gamma}_1$

Following assembly of the various matrices in (3.36), standard methods may be employed to solve for the amplitude coefficients of the aperture electric field.

$$[\underline{b}] = [\underline{S}\,\underline{R} + \underline{S}'\underline{R}']^{-1} \cdot 2 \cdot [\underline{S}] \cdot [\underline{a}_i^{(1)}] \tag{3.49}$$

Substitution of these coefficients into equation (3.29) yields the amplitude coefficients of the -z travelling modes in guide 1,

$$[\underline{a}_r^{(1)}] = [\underline{R}] \cdot [\underline{b}] - [\underline{a}_i^{(1)}] \tag{3.50}$$

from which the dominant mode reflection coefficient may be extracted.

$$\underline{\Gamma}_1 = \underline{a}_{r1}^{(1)} \tag{3.50}$$

3.4 Description of the Computer Program

The theory presented in this chapter has been implemented in FORTRAN and a program listing is provided in Appendix C. The program is written explicitly for capacitive slots symmetrical about $b/2$, but the formulas are valid for any rectangular aperture whose edges are parallel to the waveguide walls.

The program is interactive and prompts for the frequency of operation, the dimensions of the input and output guides, the width of the aperture, the relative permittivity of the material filling the output guide, and the number of modes to consider in each region. The matrix elements are then evaluated and the resulting system of equations is solved by Gaussian elimination [31]. The program outputs are the modal amplitudes of the electric field in the three regions.

3.5 Convergence of the Method

The mode matching method is potentially unstable due to a phenomenon known as "relative convergence" [34,35]. It has been shown that the numerical solutions may converge to incorrect values if an improper ratio is chosen between the number of modal terms retained in adjacent regions. Furthermore, an optimum ratio exists which leads to the fastest convergence. This ratio may be determined from the physical dimensions of the three regions. [36]

Once the ratio of the number of modes in each region is fixed, the total number of modes is increased until convergence is witnessed. Table 3.1 and Table 3.2 show the dependence of the computed reflection coefficient on the number of modes used for two aperture geometries: a full aperture and a 2 mm slot. In both cases the input and output guides had dimensions 22.86 x 10.16 mm and 22.86 x 10.86 cm, respectively. The frequency of operation was 10 GHz and the dielectric filling the output guide was water ($\hat{\varepsilon}_r = 60.4 - j32.3$ @ 10 GHz). Due to the symmetry of the structures, only the LSE_{1n} modes with n even were considered.

Table 3.1: Convergence of Mode Matching; Full Aperture

Open-ended Guide into Water at 10 GHz			
No. of Modes in Input Guide	No. of Modes in Aperture	No. of Mode in Output Guide	Calculated $\lvert \Gamma \rvert$
5	5	500	.8295
10	10	1000	.8288
15	15	1500	.8286
20	20	2000	.8285
25	25	2500	.8285
30	30	3000	.8284
35	35	3500	.8284

Table 3.2: Convergence of Mode Matching; 2 mm Aperture

2 mm Aperture into Water at 10 GHz			
No. of Modes in Input Guide	No. of Modes in Aperture	No. of Mode in Output Guide	Calculated $\lvert \Gamma \rvert$
5	1	500	.9631
10	2	1000	.9610
15	3	1500	.9605
20	4	2000	.9603
25	5	2500	.9602
30	6	3000	.9601
35	7	3500	.9601

Chapter 4:

Application of the Method of Moments to Open-Ended Waveguide Problems

4.1 Introduction

This chapter presents the final method employed to solve the open-ended waveguide problem. The method uses the equivalence principle [37] to divide the problem into two regions. The internal region consists of the interior of the waveguide, assumed to extend from $z = -\infty$ to $z = 0$, while the external region consists of the infinite half-space $z > 0$.

In the internal region, the aperture is modeled by a short circuit on which flows an equivalent magnetic current $\overrightarrow{M}$. This current is proportional to the actual tangential electric field in the aperture.

In the external region, the aperture is again replaced by a perfect electric conductor supporting an equivalent magnetic current $-\overrightarrow{M}$. This choice of the sign of the magnetic current ensures that the tangential electric field of the original problem is continuous across the aperture.

Imposing the condition of continuity of the tangential magnetic field across the aperture leads to an integral equation, in terms of the unknown magnetic current $\overrightarrow{M}$, which is solved via Galerkin's method.

Finally, once the magnetic current is known, other quantities of interest, such as the incident mode reflection coefficient, the aperture admittance, and the radiated fields, may be determined.

4.2 Geometry and Assumptions

The geometry considered here is shown in Fig. 4.1. An air-filled waveguide of cross-sectional dimensions $a \times b$ is terminated in the plane $z = 0$ by a metal screen containing one or more rectangular apertures. The half space $z > 0$ is filled with a homogeneous, isotropic, linear, non-magnetic dielectric having a relative permittivity given by $\hat{\varepsilon}_r = \varepsilon' - j\varepsilon''$. In addition, the following assumptions have been made:

1) The incident waveguide mode is the dominant TE_{10}.
2) Cross polarization is negligible.
3) The metal flange is large enough to be considered infinite in the transverse direction.
4) The edges of the aperture(s) are parallel to the walls of the waveguide.
5) All metal is perfectly conducting.

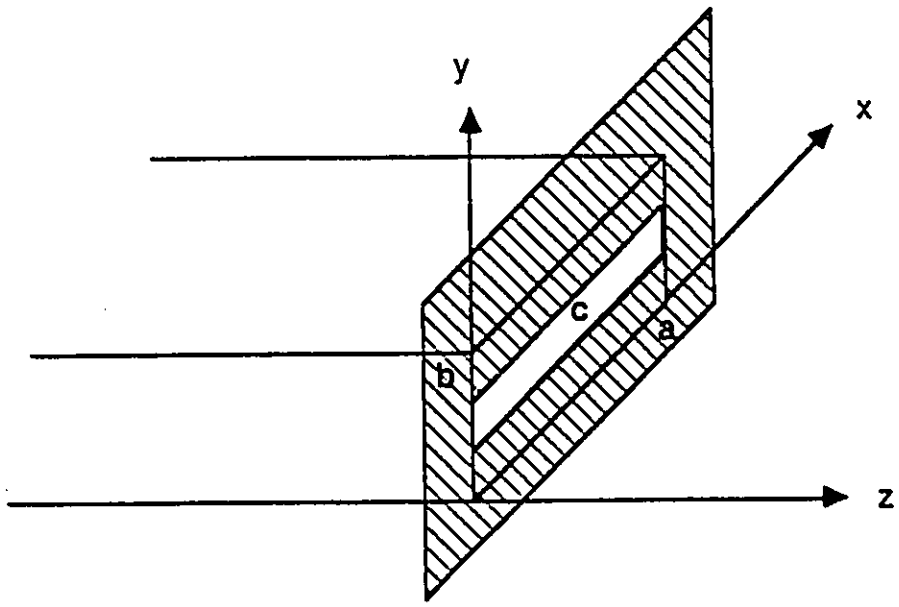

Fig. 4.1: Geometry used in the Method of Moments

4.3 Mathematical Development

4.3.1 The Operator Equation

The equivalence principle [37] is used to divide the problem into two equivalent problems as shown in Fig. 4.2. In the waveguide region, denoted R_1, the aperture is modeled by a short circuit on which flows the equivalent magnetic current,

$$\underline{\vec{M}}_1 = \vec{n}_1 \times \underline{\vec{E}}_a^1 \tag{4.1}$$

where $\vec{n}_1$ is the outward directed normal to R_1, and $\underline{\vec{E}}_a^1$ is the actual electric field in the aperture at $z = 0^-$.

Similarly, in region 2 (R_2:$z > 0$), the aperture is replaced by a perfect electric conductor supporting an equivalent magnetic current,

$$\underline{\vec{M}}_2 = \vec{n}_2 \times \underline{\vec{E}}_a^2 \tag{4.2}$$

where $\vec{n}_2$ is the outward directed normal to R_2, and $\underline{\vec{E}}_a^2$ is the actual electric field in the aperture at $z = 0^+$.

The continuity of the tangential component of the electric field across the aperture requires,

$$\underline{\vec{M}} = \underline{\vec{M}}_1 = -\underline{\vec{M}}_2 \tag{4.3}$$

The remaining boundary condition to be applied is the continuity of the tangential component of the magnetic field, $\underline{\vec{H}}_t$, across the aperture.

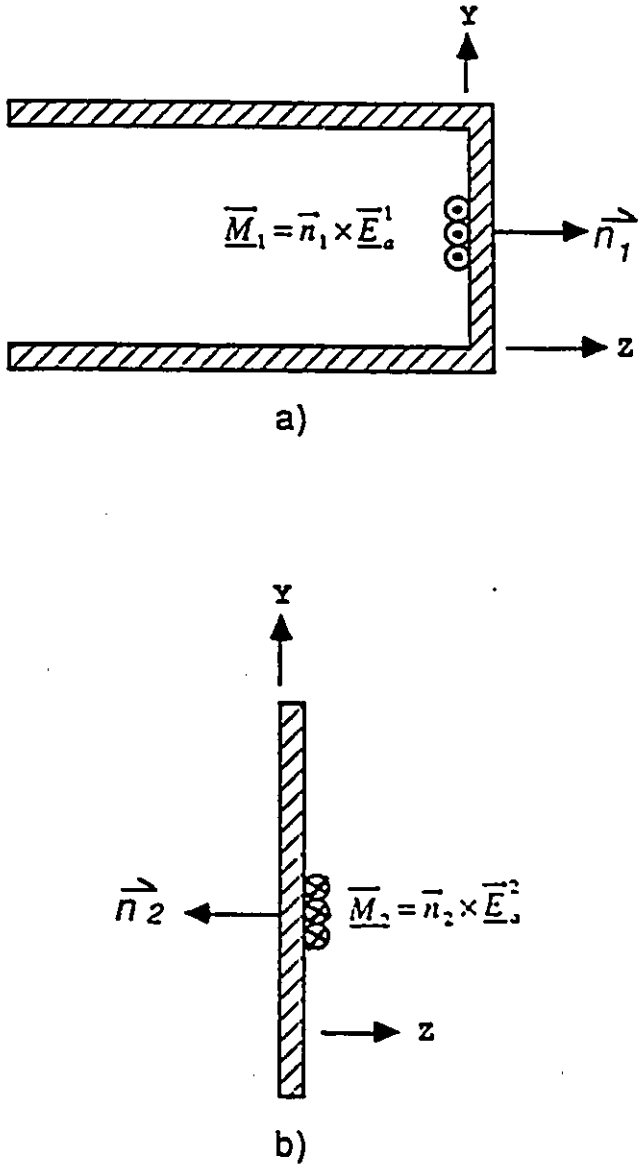

Fig. 4.2: Equivalent Magnetic Currents used in Mathematical Derivation

The tangential magnetic field at $z = 0^-$ may be expressed in terms of $\underline{\vec{M}}_1$ as,

$$\underline{\vec{H}}_t^1 = \underline{\vec{H}}_t^i + \underline{\vec{H}}_t^1(\underline{\vec{M}}_1) \tag{4.4}$$

where $\underline{\vec{H}}_t^i$ is the tangential magnetic field due to the incident waveguide mode and $\underline{\vec{H}}_t^1(\underline{\vec{M}}_1)$ is the tangential magnetic field due to the magnetic current $\underline{\vec{M}}_1$. Both of these fields are computed with the aperture covered by the perfect electric conductor.

In region 2, the magnetic field is produced by the magnetic current $\underline{\vec{M}}_2$. In operator notation,

$$\underline{\vec{H}}_t^2 = \underline{\vec{H}}_t^2(\underline{\vec{M}}_2) \tag{4.5}$$

This field is also computed in the presence of the perfect electric conductor and, hence, image theory may be applied.

Finally, imposing the continuity condition, yields,

$$-\underline{\vec{H}}_t^1(\underline{\vec{M}}) - \underline{\vec{H}}_t^2(\underline{\vec{M}}) = \underline{\vec{H}}_t^i \tag{4.6}$$

In writing (4.6) use has been made of (4.3) and the linearity of the $\underline{\vec{H}}_t$ operator.

Equation (4.6), which is in fact an integro-differential equation in $\underline{\vec{M}}$, is solved using the method of moments.

4.3.2 Galerkin's Method

Following the general method of moments, the unknown magnetic current is expressed in terms of a set of expansion functions, $\overrightarrow{M}_j$,

$$\underline{\overrightarrow{M}} = \sum_{j=1}^{N} \underline{V}_j \overrightarrow{M}_j \tag{4.7}$$

where the $\underline{V}_j$ are unknown amplitude coefficients and N is the total number of expansion functions used to approximate the magnetic current.

Substituting (4.7) into (4.6) and exploiting the linearity of the $\underline{\overrightarrow{H}}_t$ operators leads to,

$$-\sum_{j=1}^{N} \underline{V}_j \underline{\overrightarrow{H}}_t^1(\overrightarrow{M}_j) - \sum_{j=1}^{N} \underline{V}_j \underline{\overrightarrow{H}}_t^2(\overrightarrow{M}_j) = \underline{\overrightarrow{H}}_t^i \tag{4.8}$$

Next, define the symmetric product,

$$\langle \underline{\overrightarrow{A}}, \underline{\overrightarrow{B}} \rangle = \int_{Aperr.} \underline{\overrightarrow{A}} \cdot \underline{\overrightarrow{B}}\, dS \tag{4.9}$$

and choose as weighting functions the set of expansion functions (Galerkin's method),

$$\overrightarrow{W}_i = \overrightarrow{M}_i \qquad i = 1,2,3,\ldots,N$$

Finally, taking the symmetric product of (4.8) with each of the weighting functions, one obtains the following set of equations,

$$-\sum_{j=1}^{N} \underline{V}_j \langle \overrightarrow{M}_i, \underline{\overrightarrow{H}}_t^1(\overrightarrow{M}_j) \rangle - \sum_{j=1}^{N} \underline{V}_j \langle \overrightarrow{M}_i, \underline{\overrightarrow{H}}_t^2(\overrightarrow{M}_j) \rangle = \langle \overrightarrow{M}_i, \underline{\overrightarrow{H}}_t^i \rangle \qquad i = 1,2,3,\ldots,N \tag{4.10}$$

Equation (4.10) may be cast in matrix notation as,

$$[\underline{Y}^1 + \underline{Y}^2] \cdot [\underline{V}] = [\underline{I}] \tag{4.11}$$

Comparing (4.11) and (4.10), one identifies the following terms:

The generalized aperture admittance matrix seen from the waveguide side,

$$\underline{Y}^1_{ij} = -\langle \vec{M}_i, \underline{\vec{H}}^1_t(\vec{M}_j) \rangle \qquad \begin{cases} i = 1,2,\ldots,N \\ j = 1,2,\ldots,N \end{cases} \tag{4.12}$$

The generalized aperture admittance matrix seen from the half-space region,

$$\underline{Y}^2_{ij} = -\langle \vec{M}_i, \underline{\vec{H}}^2_t(\vec{M}_j) \rangle \qquad \begin{cases} i = 1,2,\ldots,N \\ j = 1,2,\ldots,N \end{cases} \tag{4.13}$$

The source vector,

$$\underline{I}_i = \langle \vec{M}_i, \underline{\vec{H}}^i_t \rangle \qquad i = 1,2,\ldots,N \tag{4.14}$$

and the coefficient vector,

$$\underline{V}_j \qquad j = 1,2,\ldots,N$$

The solution of (4.11) for the coefficients $\underline{V}_j$ gives $\underline{\vec{M}}$ according to (4.7).

4.3.3 The Expansion functions

For this particular study the method of subsectional bases is used. The aperture is divided into rectangular subareas of length $2\Delta x_j$ in the x direction and length Δy_j in the y direction. On each subsection, the magnetic current is approximated by "tent" functions, composed of triangles in the direction of current flow and pulses in the direction perpendicular to the current flow. Furthermore, following assumptions (1) and (2) there is no y-component of the magnetic current. This leads to the following definition of the expansion functions:

$$\overrightarrow{M_j} = \vec{x} T_j(x) P_j(y) \qquad j = 1,2,\ldots,N \tag{4.15}$$

where the $T_j(x)$ are triangle functions given by,

$$T_j(x) = \begin{cases} \dfrac{x - x_{j-1}}{\Delta x_j} & x_{j-1} \le x \le x_j \\ \dfrac{x_{j+1} - x}{\Delta x_j} & x_j \le x \le x_{j+1} \\ 0 & |x - x_j| > \Delta x_j \end{cases} \tag{4.16}$$

$$\textit{where} \qquad \Delta x_j = x_{j+1} - x_j = x_j - x_{j-1} \tag{4.17}$$

and the $P_j(y)$ are pulse functions given by,

$$P_j(y) = \begin{cases} 1 & y_{j-1} \le y \le y_j \\ 0 & \textit{elsewhere} \end{cases} \tag{4.18}$$

$$\textit{where} \qquad \Delta y_j = y_j - y_{j-1} \tag{4.19}$$

A typical subsection is shown in Fig. 4.3 with the various coordinates defined. This choice of expansion functions leads to a piecewise linear approximation to the x-variation of the magnetic current and a step approximation to the y-variation of the magnetic current.

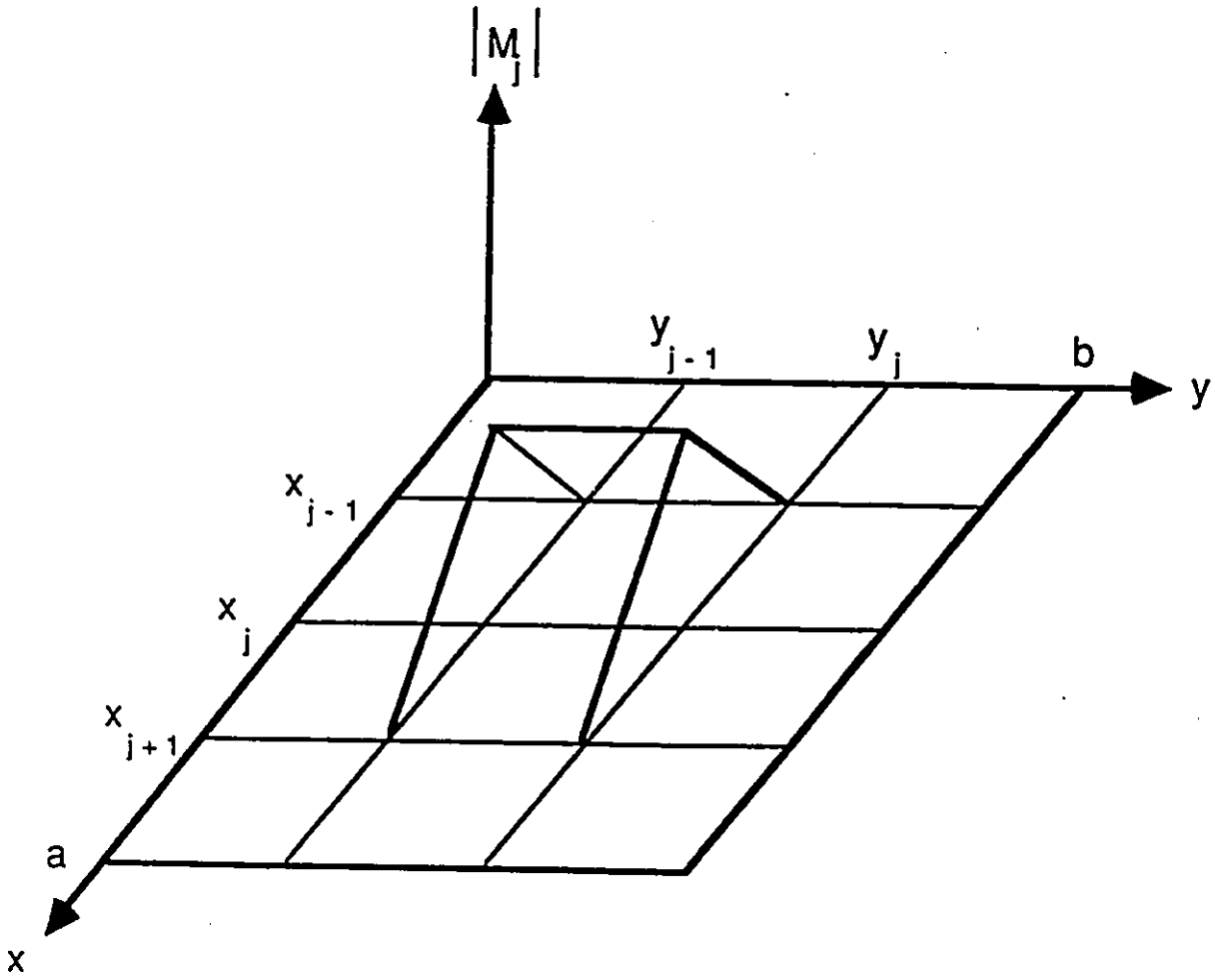

Fig. 4.3: A Typical Expansion Function

4.3.4 Calculation of $[\underline{Y}^1]$ and $[\underline{I}]$

The total transverse field (x-, and y-components) inside the guide may be written in terms of transverse mode functions as,

$$\underline{\vec{E}}_t = \underline{\vec{e}}_1 e^{-\underline{\gamma}_1 z} + \sum_{k=1}^{\infty} \underline{\Gamma}_k \underline{\vec{e}}_k e^{\underline{\gamma}_k z} \tag{4.20}$$

$$\underline{\vec{H}}_t = \underline{\vec{h}}_1 e^{-\underline{\gamma}_1 z} - \sum_{k=1}^{\infty} \underline{\Gamma}_k \underline{\vec{h}}_k e^{\underline{\gamma}_k z} \tag{4.21}$$

Here the $\underline{\gamma}_k$ represent the modal propagation constants defined by,

$$\underline{\gamma}_k = \begin{cases} jk_0\sqrt{1-\left(\dfrac{f_k}{f}\right)^2} & f > f_k \\ k_k\sqrt{1-\left(\dfrac{f}{f_k}\right)^2} & f < f_k \end{cases} \tag{4.22}$$

where k_0 is the free space wave number, f is the frequency of operation, and k_k and f_k are the cutoff wavenumber and the cutoff frequency of the kth mode, respectively. Similarly, $\underline{\Gamma}_k$ is the complex amplitude coefficient of the -z travelling component of the kth mode. In particular, the index 1 refers to the incident mode, assumed to be the dominant mode with unit amplitude.

Due to assumptions (1) and (2), there is no x-component of the electric field present inside the guide. For this reason a suitable mode set is the LSE_{mn} (TE^x) mode set, for which the transverse mode functions are [33],

$$\underline{\vec{e}}_k = \vec{y}\sqrt{\frac{2\varepsilon_n}{ab}}\sin\frac{m\pi x}{a}\cos\frac{n\pi y}{b} \tag{4.23}$$

$$\underline{\vec{h}}_k = -\sqrt{\frac{2\varepsilon_n}{ab}}\left\{\vec{x}\,\underline{Y}_k\sin\frac{m\pi x}{a}\cos\frac{n\pi y}{b} + \vec{y}\left(\frac{mn\pi^2}{j\omega\mu_0 ab\underline{\gamma}_k}\right)\cos\frac{m\pi x}{a}\sin\frac{n\pi y}{b}\right\} \tag{4.24}$$

The various quantities appearing in these two equations are:

The z-directed wave admittance,

$$\underline{Y}_k = \frac{\left(\frac{m\pi}{a}\right)^2 - k_0^2}{j\omega\mu_0\underline{\gamma}_k} \tag{4.25}$$

and the Neumann factor,

$$\varepsilon_n = \begin{cases} 1 & n = 0 \\ 2 & n > 0 \end{cases} \tag{4.26}$$

These mode functions are orthogonal [33] and have been normalized such that,

$$\int_{guide} \underline{\vec{e}}_m \cdot \underline{\vec{e}}_n \, ds = \begin{cases} 1 & n = m \\ 0 & n \neq m \end{cases} \tag{4.27}$$

Where the integration is performed over the cross section of the waveguide.

The transverse fields due to the magnetic current $\overrightarrow{M_j}$ are similar to (4.20) and (4.21), except that the incident mode is not present. Hence, this field is,

$$\overrightarrow{\underline{E}_t}(\overrightarrow{M_j}) = \sum_{k=1}^{\infty} \underline{A}_{jk} \overrightarrow{\underline{e}}_k e^{\underline{\gamma}_k z} \tag{4.28}$$

$$\overrightarrow{\underline{H}_t}(\overrightarrow{M_j}) = -\sum_{k=1}^{\infty} \underline{A}_{jk} \overrightarrow{\underline{h}}_k e^{\underline{\gamma}_k z} \tag{4.29}$$

where the $\underline{A}_{ij}$ are the modal amplitudes.

Now, at z=0, equation (4.1) must hold. Therefore,

$$\overrightarrow{M_j} = \sum_{k=1}^{\infty} \underline{A}_{jk} (\vec{z} \times \overrightarrow{\underline{e}}_k) \tag{4.30}$$

Taking the symmetric product of (4.30) with $(\vec{z} \times \overrightarrow{\underline{e}}_l)$ yields,

$$\int_{guide} \overrightarrow{M_j} \cdot (\vec{z} \times \overrightarrow{\underline{e}}_l) ds = \sum_{k=1}^{\infty} \underline{A}_{jk} \int_{guide} (\vec{z} \times \overrightarrow{\underline{e}}_k) \cdot (\vec{z} \times \overrightarrow{\underline{e}}_l) ds \tag{4.31}$$

where the integration is performed over the cross section of the guide. However, due to the orthogonality of the mode functions, (4.27), all the terms of (4.31) vanish except for the term l=k from which:

$$\underline{A}_{jk} = \int_{Apert.} \overrightarrow{M_j} \cdot (\vec{z} \times \overrightarrow{\underline{e}}_k) ds \tag{4.32}$$

Note that the integration over the guide cross section is replaced by an integration over the aperture, since $\overrightarrow{M_j}$ is non-zero only on the aperture.

Substitution of (4.29) into (4.12) gives

$$\underline{Y}_{ij}^{1} = \int_{Apert.} \overrightarrow{M}_i \sum_{k=1}^{\infty} \underline{A}_{jk} \overrightarrow{\underline{h}}_k \, ds$$

$$= \sum_{k=1}^{\infty} \underline{A}_{jk} \int_{Apert.} \overrightarrow{M}_i \cdot \overrightarrow{\underline{h}}_k \, ds \tag{4.33}$$

In this last equation, only the x-component of $\overrightarrow{\underline{h}}_k$ contributes to the integration. Furthermore, inspection of (4.23) and (4.24) reveals the following relationship,

$$\vec{x} \cdot \overrightarrow{\underline{h}}_k = \underline{Y}_k \vec{x} \cdot (\vec{z} \times \overrightarrow{\underline{e}}_k) \tag{4.34}$$

Hence, (4.33) may be recast in terms of $\overrightarrow{\underline{e}}_k$ as,

$$\underline{Y}_{ij}^{1} = \sum_{k=1}^{\infty} \underline{A}_{jk} \underline{Y}_k \int_{Apert.} \overrightarrow{M}_i \cdot (\vec{z} \times \overrightarrow{\underline{e}}_k) \, ds \tag{4.35}$$

Finally, the integration in (4.35) may be replaced by (4.32) to yield the more compact form,

$$\underline{Y}_{ij}^{1} = \sum_{k=1}^{\infty} \underline{A}_{jk} \underline{Y}_k \underline{A}_{ik} \tag{4.36}$$

For computational purposes the series in (4.36) is truncated to NM modes.

Next the source vector, $[I]$ is evaluated. The incident magnetic field is given by the first term of (4.21). When the aperture is covered by the electric conductor the guide is short circuited. According to image theory, the tangential magnetic field at z=0 is just twice the incident wave. i.e.

$$\overrightarrow{\underline{H}}_t^i = 2\overrightarrow{\underline{h}}_1 \tag{4.37}$$

Using (4.37) in (4.14) leads to the following expression for the source vector

$$\underline{I}_i = 2 \int_{Apert.} \overrightarrow{M}_i \cdot \overrightarrow{\underline{h}}_1 \, ds \tag{4.38}$$

The same considerations used to arrive at (4.36) may be used to rewrite this equation in terms of $\overrightarrow{\underline{e}}_1$ as,

$$\underline{I}_i = 2\underline{Y}_1 \int_{Apert.} \overrightarrow{M}_i \cdot (\overrightarrow{z} \times \overrightarrow{\underline{e}}_1) \, ds$$

$$= 2\underline{Y}_1 \underline{A}_{i1} \tag{4.39}$$

4.3.5 Calculation of $[\underline{Y}^2]$

From (4.13),

$$\underline{Y}_{ij}^2 = -\langle \vec{M}_i, \underline{\vec{H}}_t^2(\vec{M}_j) \rangle$$

where $\underline{\vec{H}}_t^2$ is the magnetic field at $z=0^+$ due to the magnetic current $\vec{M}_j$ flowing in front of the conductor. Applying image theory,

$$\underline{\vec{H}}_t^2(\vec{M}_j) = -j\omega \underline{\vec{F}}(2\vec{M}_j) - \nabla \underline{\psi}(2\vec{M}_j) \tag{4.40}$$

where $\underline{\vec{F}}$ is the electric vector potential and $\underline{\psi}$ is the magnetic scalar potential.

These quantities may be computed from the following potential integrals:

$$\underline{\vec{F}}(2\vec{M}_j) = 2\underline{\vec{F}}(\vec{M}_j) = 2\frac{\underline{\varepsilon}}{4\pi} \int_{Apert.} \vec{M}_j \frac{e^{-j\underline{k}|\vec{r}-\vec{r}'|}}{|\vec{r}-\vec{r}'|} ds' \tag{4.41}$$

$$\underline{\psi}(2\vec{M}_j) = 2\underline{\psi}(\vec{M}_j) = 2\frac{1}{4\pi\mu_0} \int_{Apert.} \underline{m}_j \frac{e^{-j\underline{k}|\vec{r}-\vec{r}'|}}{|\vec{r}-\vec{r}'|} ds' \tag{4.42}$$

where $\underline{\varepsilon} = \varepsilon_0 \hat{\varepsilon}_r$ is the complex permittivity of the material filling the half space, $\underline{k}$ is the complex wavenumber in this material, $|\vec{r}-\vec{r}'|$ is the distance between the source point (primed coordinates) and the field point (unprimed coordinates) and $\underline{m}_j$ is the magnetic charge density.

The equivalent magnetic charge density is related to the magnetic current density through the equation of continuity,

$$\underline{m}_j = -\frac{\nabla \cdot \vec{M}_j}{j\omega} \tag{4.43}$$

Substitution of (4.40) into (4.13) gives,

$$\underline{Y}^2_{ij} = 2 \int_{Apert.} \vec{M}_i \cdot \left(j\omega \vec{\underline{F}}_j + \nabla \underline{\Psi}_j \right) ds$$

$$= 2j\omega \int_{Apert.} \vec{M}_i \cdot \vec{\underline{F}}_j \, ds + 2 \int_{Apert.} \vec{M}_j \cdot \nabla \underline{\Psi}_j \, ds \qquad (4.44)$$

The second integral in (4.44) may be simplified as follows. A vector identity and the divergence theorem are used to write,

$$\int_{Apert.} \vec{M}_i \cdot \nabla \underline{\Psi}_j \, ds = \oint_C \underline{\Psi}_j \vec{M}_i \cdot \vec{n} \, dl - \int_{Apert.} \underline{\Psi}_j \nabla \cdot \vec{M}_i \, ds \qquad (4.45)$$

where the contour C corresponds to the perimeter of the aperture. Under assumption (4) [p. 43] this line integral vanishes, since

$$\vec{M}_i \cdot \vec{n} = 0 \qquad on \quad C \qquad (4.46)$$

Under these conditions (4.44) becomes,

$$\underline{Y}^2_{ij} = 2j\omega \int_{Apert.} \left(\vec{M}_i \cdot \vec{\underline{F}}_j + \underline{\Psi}_j \underline{m}_i \right) ds \qquad (4.47)$$

The mathematical details for the evaluation of (4.47) are given in Appendix A.

The total aperture admittance matrix may now be assembled according to (4.11) and the resulting system solved for the unknown coeficients.

$$[V] = [\underline{Y}^1 + \underline{Y}^2]^{-1} \cdot [\underline{I}] \qquad (4.48)$$

Once these coefficients are found, $\vec{\underline{M}}$ is obtained from equation (4.7).

4.3.6 Calculation of $\underline{\Gamma}_1$

The quantity of prime interest in this study is the dominant mode reflection coefficient, $\underline{\Gamma}_1$. Combining equations (4.20) and (4.1) allows one to write,

$$\underline{\vec{M}} = \vec{z} \times \underline{\vec{E}}_t|_{z=0} = \vec{z} \times \underline{\vec{e}}_1 + \sum_{k=1}^{M} \underline{\Gamma}_k (\vec{z} \times \underline{\vec{e}}_k) \tag{4.49}$$

Multiply this equation by $(\vec{z} \times \underline{\vec{e}}_l)$ and integrate over the guide cross section. Due to the orthogonality relationship (4.27) all the terms in the summation vanish except the term l=k, for which

$$\int_{guide} \underline{\vec{M}} \cdot (\vec{z} \times \underline{\vec{e}}_k) ds = \begin{cases} 1 + \underline{\Gamma}_1 & k = 1 \\ \underline{\Gamma}_k & k \neq 1 \end{cases} \tag{4.50}$$

Next, substitute equation (4.7) into (4.50) to obtain,

$$\sum_{j=1}^{N} \underline{V}_j \int_{guide} \vec{M}_j \cdot (\vec{z} \times \underline{\vec{e}}_k) ds = \begin{cases} 1 + \underline{\Gamma}_1 & k = 1 \\ \underline{\Gamma}_k & k \neq 1 \end{cases} \tag{4.51}$$

Finally, (4.32) may be used to replace the integral in (4.51) yielding the expression used to calculate the reflection coefficients.

$$\sum_{j=1}^{N} \underline{V}_j \underline{A}_{jk} = \begin{cases} 1 + \underline{\Gamma}_1 & k = 1 \\ \underline{\Gamma}_k & k \neq 1 \end{cases} \tag{4.52}$$

4.4 Description of the Computer Program

A FORTRAN program developed to analyze the modified open-ended waveguide structure via the method of moments is included in Appendix D. The program is interactive and may be divided into four major sections: initialization, discretization, matrix assembly, and solution of the system of equations.

In the first section, the various parameters defining the problem are initialized. These include the frequency of operation, the permittivity of the half-space, the dimensions of the guide, and the number of waveguide modes to consider.

The discretization of the aperture is performed by the subroutine GRID. The aperture geometry is defined interactively in terms of rectangular sub-patches and the number of expansion functions desired is entered. This approach is very versatile, allowing one to analyze a large class of aperture geometries. Any aperture which is composed of rectangular sub-patches, such as L-shaped, T-shaped, etc., can be treated. Multiple apertures are also possible.

The matrix assembly is performed by the subroutines YWG and YHS, which initialize the generalized admittance matrices of the waveguide and half-space regions, respectively. The excitation vector, $[\underline{I}]$, is also initialized in the subprogram YWG.

The resulting system of equations is solved by the LINPACK [31] subroutines ZGECO and ZGESL, yielding the amplitude coefficients of the magnetic current. This information is then used to calculate the modal amplitudes of the reflected waveguide modes and the aperture admittance seen by the dominant mode.

4.5 Convergence of the Method

Convergence of the method of moments is governed by three parameters: the number of waveguide modes retained, the number of expansion functions used in the x-direction, and the number of expansion functions used in the y-direction. When the aperture consists of a symmetrical capacitive slot, the experience gained from the mode matching analysis may be used to fix the number of modes. Twenty-five $\tilde{\text{L}}\text{SE}_{1n}$ modes, with n even were used. (cf. Table 3.2)

The effect of varying the number of expansion functions on the computed reflection coefficient is illustrated in Fig. 4.4 and Fig. 4.5. These results are for transmission from X-band guide into water at 10 GHz, for the case of a full aperture and a 2 mm aperture. There are four curves per figure, each corresponding to a fixed number of expansion functions in the x-direction. The number of expansion functions used in the y-direction varied from 5 to 15. The total number of unknowns was computed according to $N = (n_x - 1) \cdot n_y$.

Fig. 4.4: Convergence of MOM
Open–end Radiating into Water

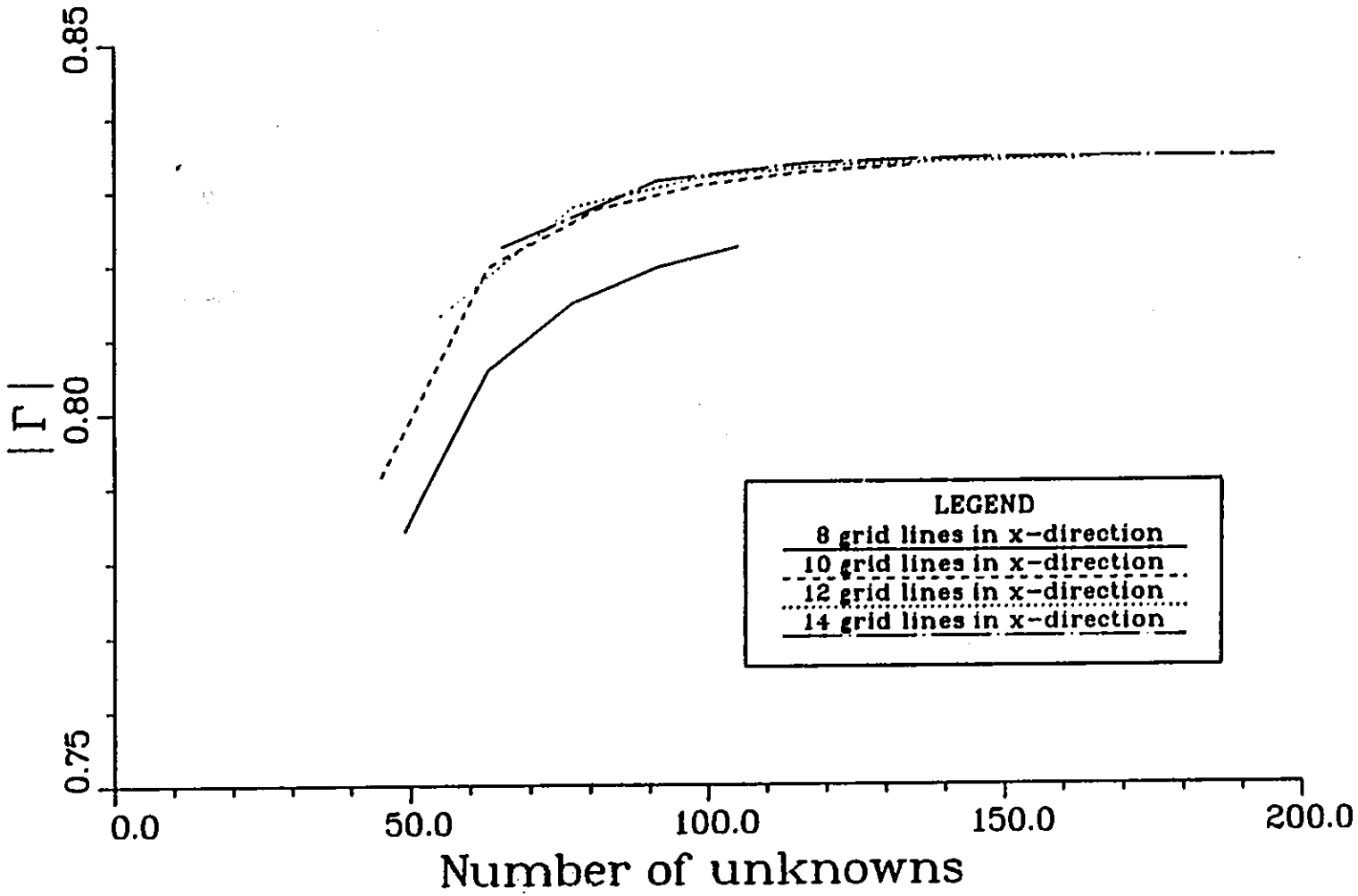

Fig. 4.4: Convergence of MOM
Open–end Radiating into Water

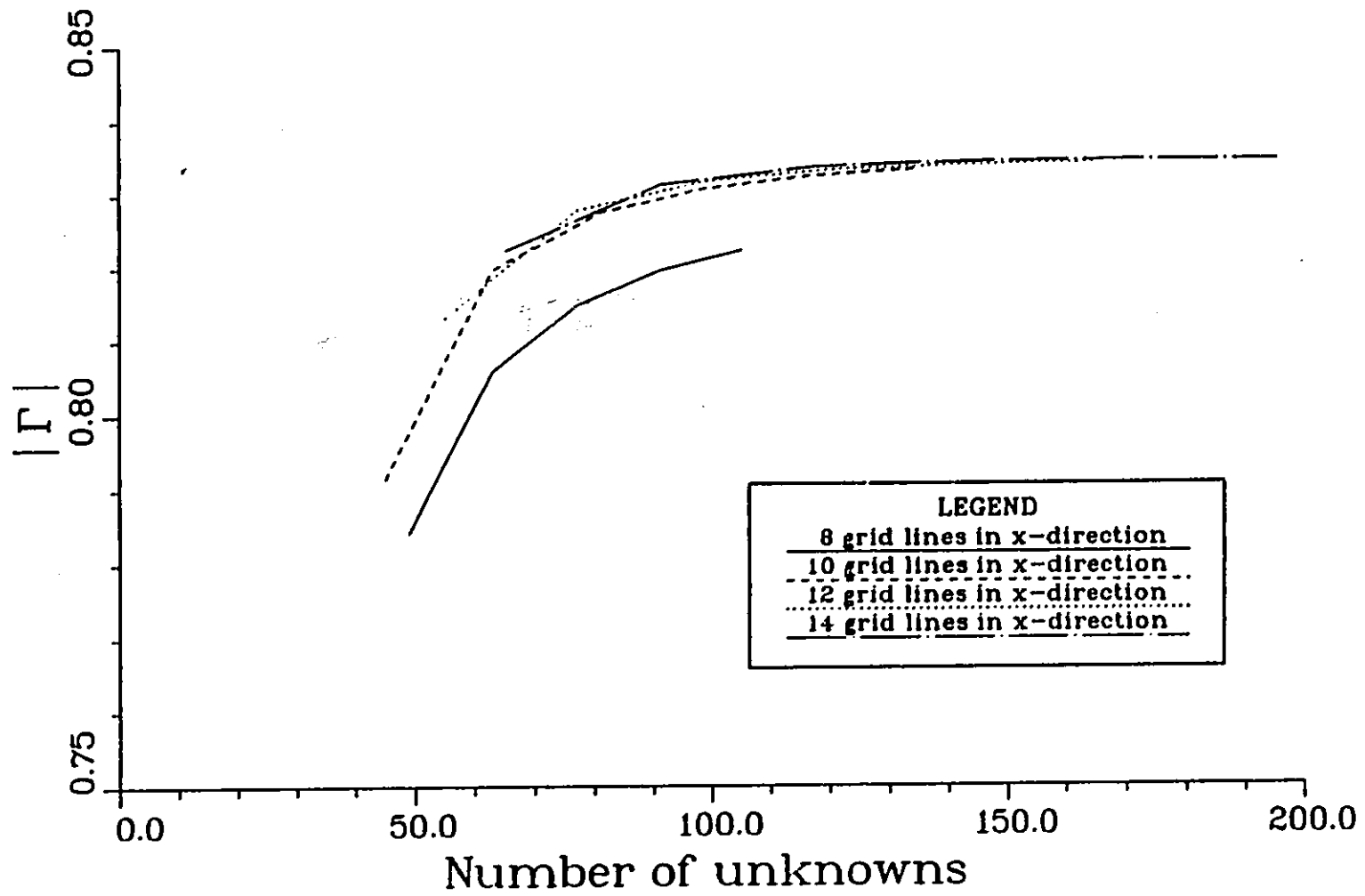

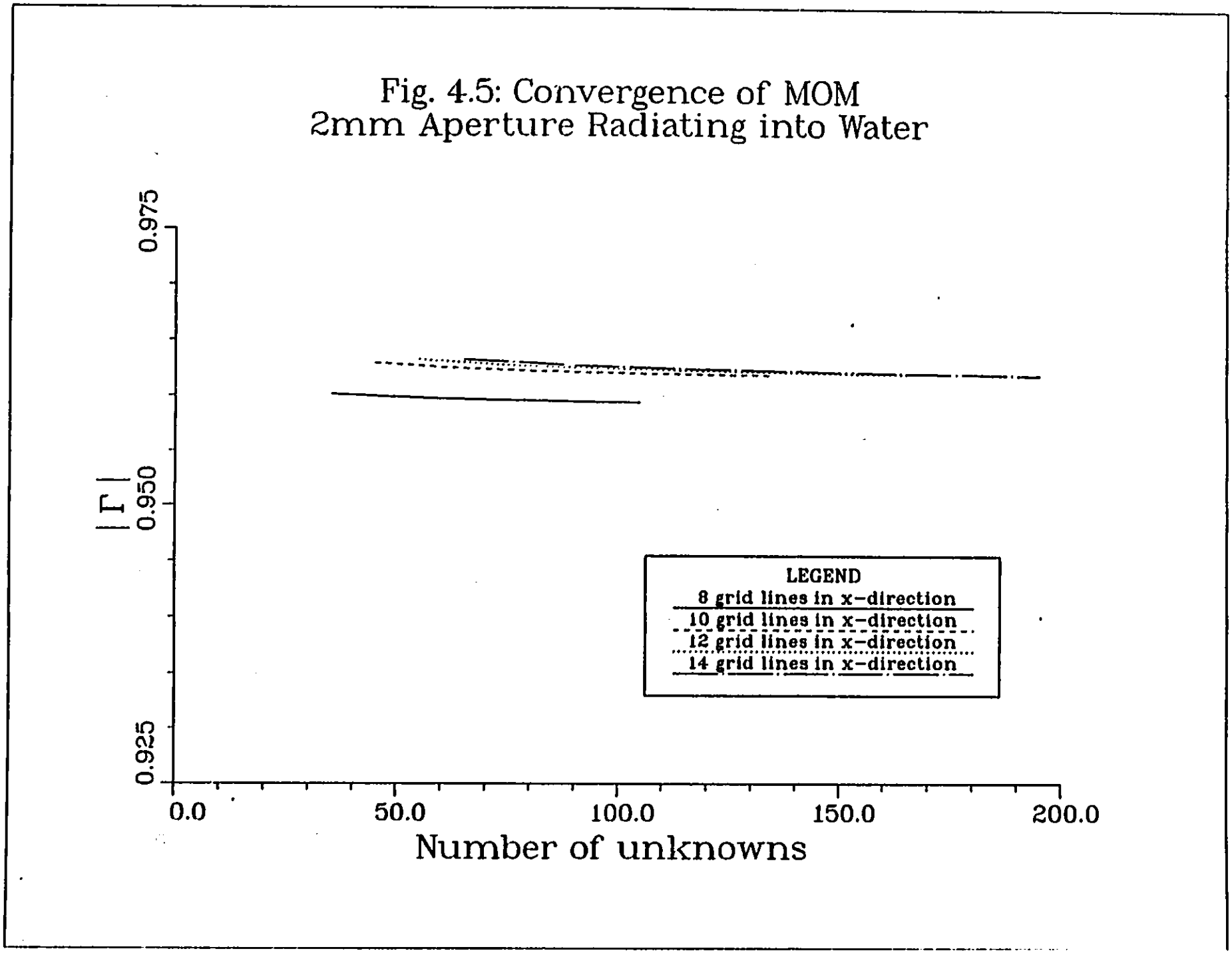
Fig. 4.5: Convergence of MOM
2mm Aperture Radiating into Water
0.975
0.950
0.925
|Γ|
0.0
50.0
100.0
150.0
200.0
Number of unknowns
LEGEND
8 grid lines in x-direction
10 grid lines in x-direction
12 grid lines in x-direction
14 grid lines in x-direction

Table 5.1: Calculated Permittivity of Water and Methanol at 20°C

Frequency [GHz]	$\hat{\varepsilon}$, of Water	$\hat{\varepsilon}$, of Methanol
8.5	64.6-j29.7	8.2-j9.2
9.0	63.2-j30.7	7.9-j8.8
9.5	61.8-j31.5	7.6-j8.4
10.0	60.4-j32.3	7.4-j8.1
10.5	59.0-j33.0	7.1-j7.8
11.0	57.6-j33.7	6.9-j7.5
11.5	56.2-j34.3	6.8-j7.3

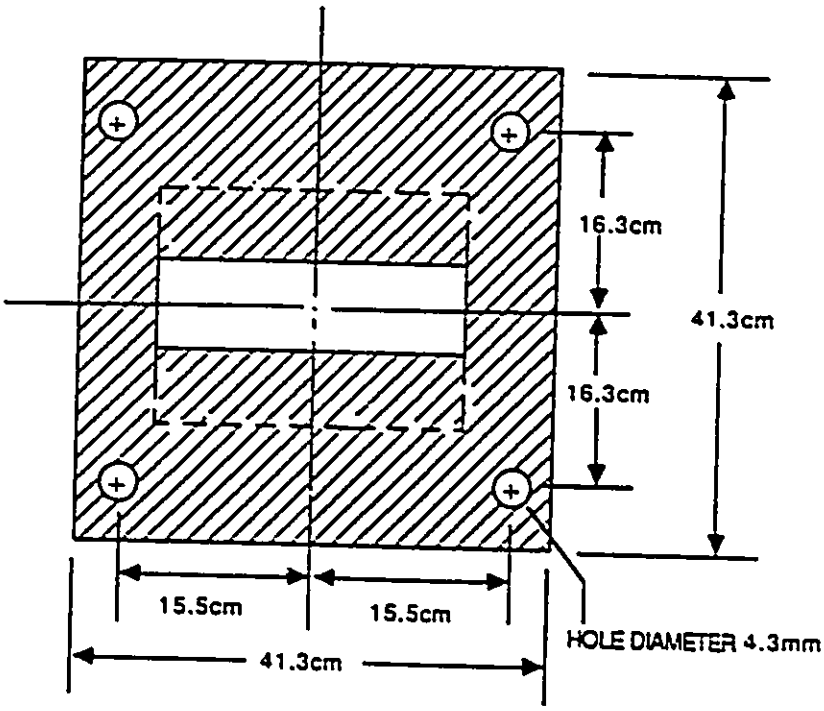

Fig. 5.1: The Experimental Sensor

5.2 Experimental Arrangement

An automated network analyzer operating in the frequency range 8.5 - 11.5 GHz has been used for the measurement of the structure reflection coefficient. A block diagram of this system is given in Fig. 5.2.

The analyzer consists of an HP8410B network analyzer, an HP8743A reflection/transmission test set, an HP8620C RF signal source, an HP8412 rectilinear display, and an HP8414 polar display. The system also incorporates a source phase-lock subsystem, consisting of the HP8656A synthesized signal generator and the HP8709A synchronizer, which provides increased frequency accuracy and repeatability. All these instruments are controlled by an IBM PC interfaced through the IEEE-488 GPIB.

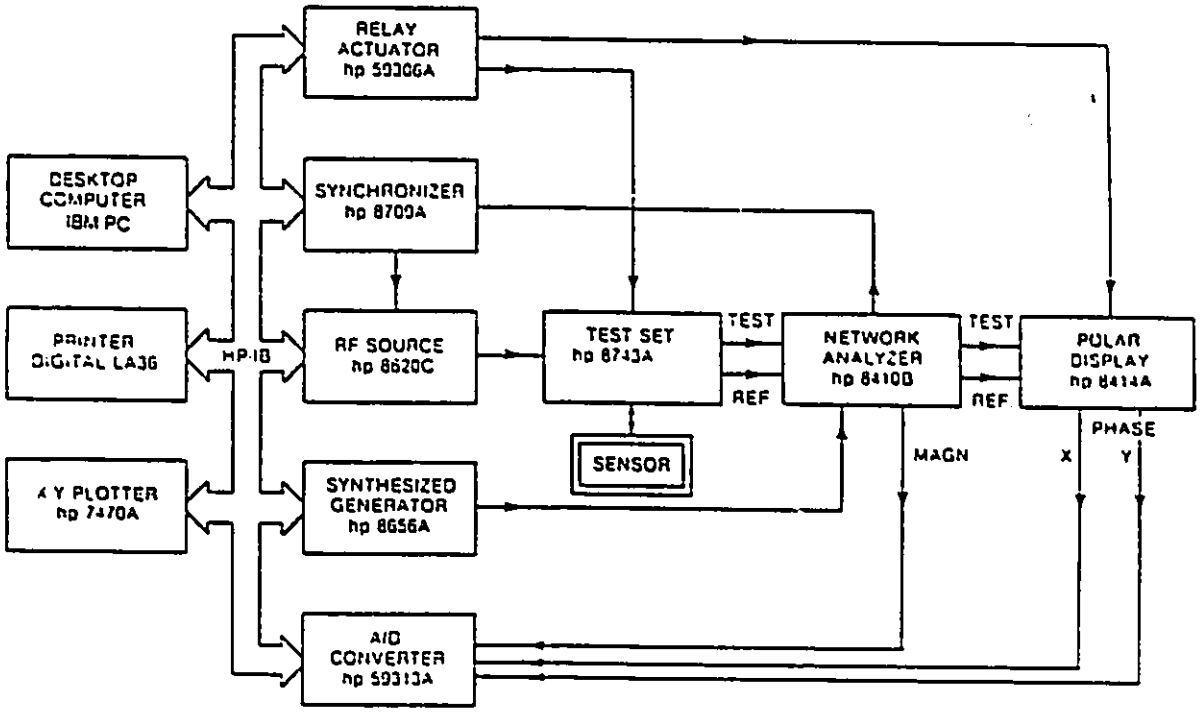

Fig. 5.2: Block Diagram of Measurement System

Operation in waveguide is accomplished by using a waveguide adapter. A Maury Microwave model X209D2 APC-7-to-waveguide transition connects a section of X-band waveguide to the test port of the HP8743 test set. This arrangement prevents high-order mode coupling between the aperture and the waveguide adapter. Figure 5.3 illustrates this setup and indicates the reference plane A-A used for calibration.

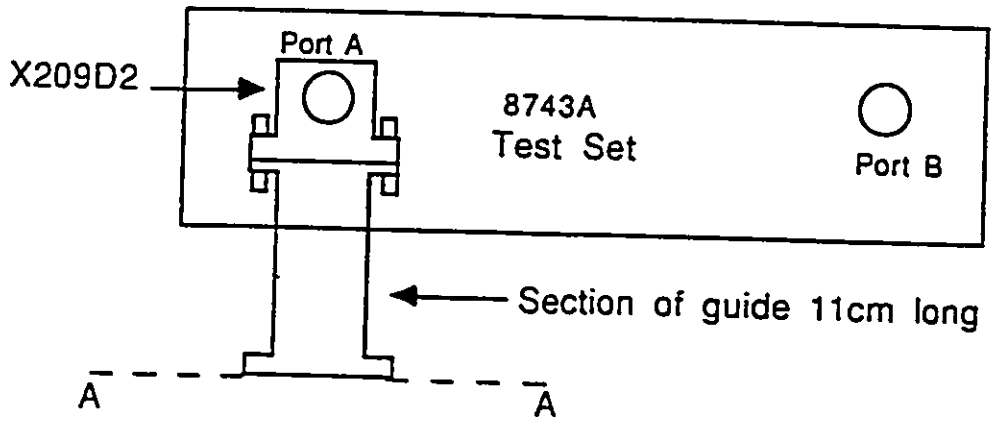

Fig. 5.3: Reference Plane for Reflection Measurements

Calibration of the network analyzer for reflection measurements is the most important part of the measurement procedure. A computer program was written which uses a three term accuracy enhancement algorithm to remove directivity, source match, and frequency response errors [42]. The method uses the expected and measured responses of three calibration terminations to quantify these systemaic errors at each frequency point. The terminations used for calibration were an HPX914A moving load, and two short circuits (HPX923A), one at the reference plane

and one offset from the reference plane by 0.99 cm ($\lambda_g/2$ @ 10GHz). During the measurement sequence, the network analyzer is tuned back to each calibration frequency, the sensors response is measured and an error correction computation is performed.

Three sensors were manufactured according to the specifications given is Fig. 5.1. A thin metal foil (thickness 0.2 mm) containing the aperture was soldered to a waveguide spacer. The spacer had the outside dimensions of a standard UG-135/U waveguide flange, the inside dimensions of WR90 waveguide and a thickness of 0.99 cm. The four threaded holes provided a means of attaching the sensor to the test port waveguide.

Following calibration, the sensor was attached to the test port and Saran Wrap was streched over the aperture to prevent liquid from entering the guide. The sensor was immersed in the dielectric, either water or methanol, and the reflection coeffiecient was measured. The transformation from the measurement plane to the aperture plane was performed mathematically according to the formula:

$$\underline{\Gamma}_{ap} = \underline{\Gamma}_{A} e^{2j\beta d} \tag{5.1}$$

where: $\underline{\Gamma}_{ap}$ is the reflection coefficient in the plane of the aperture,

$\underline{\Gamma}_{A}$ is the measured reflection coefficient in the plane A-A,

β is the dominant mode propogation constant in the guide, and

d is the thickness of the spacer.

5.3 Results

For brevity, the results for two representative cases are presented: the full aperture, and the 2 mm slot. Figures 5.4 and 5.5 show the reflection coefficient at the plane of the aperture vs. frequency for the full aperture radiating into water and methanol, respectively. The curves represent the computed values while the points correspond to measured quantities. Figures 5.6 and 5.7 are similar plots for the 2 mm aperture. In all cases there is good agreement between experiment and theory, except for the shift in the measured values for the 2mm aperture. Estimated uncertainties in the measured reflection coefficient are ± 0.05 *dB* and $\pm 0.2°$ for phase. No attempt has been made to determine the error in the computed values.

Since the objective of this work was to minimize the uncertainty in the measurement of material properties, it is instructive to examine the change in the reflection coefficient resulting from a change in the permittivity of the material. This may be done on Fig. 5.8, which shows the calculated reflection coefficient of the sensor in contact with water and methanol for the full aperture (solid lines) and the 2 mm slot (dashed lines). These curves were obtained by the method of moments.

Fig. 5.5: Reflection Coefficient
of Open–Ended Guide
Radiating into Methanol

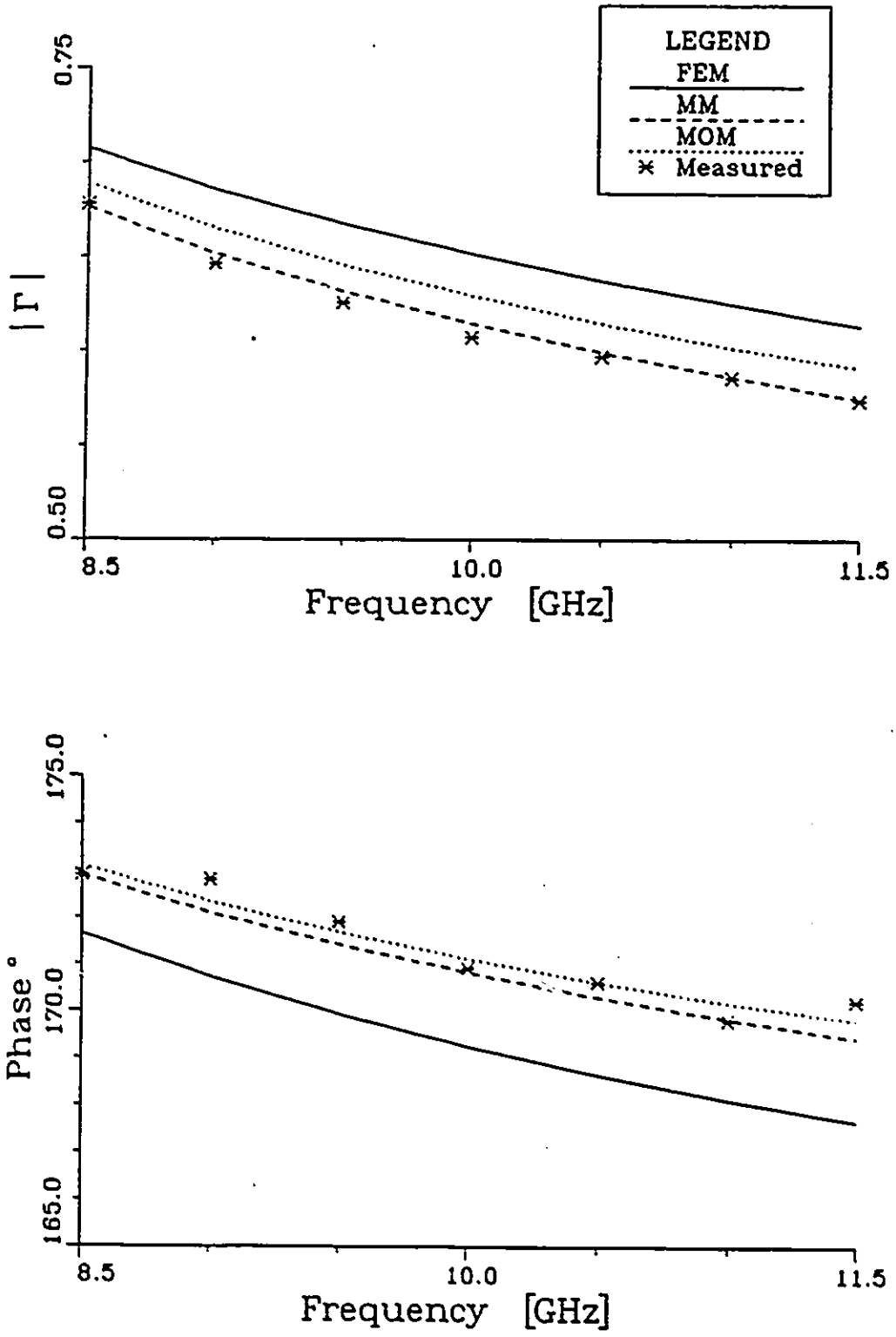

Fig. 5.6: Reflection Coefficient
of 2mm Aperture
Radiating into Water

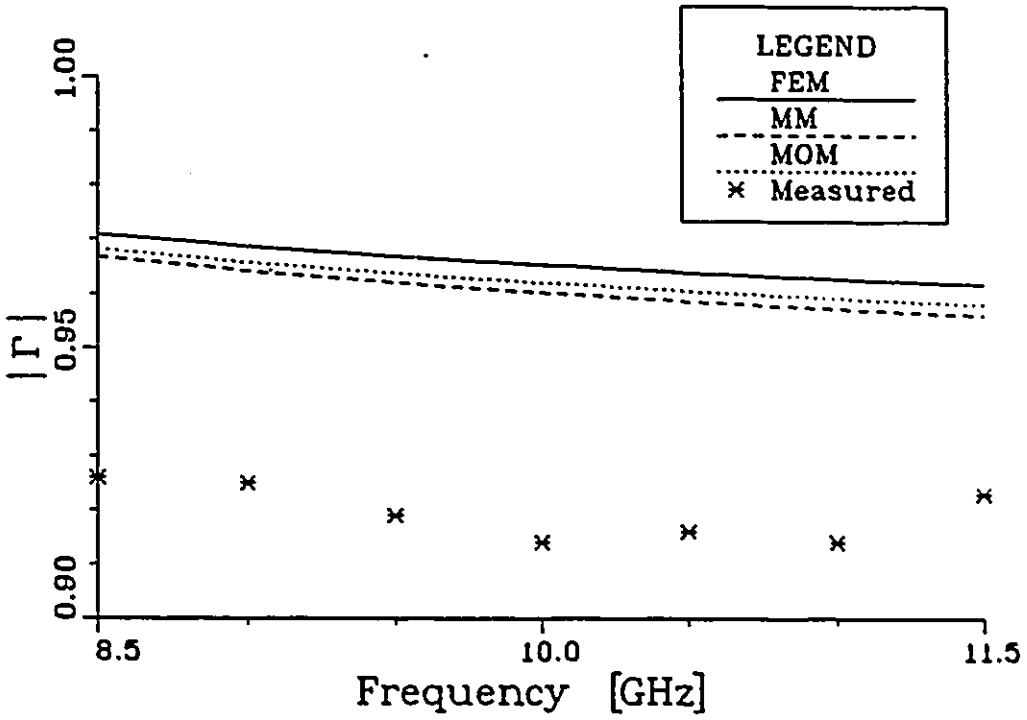

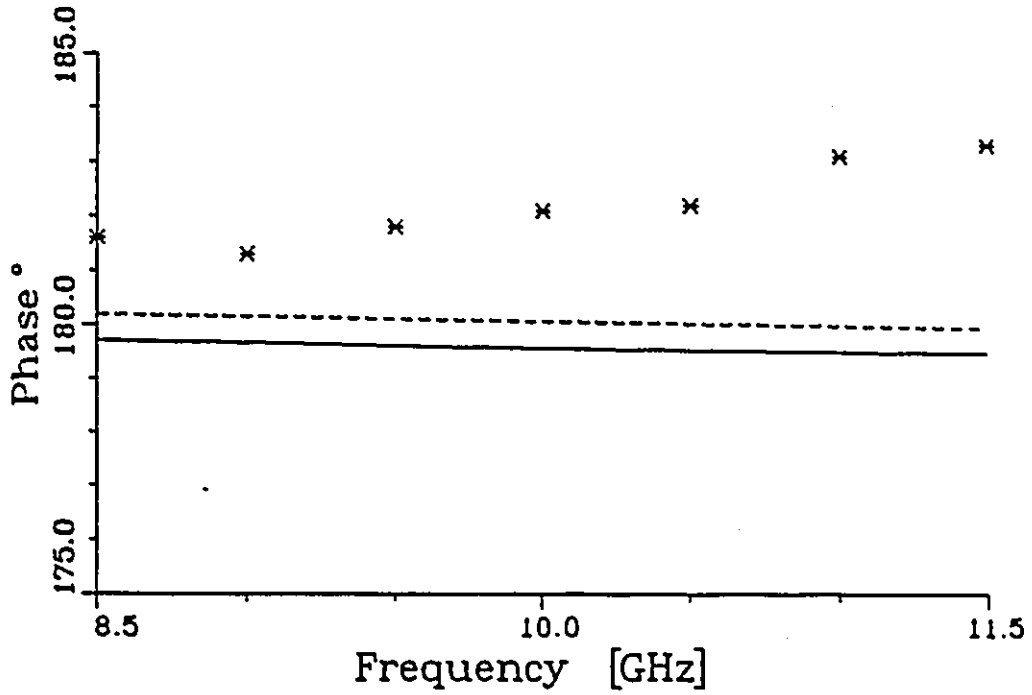

Fig. 5.7: Reflection Coefficient
of 2mm Aperture
Radiating into Methanol

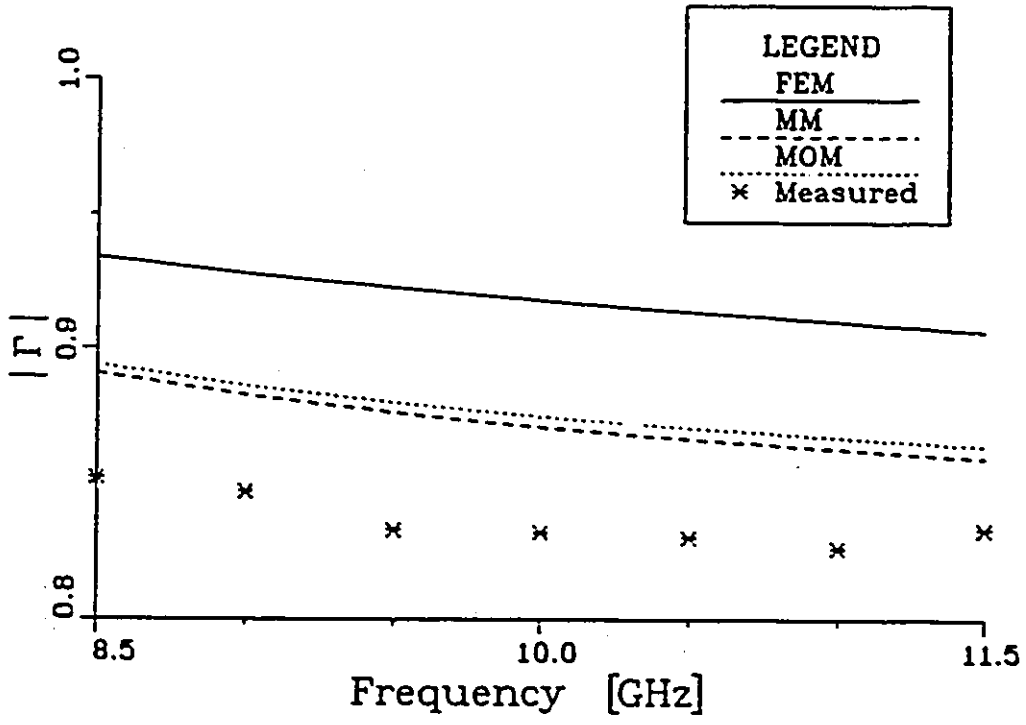

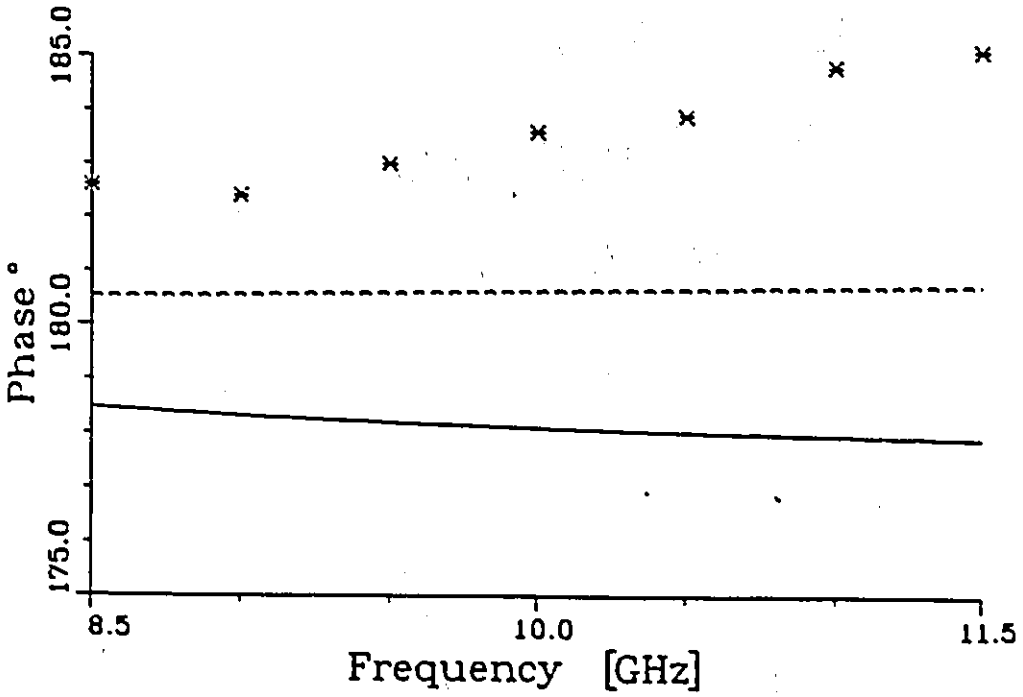

Fig. 5.8: Comparison of Sensitivity
of Open–Ended Guide and 2 mm Aperture

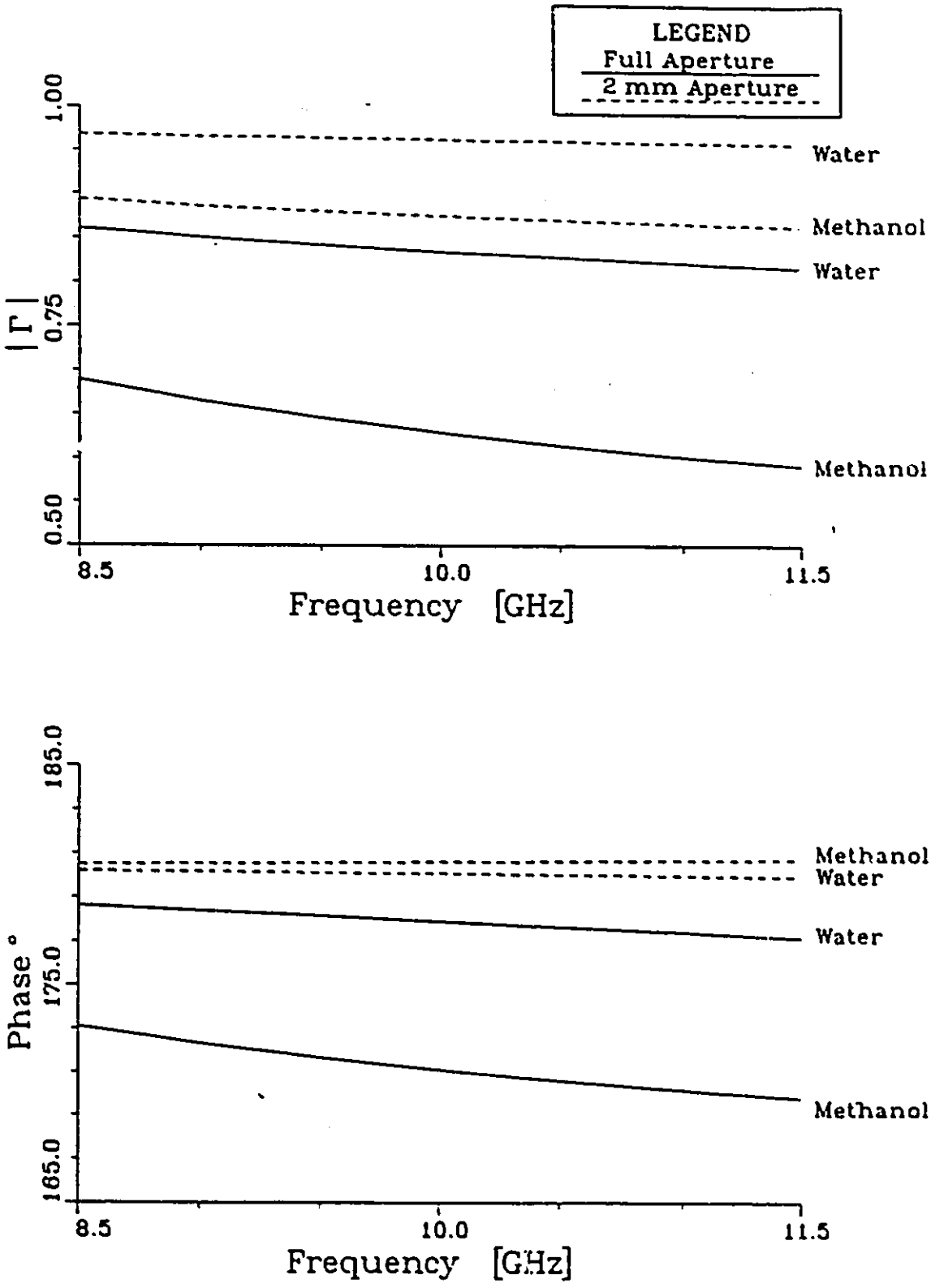

Fig. 5.8: Comparison of Sensitivity
of Open–Ended Guide and 2 mm Aperture

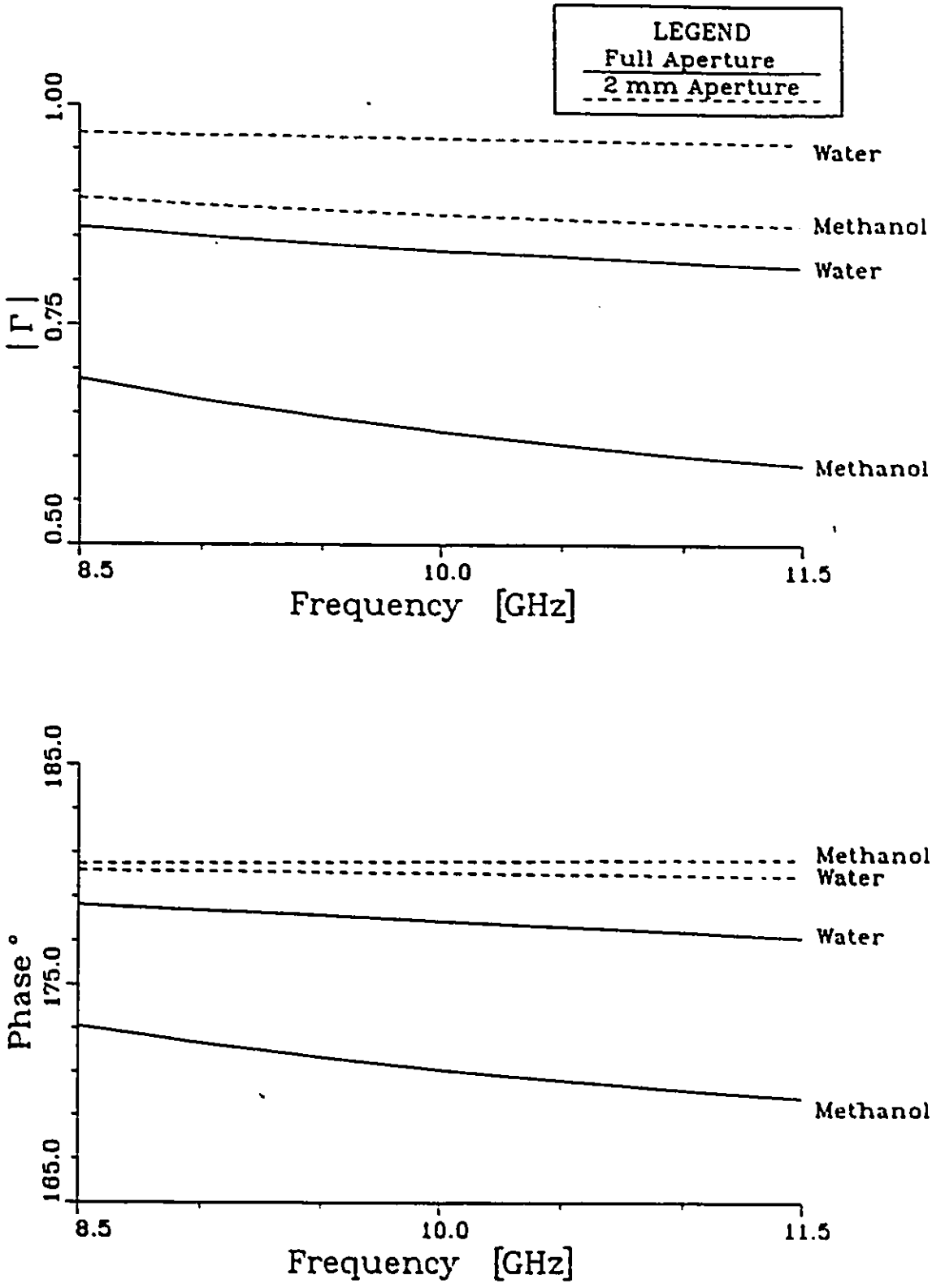

Chapter 6:

Discussion and Conclusions

6.1 Discussion

The results presented in Figures 5.4 and 5.5 for the open-ended guide show excellent agreement between measurement and theory. In particular, the results of the mode matching technique are within 1 percent of the measured values for both dielectrics over the entire frequency range. The agreement between measurement and theory is not as good for the 2mm aperture, for which the difference approaches 5 percent. There are several possible sources for this larger difference. In the numerical analysis, the thickness of the metal forming the aperture, and the presence of the saran wrap were neglected. These factors could lead to small errors, however, it is felt that the largest error was due to the measurement arrangement. Although the uncertainty in the measured reflection coefficient is generally assumed to be ±.05 dB and .2° [13], these uncertainties depend upon the actual value of the reflection coefficient. A qualitative expression for the uncertainty in the measured value of the reflection coefficient is [43]

$$\Delta|\Gamma| = D + T_R|\Gamma_a| + M_S|\Gamma_a|^2 \tag{6.1}$$

where Γ_a represents the actual reflection coefficient of the device and D, T_R, and M_S are the residual directivity, frequency tracking and source match error, respectively, remaining after calibration. From (6.1) it is evident that for devices having large reflections the source mismatch terms dominates and the uncertainty increases.

Phase uncertainty may be related to the magnitude uncertainty by:

$$\Delta\theta = \sin^{-1}\left(\frac{\Delta|\Gamma|}{|\Gamma|}\right) \tag{6.2}$$

and, hence, also increases with increasing $|\Gamma_a|$.

In all cases, the moment method and the mode matching method yielded almost identical results. From Figures 5.5 and 5.7 one notices that the results of the Finite-Element method differed by as much as 6 percent. This may be attributed to the failure of the impedance boundary condition. As the relative permittivity of the dielectric, $|\hat{\varepsilon}|$ decreases, the approximation inherent in equation (2.12) of Section 2.3.2 worsens. Methanol, which has $|\hat{\varepsilon}| = 10$, lies at the lower limit of validity of this boundary condition [28].

A comparison of the three numerical methods with respect to CPU usage is made in Table 6.1. This data was obtained for the case of the full aperture radiating into water. All computations were performed using double precision complex (16 byte word) arithmetic on a Digital 11/RC VAXstation.

Table 6.1: CPU Usage of the Numerical Methods

	FEM	MOM	MM
No. of Unknowns	520	143	625
CPU time [sec]	1240	700	390

The major advantage of the Finite-Element method over the other methods employed is it's simplicity. This method required the least amount of analytical pre-processing. The method is also versatile, allowing a broad class of aperture geometries to be treated. An undesirable feature

of the method is the impedance boundary condition used to artificially bound the problem. This condition restricts the analysis to materials having large permittivities. In addition, the execution time was long.

The mode matching method was the most efficient method in terms of execution time. Unfortunately, the program is very specific with respect to the aperture geometry. A change in the aperture geometry would require the development of new eigenmodes. Furthermore, the approximation made by introducing the over-sized waveguide restricts the analysis to lossy dielectrics.

The most versatile technique was the method of moments. This method allowed the same freedom in the aperture geometry as the finite-element method without restricting the analysis to lossy dielectrics. The execution time was also more favorable than the finite-element method. This method, however, was the most mathematically intensive.

The primary objective of this thesis was to determine an aperture geometry which would reduce the uncertainty in the measurement of material permittivity. One factor governing the measurement uncertainty is the sensor's sensitivity to changes in the material permittivity. One desires a small change in permittivity to produce a relatively large change in the reflection coefficient. Figure 5.8 shows the reflection coefficient of the full aperture and the 2 mm aperture in contact with water and methanol. From this figure it is evident that the full aperture provides the greater sensitivity. In fact, of all the apertures investigated, the open-ended guide provided the greatest sensitivity.

6.2 Conclusions

Three numerical techniques have been applied to the analysis of a waveguide-fed aperture radiating into a lossy dielectric. The objective of the study was to determine an aperture geometry which would minimize the uncertainty in the non-destructive measurement of material permittivity. Four aperture geometries were chosen for detailed study: the full aperture, and three reduced apertures. The reflection coefficient of the aperture in contact with water and methanol was calculated in the frequency range 8.5-11.5 GHz. The theoretical results were validated by measurements performed on an HP8410B automatic network analyzer.

A sample of the experimental and numerical results was given, showing good agreement between theory and experiment. The numerical techniques were compared with the conclusion that the method of moments was the most suitable method for this type of problem.

Of the apertures investigated the open-ended guide provided the best sensitivity to changes in the material permittivity. This indicates that the analogy with TEM structures is not valid. The increased static capacitance of the sensor is overwhelmed by the reduced aperture area which limits the interaction of the waveguide fields with the sample. Although the primary expectation of this study was not fulfilled, the tools have been developed that would allow further analysis. Possible structures for further analysis are ridged waveguide and tapered waveguides.

A logical extension to this work would be to investigate other apertures and to develop an equivalent circuit which would allow one to invert the problem.

Appendix A:

Evaluation of $[\underline{Y}^2]$

The expression for the elements of the generalized admittance matrix for the half-space region was derived in section 4.3.5. From equation (4.47) of that section, we have,

$$\underline{Y}_{ij}^2 = 2j\omega \int_{Apert.} \left(\overline{M}_i \cdot \underline{F}_j + \underline{\Psi}_j \underline{m}_i\right) ds \qquad (A.1)$$

where the electric vector potential, $\overline{\underline{F}}_j$, and the scalar magnetic potential, $\underline{\Psi}_j$, are given by equations (4.41) and (4.42) respectively. The testing functions $\overline{M}_i$ and $\underline{m}_i$ are obtained from equation (4.15) and the equation of continuity, (4.43), by replacing the subscript j by the subscript i. Expanding (A.1) using these definitions yields,

$$\underline{Y}_{ij}^2 = 2j\omega \int_{y_{i-1}}^{y_i} \int_{x_{i-1}}^{x_{i+1}} \underline{F}_j(x,y) T_i(x) P_i(y) dx dy$$

$$+ 2j\omega \int_{y_{i-1}}^{y_i} \int_{x_{i-1}}^{x_{i+1}} \underline{\Psi}_j(x,y) P_i(y) \left\{ \frac{P_{i+1}(x) - P_i(x)}{j\omega \Delta x} \right\} dx dy \qquad (A.2)$$

The integration over the field coordinates (unprimed coordinates) in (A.2) may be approximated by a two term triangle rule,

$$\underline{Y}_{ij}^2 = j\omega \Delta x_i \Delta Y_i \{\underline{F}_j(x_c, y_c) + \underline{F}_j(x_{c+1}, y_c)\}$$

$$+ 2\Delta y_i \{\underline{\Psi}_j(x_{c+1}, y_c) - \underline{\Psi}_j(x_c, y_c)\} \qquad (A.3)$$

where the samples are taken at,

$$x_c = x_i - \frac{\Delta x_i}{2} \tag{A.4}$$

$$x_{c+1} = x_i + \frac{\Delta x_i}{2} \tag{A.5}$$

$$y_c = y_i - \frac{\Delta y_i}{2} \tag{A.6}$$

Substituting these coordinates into (4.41) one obtains the collowing expression for $\underline{F}_j(x_c, y_c)$:

$$\underline{F}_j(x_c, y_c) = \frac{\varepsilon}{4\pi} \int_{y_{j-1}}^{y_j} \int_{x_{j-1}}^{x_{j+1}} T_j(x') P_j(y') \frac{e^{-jk\sqrt{(x_c - x')^2 + (y_c - y')^2}}}{\sqrt{(x_c - x')^2 + (y_c - y')^2}} dx' dy' \tag{A.7}$$

Letting,

$$x = x' - x_c \tag{A.8}$$

$$y = y' - y_c \tag{A.9}$$

(A.7) becomes,

$$\underline{F}_{ij}(x_c, y_c) = \frac{\varepsilon}{4\pi} \{ \int_{v-\frac{\Delta y_j}{2}}^{v+\frac{\Delta y_j}{2}} \int_{t-\frac{\Delta x_j}{2}}^{t+\frac{\Delta x_j}{2}} \frac{x e^{-jkr}}{\Delta x_j r} dx dy - \int_{v-\frac{\Delta y_j}{2}}^{v+\frac{\Delta y_j}{2}} \int_{u-\frac{\Delta x_j}{2}}^{u+\frac{\Delta x_j}{2}} \frac{x e^{-jkr}}{\Delta x_j r} dx dy$$

$$+ \left(u + \frac{\Delta x_j}{2}\right) \int_{v-\frac{\Delta y_j}{2}}^{v+\frac{\Delta y_j}{2}} \int_{u-\frac{\Delta x_j}{2}}^{u+\frac{\Delta x_j}{2}} \frac{e^{-jkr}}{\Delta x_j r} dx dy - \left(t - \frac{\Delta x_j}{2}\right) \int_{v-\frac{\Delta y_j}{2}}^{v+\frac{\Delta y_j}{2}} \int_{t-\frac{\Delta x_j}{2}}^{t+\frac{\Delta x_j}{2}} \frac{e^{-jkr}}{\Delta x_j r} dx dy \} \tag{A.10}$$

where,

$$r = \sqrt{x^2 + y^2} \tag{A.11}$$

$$t = (x_j - x_i) + \frac{\Delta x_i}{2} - \frac{\Delta x_j}{2} \tag{A.12}$$

$$u = (x_j - x_i) + \frac{\Delta x_i}{2} + \frac{\Delta x_j}{2} \tag{A.13}$$

$$v = (y_j - y_i) + \frac{\Delta y_i}{2} - \frac{\Delta y_j}{2} \tag{A.14}$$

By defining the following integrals,

$$I_c(\alpha,\beta) = k \int_{\beta-\frac{\Delta y_j}{2}}^{\beta+\frac{\Delta y_j}{2}} \int_{\alpha-\frac{\Delta x_j}{2}}^{\alpha+\frac{\Delta x_j}{2}} \frac{e^{-jkr}}{\Delta x_j r} dx dy \tag{A.15}$$

$$I_x(\alpha,\beta) = k \int_{\beta-\frac{\Delta y_j}{2}}^{\beta+\frac{\Delta y_j}{2}} \int_{\alpha-\frac{\Delta x_j}{2}}^{\alpha+\frac{\Delta x_j}{2}} \frac{x e^{-jkr}}{\Delta x_j r} dx dy \tag{A.16}$$

equation (A.10) may be written more compactly as,

$$\underline{F}_{ij}(x_c, y_c) = \frac{\varepsilon}{4\pi k}\left\{I_x(t,v) - I_x(u,v) + \left(u + \frac{\Delta x_j}{2}\right) I_c(u,v) - \left(t - \frac{\Delta x_j}{2}\right) I_c(t,v)\right\} \tag{A.17}$$

Similar manipulations on $\underline{F}_j(x_{c+1}, y_c)$, $\underline{\Psi}_j(x_{c+1}, y_c)$, and $\underline{\Psi}_j(x_c, y_c)$ yield,

$$\underline{F}_{ij}(x_{c+1}, y_c) = \frac{\varepsilon}{4\pi k}\left\{I_x(w,v) - I_x(s,v) + \left(s + \frac{\Delta x_j}{2}\right) I_c(s,v) - \left(w - \frac{\Delta x_j}{2}\right) I_c(w,v)\right\} \tag{A.18}$$

$$\underline{\Psi}_{ij}(x_c, y_c) = \frac{1}{4\pi j \omega \mu k}\{I_c(u,v) - I_c(t,v)\} \tag{A.19}$$

$$\underline{\Psi}_{ij}(x_{c+1}, y_c) = \frac{1}{4\pi j\omega\mu k}\{I_e(s,v) - I_e(w,v)\} \tag{A.20}$$

where

$$w = (x_j - x_i) - \frac{\Delta x_i}{2} - \frac{\Delta x_j}{2} \tag{A.21}$$

$$s = (x_j - x_i) - \frac{\Delta x_i}{2} + \frac{\Delta x_j}{2} \tag{A.22}$$

Substitution of (A.17) - (A.20) into (A.3) yields the final expression for $\underline{Y}_{ij}^2$,

$$\begin{aligned}\underline{Y}_{ij}^2 \approx \frac{j\omega\epsilon\Delta x_i\Delta y_i}{4\pi k}\{&I_x(t,v) - I_x(u,v) + \left(u + \frac{\Delta x_j}{2}\right)I_e(u,v) \\ &- \left(t - \frac{\Delta x_j}{2}\right)I_e(t,v) + I_x(w,v) - I_x(s,v) \\ &\left(s + \frac{\Delta x_j}{2}\right)I_e(s,v) - \left(w - \frac{\Delta x_j}{2}\right)I_e(w,v) \\ &\frac{2}{k^2\Delta x_i}[I_e(w,v) - I_e(s,v) - I_e(t,v) + I_e(u,v)]\}\end{aligned} \tag{A.23}$$

The integrals defined in (A.15) and (A.16) may be evaluated analytically if an approximation to the exponential is made. For this purpose, a four term Taylor series with center

$$r_0 = \sqrt{\alpha^2 + \beta^2} \tag{A.24}$$

is used to write:

$$e^{-jkr} \approx e^{-jkr_0}\left\{1 - jk(r - r_0) - \frac{k^2}{2}(r - r_0)^2 + j\frac{k^3}{6}(r - r_0)^3\right\} \tag{A.25}$$

Substituting this last equation into (A.15), one obtains:

$$I_c(\alpha,\beta) \approx \frac{e^{-jkr_0}}{\Delta x_j}\{j\frac{k^4}{6}\int\int r^2 dxdy - \frac{k^3}{2}[jkr_0+1]\int\int r dxdy$$
$$k^2\left[j\frac{k^2r_0^2}{2}+kr_0-j\right]\int\int dxdy$$
$$k\left[-j\frac{k^3r_0^3}{6}-\frac{k^2r_0^2}{2}+jkr_0+1\right]\int\int\frac{1}{r}dxdy\} \qquad (A.26)$$

where the limits of integration are given in (A.15).

Similarly, (A.16) may be approximated by:

$$I_c(\alpha,\beta) \approx \frac{e^{-jkr_0}}{\Delta x_j}\{j\frac{k^4}{6}\int\int x r^2 dxdy - \frac{k^3}{2}[jkr_0+1]\int\int x r dxdy$$
$$k^2\left[j\frac{k^2r_0^2}{2}+kr_0-j\right]\int\int x dxdy$$
$$k\left[-j\frac{k^3r_0^3}{6}-\frac{k^2r_0^2}{2}+jkr_0+1\right]\int\int\frac{x}{r}dxdy\} \qquad (A.27)$$

Finally, the integrals appearing in (A.26) and (A.27) are evaluated analytically.

Appendix B:

Computer Program for the Finite-Element Method

```
c     Description:
c     ------------
c     This program calculates the input reflection coefficient and Hertian
c     magnetic potential of a waveguide in contact with a lossy dielectric.
c     The waveguide is terminated in a conducting screen with one or more
c     apertures symetrically placed about the planes x=a/2, y=b/2.
c     The geometry of the aperture(s) is defined interactively and
c     consists of rectangular patches which are either metal or open.
c     The finite element method, based on Galerkins method, is used to solve
c     the Helmholtz equation for the unknown magnetic Hertzian potential.
c     This potential is assumed to have only an x-component (LSE modes).
c     Rectangular "brick" elements are used, and 2nd order interpolatory
c     functions are employed.
c
c    Variables:
c    ----------
c     pot(nnode)  : the node potentials.
c     lhs(nn,nn)  : the coefficient matrix of problem to be solved.
c     rhs(nn)     : the right hand side of matrix equation.
c     smat        : one element of the stiffness matrix.
c     tmat        : one element of the T matrix.
c     l1mat       : contribution from surface element at z=0
c     l2mat       : contribution from surface element at z=d
c     ko          : the free space wave number. [rad/cm]
c     kz          : the guided wave number of dominant mode. [rad/cm]
c     epso        : dielectric constant of free space.
c     epsr        : the relative permittivity  of dielectric.
c     miuo        : the permeability of free space.
c     freq        : the operating frequency.
c     lambo       : the free space wavelength [cm]
c     lambg       : the guide wavelength. [cm]
c     omeg        : the angular frequency.
c     pi          : 3.14159....
c     a           : the broad dimension of waveguide. [cm]
c     b           : the narrow dimension of waveguide. [cm]
c     d           : the distance from z=0 to aperture. [cm]
c     xa          : x coordinate of 1st air/metal transition in x direction [cm]
c     xb          : x coordinate of 2nd air/metal transition in x direction [cm]
c     xg1         : # of grid lines 0<=x<=xa
c     xg2         : # of grid lines xa=x<=xb
c     xg3         : # of grid lines xb<=x<=a/2
c     xg          : total number of grid lines in x. (xg=xg1+xg2+xg3-2)
c     ya          : y coordinate of 1st air/metal transition in y direction [cm]
c     yb          : y coordinate of 2nd air/metal transition in y direction [cm]
c     yg1         : # of grid lines 0<=y<=ya.
c     yg2         : # of grid lines ya<=y<=yb
c     yg3         : # of grid lines yb<=y<=b/2
c     yg          : total number of grid lines in y. (yg=yg1+yg2+yg3-2)
```

```
c     zg          : total number of grid lines in z-direction
c     nnode       : the total number of nodes. ( free nodes + dirichlet )
c     nbric       : the number of brick elements
c     nol1        : the number of surface elements at z=0
c     nol2        : the number of surface elements at z=d
c     ndir        : the number of dirichlet nodes.
c     nn          : the number of free nodes, i.e. number of unknowns.
c     x(nnode)    : the x coordinates of nodes.
c     y(nnode)    : the y coordinates of nodes.
c     z(nnode)    : the z coordinates of nodes.
c     dx          : the x dimension of bricks or surface patch.
c     dy          : the y dimension of bricks or surface patch.
c     dz          : the z dimension of bricks or surface patch.
c     iv(27,nbric) : the global node numbers for each brick.
c                    iv(i,j) = global node number of node i of brick j.
c     liv1(9,nol1) : the global node number of each surface element (z=0)
c     liv2(9,nol2) : the global node number of each surface element (z=d)
c     it,i,k,l,m,n,o,p,q : loop counters.
c     row           : index of row in lhs.
c     col           : index of column in lhs.
c     j             : sqrt(-1)
c
c  Common variables:
c  ----------------
c     a             : the broad dimension of guide [cm]
c     b             : the narrow dimension of guide [cm]
c     d             : the length of guide from z=0 to aperture [cm]
c     xa,xb         : see above
c     ya,yb         : see above
c
c     Functions/Constants:
c     --------------------
c       f(k,n)   : results of integrating product of 2 legrange polynomials.
c       fd(k,n)  : results of integrating derivatives of legrange polynomials.
c       g(k,n)   : integration of the product of legrange polynomial and 2nd
c                  derivative of legrange.
c       u(k)     : integration of single legrange poly.
c       s(k)     : integration of product of legrange poly. and sin(pi*x/a)
c
c     Subroutines:
c     ------------
c       grid : calclates node co-ordinates, assigns node numbers and
c              initializes iv,liv1,liv2.
c       zgeco: solves the final linear system of equations.
c       sht  : calculates the analytical solution for short circuit guide.

      IMPLICIT none
      PARAMETER pxg=9,pyg=9,pzg=13
      PARAMETER dim1=pxg*pyg*pzg
      PARAMETER dim2=(pxg-1)*(pyg-1)/4
      PARAMETER dim3=(pxg-1)*(pyg-1)*(pzg-1)/8
      PARAMETER dim4=dim1-pyg*pzg
      COMPLEX*16 cdsqrt,cdcos,cdsin,sht
      COMPLEX*16 smat,tmat,l1mat,l2mat,j,epsr,ref,sum
      REAL*8 pi,epso,freq,miuo,omeg,rcond
      REAL*8 kz,ko,lambo,lambg,a,b,d,xa,xb,ya,yb
      REAL*8 dx,dy,dz,xl,yl
      REAL*8 cx1,cx3,sx1,sx3
```

```
      REAL*8 f(3,3),fd(3,3),g(3,3),u(3),s(3)
      INTEGER*4 i,k,l,m,n,o,p,q,xg3,yg3
      INTEGER*4 job,nrow,it,row,col,xg1,xg2,xg,yg1,yg2,yg,zg
      CHARACTER*1 ans
      INTEGER*4 nnode,ndir,nn,nbric,no11,no12
      COMPLEX*16 pot(dim1),lhs(dim4,dim4),rhs(dim4),work(dim4)
      REAL*8 x(dim1),y(dim1),z(dim1)
      INTEGER*4 iv(27,dim3),liv1(9,dim2),liv2(9,dim2),piv(dim4)
      COMMON /geo/a,b,d,xa,xb,ya,yb
c*********
c     Constant definitions
c*********
      f(1,1)=2.0d0/15.0d0
      f(1,2)=1.0d0/15.0d0
      f(1,3)=-1.0d0/30.0d0
      f(2,1)=f(1,2)
      f(2,2)=8.0d0/15.0d0
      f(2,3)=1.0d0/15.0d0
      f(3,1)=f(1,3)
      f(3,2)=f(2,3)
      f(3,3)=2.0d0/15.0d0
      fd(1,1)=7.0d0/3.0d0
      fd(1,2)=-8.0d0/3.0d0
      fd(1,3)=1.0d0/3.0d0
      fd(2,1)=fd(1,2)
      fd(2,2)=16.0d0/3.0d0
      fd(2,3)=-8.0d0/3.0d0
      fd(3,1)=fd(1,3)
      fd(3,2)=fd(2,3)
      fd(3,3)=7.0d0/3.0d0
      g(1,1)=2.0d0/3.0d0
      g(1,2)=-4.0d0/3.0d0
      g(1,3)=2.0d0/3.0d0
      g(2,1)=8.0d0/3.0d0
      g(2,2)=-16.0d0/3.0d0
      g(2,3)=8.0d0/3.0d0
      g(3,1)=2.0d0/3.0d0
      g(3,2)=-4.0d0/3.0d0
      g(3,3)=2.0d0/3.0d0
c********
c     get input data
c********
      nrow=dim4
      a=2.286d0
      b=1.016d0
      write(*,'(a$)') ' enter d [in terms of lambg] --->'
      read(*,*) d
      write(*,'(a$)') ' enter xa [cm]--->'
      read(*,*) xa
      if (xa .eq. 0.0d0) then
        xg1=1
      else
        write(*,'(a)') ' enter # of grid lines 0 < x < xa'
        write(*,'(a$)') ' MUST BE ODD---->'
        read(*,*) xg1
      endif
      write(*,'(a$)') ' enter xb [cm]--->'
      read(*,*) xb
```

```
if (xb .eq. 0.0d0) then
  xg2=1
else
  write(*,'(a)') ' enter # of grid lines xa < x < xb'
  write(*,'(a$)') ' MUST BE ODD---->'
  read(*,*) xg2
endif
write(*,'(a)') ' enter # of grid lines xb < x < a/2'
write(*,'(a$)') ' MUST BE ODD---->'
read(*,*) xg3
xg=xg1+xg2+xg3-2
write(*,'(a$)') ' enter ya [cm]--->'
read(*,*) ya
if (ya .eq. 0.0d0) then
  yg1=1
else
  write(*,'(a)') ' enter # of grid lines 0 < y < ya'
  write(*,'(a$)') ' MUST BE ODD---->'
  read(*,*) yg1
endif
write(*,'(a$)') ' enter yb [cm]--->'
read(*,*) yb
if (yb .eq. 0.0d0) then
  yg2=1
else
  write(*,'(a)') ' enter # of grid lines ya < y < yb'
  write(*,'(a$)') ' MUST BE ODD---->'
  read(*,*) yg2
endif
write(*,'(a)') ' enter # of grid lines yb < y < b/2'
write(*,'(a$)') ' MUST BE ODD---->'
read(*,*) yg3
yg=yg1+yg2+yg3-2
write(*,'(a$)') ' enter # of grid lines in 0 < z < d'
write(*,'(a,i2,a,$)') ' MUST BE ODD,MAXIMUM OF ',pzg,' ---->'
read(*,*) zg
noll=(xg-1)*(yg-1)/4
nbric=noll*(zg-1)/2
nnode=xg*yg*zg
ndir=zg*yg
nn=nnode-ndir
if(nnode .gt. dim1) then
  write(*,'(a)') ' TOO MANY NODES '
  stop
endif
if(noll .gt. dim2) then
  write(*,'(a)') ' TOO MANY SURFACES '
  stop
endif
if(nbric .gt. dim3) then
  write(*,'(a)') ' TOO MANY BRICS '
  stop
endif
if(nn .gt. dim4) then
  write(*,'(a)') ' TOO MANY UNKNOWNS '
  stop
endif
write(*,*) ' nn = ',nn,' nnode = ',nnode,' nbric = ',nbric
```

```
c********
c     initialize variables and constants
c********
      nol2=0
      smat=(0.0d0,0.0d0)
      tmat=(0.0d0,0.0d0)
      l1mat=(0.0d0,0.0d0)
      l2mat=(0.0d0,0.0d0)
      pi=dacos(-1.d0)
      j=dcmplx(0.0d0,1.0d0)
1     continue
      write(*,'(a,$)') ' enter operating frequency: [Hz] '
      read(*,*) freq
      lambo=2.997925d10/freq
      if(lambo .gt. 2.d0*a) then
        write(*,*) ' waveguide below cutoff'
        goto 1
      endif
      lambg=lambo/dsqrt(1.d0-(lambo/2.d0/a)**2)
      write(*,*) ' guided wavelength is:',lambg
      d=lambg*d
      write(*,'(a$)') ' enter eps rel (real,imag)--->'
      read(*,*) epsr
      omeg=2.*pi*freq
      epso=1./(35.950336d+011*pi)
      miuo=4.d-09*pi
      ko=2.0d0*pi/lambo
      kz=2.0d0*pi/lambg
      do 6 i=1,nn
      rhs(i)=(0.d0,0.d0)
      do 6 k=1,nn
6     lhs(i,k)=(0.d0,0.d0)
      do 603 i=ndir+1,nnode
603   pot(i)=(0.d0,0.d0)
c**********
c     initalize bricks and surface elements. ( triangulate region )
c**********
      call grid(nnode,ndir,nbric,nol1,nol2,xg1,xg2,xg3,xg,yg1,yg2,
     &          yg3,yg,zg,x,y,z,iv,liv1,liv2,pot)
c**********
c     Add contribution from bricks
c**********
      do it=1,nbric
       dx=x(iv(27,it))-x(iv(1,it))
       dy=y(iv(27,it))-y(iv(1,it))
       dz=z(iv(27,it))-z(iv(1,it))
       i=0
       do n=1,3
        do m=1,3
         do l=1,3
          i=i+1
          row=iv(i,it)-ndir
          if(iv(i,it) .gt. ndir) then
           k=0
           do q=1,3
            do p=1,3
             do o=1,3
              k=k+1
```

```
              smat=dy*dz*fd(l,o)*f(m,p)*f(n,q)/dx+
     &             dx*dz*f(l,o)*fd(m,p)*f(n,q)/dy+
     &             dx*dy*f(l,o)*f(m,p)*fd(n,q)/dz
              tmat=ko**2*dx*dy*dz*f(l,o)*f(m,p)*f(n,q)
              if (iv(k,it) .le. ndir) then
               rhs(row)=rhs(row)+pot(iv(k,it))*(tmat-smat)
              else
               col=iv(k,it)-ndir
               lhs(row,col)=lhs(row,col)+smat-tmat
              endif
             end do
            end do
           end do
          endif
         end do
        end do
       end do
      end do
c**********
c     Now add contribution from surface elements (z=0)
c**********
      do it=1,noll
       dx=x(livl(9,it))-x(livl(1,it))
       dy=y(livl(9,it))-y(livl(1,it))
       u(1)=dy/6.0d0
       u(2)=4.0d0*u(1)
       u(3)=u(1)
       cx3=dcosd(180.0d0*x(livl(9,it))/a)
       cxl=dcosd(180.0d0*x(livl(1,it))/a)
       sx3=dsind(180.0d0*x(livl(9,it))/a)
       sxl=dsind(180.0d0*x(livl(1,it))/a)
       s(1)=3.0d0*sxl+sx3+dx*(pi/a)*cxl+4.0d0*(a/pi)*(cx3-cxl)/dx
       s(1)=(a/pi)**2*s(1)/dx
       s(2)=-sx3-sxl-2.0d0*(a/pi)*(cx3-cxl)/dx
       s(2)=4.0d0*(a/pi)**2*s(2)/dx
       s(3)=3.0d0*sx3+sxl-dx*(pi/a)*cx3+4.0d0*(a/pi)*(cx3-cxl)/dx
       s(3)=(a/pi)**2*s(3)/dx
       i=0
       do m=1,3
        do l=1,3
         i=i+1
         row=livl(i,it)-ndir
         if(livl(i,it) .gt. ndir) then
          rhs(row)=rhs(row)+2.0d0*s(l)*u(m)
          k=0
          do p=1,3
           do o=1,3
            k=k+1
            llmat=j*kz*dx*dy*f(l,o)*f(m,p)
            if(livl(k,it) .le. ndir) then
              rhs(row) = rhs(row)-pot(livl(k,it))*llmat
            else
              col = livl(k,it)-ndir
              lhs(row,col) = lhs(row,col)+llmat
            endif
           end do
          end do
         endif
```

```
        end do
       end do
      end do
c**********
c     Now add contribution from surface elements (z=d)
c**********
      do it=1,nol2
       dx=x(liv2(9,it))-x(liv2(1,it))
       dy=y(liv2(9,it))-y(liv2(1,it))
       i=0
       do m=1,3
        do l=1,3
         i=i+1
         row=liv2(i,it)-ndir
         if(liv2(i,it) .gt. ndir) then
          k=0
          do p=1,3
           do o=1,3
            k=k+1
            l2mat=j*dy*f(m,p)*(g(l,o)/dx+dx*ko**2*f(l,o))/ko
            l2mat=l2mat/cdsqrt(epsr)
            if(liv2(k,it) .le. ndir) then
              rhs(row) = rhs(row)-pot(liv2(k,it))*l2mat
            else
              col = liv2(k,it)-ndir
              lhs(row,col) = lhs(row,col)+l2mat
            endif
           end do
          end do
         endif
        end do
       end do
      end do
c***********
c     solve the system
c***********

      call zgeco(lhs,nrow,nn,piv,rcond,work)
      write(*,*) ' condition # is: ',rcond
      job=0
      call zgesl(lhs,nrow,nn,piv,rhs,job)
      do 300 k = 1,nn
        i=ndir+k
        pot(i)=rhs(k)
300   continue
c***********
c     output
c***********
      open(25,file='bric.out',status='new')
      write(25,*) ' condition # is: ',rcond
      write(25,497) a,b,d,xa,xb,ya,yb
497   format(' a [cm]: ',1pd10.3,' b [cm]: ',1pd10.3,
     &       ' d [cm]: ',1pd10.3,/,' xa [cm]: ',1pd10.3,
     &       ' xb [cm]: ',1pd10.3,' ya [cm]: ',1pd10.3,
     &       ' yb [cm]: ',1pd10.3)
      write(25,82) ndir,nnode,nbric,nol1,nol2
82    format(' ndir: ',i4,' nnode: ',i4,' nbric: ',i4,' nol1: ',i4,
     &       ' nol2',i4,/)
```

```
      write(25,498) epsr
      write(25,'(a,f7.3)') '  frequency [GHz] ',freq*1.d-9
498   format(' eps rel.:',1pd10.3,1x,1pd10.3)
      write(*,'(a$)') ' output all potentials (y/n)? '
      read(*,'(A)') ans
      if(ans .eq. 'y' .or. ans .eq. 'Y') then
       do 500 i=1,nnode
        if(nol2 .eq. 0) then
         write(25,510) i,x(i),y(i),z(i),pot(i),sht(x(i),z(i),kz)
510      format(' node(',i3,')  x',1pe11.3,'  y',1pe11.3,'  z',1pe11.3,
     &          '  phi ',2(1pe12.4,1x),'  sht ',2(1pe12.4,1x))
        else
         write(25,511) i,x(i),y(i),z(i),pot(i)
511      format(' node(',i3,')  x',1pe11.3,'  y',1pe11.3,'  z',1pe11.3,
     &          '  phi ',2(1pe12.4,1x))
        endif
500    continue
      endif
      write(25,515)
515   format(//)
      sum=(0.0,0.0)
      do 520 i=1,nol1
        x1=x(liv1(5,i))
        y1=y(liv1(5,i))
        ref=1.0d0-pot(liv1(5,i))*j*kz/dsind(180.0d0*x1/a)
        sum=sum+ref
        write(25,525) liv1(5,i),x1,y1,ref,cdabs(ref)
525     format(' node(',i3,')   x',1pe12.4,'  y',1pe12.4,'  ref. coef.',
     &          2(1pe12.4),' !ref! ',1pd12.4)
        x1=x(liv1(6,i))
        y1=y(liv1(6,i))
        ref=1.0d0-pot(liv1(6,i))*j*kz/dsind(180.0d0*x1/a)
        sum=sum+ref
        write(25,525) liv1(6,i),x1,y1,ref,cdabs(ref)
526     format(' node(',i3,')   x',1pe12.4,'  y',1pe12.4,'  ref. coef.',
     &          2(1pe12.4),' !ref! ',1pd12.4)
        x1=x(liv1(8,i))
        y1=y(liv1(8,i))
        ref=1.0d0-pot(liv1(8,i))*j*kz/dsind(180.0d0*x1/a)
        sum=sum+ref
        write(25,525) liv1(8,i),x1,y1,ref,cdabs(ref)
527     format(' node(',i3,')   x',1pe12.4,'  y',1pe12.4,'  ref. coef.',
     &          2(1pe12.4),' !ref! ',1pd12.4)
        x1=x(liv1(9,i))
        y1=y(liv1(9,i))
        ref=1.0d0-pot(liv1(9,i))*j*kz/dsind(180.0d0*x1/a)
        sum=sum+ref
        write(25,525) liv1(9,i),x1,y1,ref,cdabs(ref)
528     format(' node(',i3,')   x',1pe12.4,'  y',1pe12.4,'  ref. coef.',
     &          2(1pe12.4),' !ref! ',1pd12.4)
520    continue
      sum=sum/nol1/4.0d0
      write(25,552) sum,cdabs(sum)
552   format(//,'average ref: ',2(1pd12.4),' average !ref!: ',1pd12.4)
      close(25)
      stop
      end
```

```
c*********
      complex*16 function sht(x,z,kz)
c*********
      complex*16 temp
      real*8 a,b,d,xa,xb,ya,yb,x,z,kz,pi
      common /geo/a,b,d,xa,xb,ya,yb
      pi=dacos(-1.0d0)
      temp=dcmplx(0.0d0,-dsind(180.0d0*x/a)/kz)
      sht=temp*(cdexp(dcmplx(0.0d0,-kz*z))+
     &          cdexp(dcmplx(0.0d0,kz*(z-2.0d0*d))))
      return
      end
c*********
      subroutine grid(nncde,ndir,nbric,nol1,nol2,xg1,xg2,xg3,
     &    xg,yg1,yg2,yg3,yg,zg,x,y,z,iv,liv1,liv2,pot)
c*********
c     description:
c     ------------
c       this routine generates the brick and surface elements for
c     a finite elements problem. the problem is a waveguide in contact
c     with a lossy dielectric. The waveguide has a conducting screen
c     with rectangular aperture(s) cut in it. The exact position of
c     metal/dielectric is defined in this routine.
      IMPLICIT none
      INTEGER*4 xg1,xg2,xg3,xg,yg1,yg2,yg3,yg,zg
      INTEGER*4 nnode,ndir,nbric,nol1,nol2,iv(27,*),liv1(9,*)
      INTEGER*4 liv2(9,*),patch
      INTEGER*4 i,j,k,p,q,r,n,m,node(25,25,25)
      COMPLEX*16 pot(nnode)
      REAL*8 z(nnode),x(nnode),y(nnode),dx1,dx2,dy1,dy2,dz
      REAL*8 a,b,d,xa,xb,ya,yb,tx(25),ty(25),tz(25),pi
      REAL*8 dx3,dy3
      character*1 resp
      COMMON /geo/a,b,d,xa,xb,ya,yb
      pi=dacos(-1.0d0)

c********
c     calculate x coordinate of vertical grid lines.
c********
      if(xg1 .eq. 1) then
        dx1=0.0d0
      else
        dx1=xa/(xg1-1)
      end if
      if(xg2 .eq. 1) then
        dx2=0.0d0
      else
        dx2=(xb-xa)/(xg2-1)
      end if
      dx3=(a/2.0d0-xb)/(xg3-1)
        do i=1,xg1
        tx(i)=(i-1)*dx1
      end do
        do i=xg1,xg1+xg2-1
        tx(i)=(i-xg1)*dx2+xa
      end do
```

```
      do i=xg1+xg2-1,xg
        tx(i)=(i-xg1-xg2+1)*dx3+xb
      end do
c********
c     calculate the y coordinate of horizontal grid lines.
c********
        if(yg1 .eq. 1) then
          dy1=0.0d0
        else
          dy1=ya/(yg1-1)
        endif
        if(yg2 .eq. 1) then
          dy2=0.0d0
        else
          dy2=(yb-ya)/(yg2-1)
        endif
        dy3=(b/2.0d0-yb)/(yg3-1)
        do i=1,yg1
          ty(i)=(i-1)*dy1
        end do
        do i=yg1,yg1+yg2-1
          ty(i)=(i-yg1)*dy2+ya
        end do
        do i=yg1+yg2-1,yg
          ty(i)=(i-yg1-yg2+1)*dy3+yb
        end do
c*******
c     calculate z coordinate of grid lines
c*******
      do i=1,zg
        tz(i)=(i-1)*d/(zg-1)
      end do
c********
c     now assign node numbers and potentials
c********
      m=ndir+1
      n=1
      do k=1,zg
        do j=1,yg
        do i=1,xg
            if(i .eq. 1) then
              node(i,j,k)=n
              x(n)=tx(i)
              y(n)=ty(j)
              z(n)=tz(k)
              pot(n)=0.0d0
              n=n+1
            else
              node(i,j,k)=m
              x(m)=tx(i)
              y(m)=ty(j)
              z(m)=tz(k)
              m=m+1
            endif
          end do
        end do
      end do
```

```
c*******
c     number bricks and assign nodes.
c*******
      n=1
      do  k=1,zg-2,2
        do  j=1,yg-2,2
          do  i=1,xg-2,2
            m=0
            do r=0,2
              do q=0,2
                do p=0,2
                  m=m+1
                  iv(m,n)=node(i+p,j+q,k+r)
                end do
              end do
            end do
            n=n+1
          end do
        end do
      end do
c*******
c     assign node nurbers to surface elements at z=0
c*******
      n=1
      do j=1,yg-2,2
        do i=1,xg-2,2
          m=0
          do q=0,2
            do p=0,2
              m=m+1
              liv1(m,n)=node(i+p,j+q,1)
            end do
          end do
          n=n+1
        end do
      end do
c*******
c     assign node numbers to surface elements at z=d
c*******
      patch=0
      n=1
      do j=1,yg-2,2
       do i=1,xg-2,2
        patch=patch+1
        write(*,'(a,i2,a$)') ' is patch ',patch,' metal (y/n)?-->'
        read(*,'(a)') resp
        if(resp .eq. 'n' .or. resp .eq. 'N') then
          m=0
          do q=0,2
            do p=0,2
              m=m+1
              liv2(m,n)=node(i+p,j+q,zg)
            end do
          end do
          n=n+1
          nol2=nol2+1
```

```
        end if
       end do
      end do
c*******
c     output calculated values
c*******
      write(*,'(a,$)') ' create map file? (y/n)-->'
      read(*,'(a)') resp
      if(resp .eq. 'y' .or. resp .eq. 'Y') then
      open(33,file='brick.map',status='new')
      write(33,82) ndir,nnode,nbric,nol1,nol2
82    format(' ndir: ',i4,' nnode: ',i4,' nbric: ',i4,' nol1: ',i4,
     &       ' nol2',i4,/)
      write(33,83) a,b,d,xa,xb,ya,yb
83    format(' a [cm]:',1pd10.3,' b [cm]:',1pd10.3,
     &       ' d [cm]:',1pd10.3,/,' xa [cm]:',1pd10.3,
     &       ' xb [cm]:',1pd10.3,' ya [cm]:',1pd10.3,
     &       ' yb [cm]:',1pd10.3)
      do i=1,nnode
        write(33,95) i,x(i),y(i),z(i),pot(i)
95      format(' node(',i3,')  x',1pe12.4,'  y',1pe12.4,'  z',1pe12.4,
     &         '  pot', 2(1pe12.4,1x))
      end do
      do k=1,zg
        write(33,96) ' nodes in plane z=',tz(k)
96      format(//,a,1pe12.4,/)
        do j=yg,1,-1
          write(33,98) (node(i,j,k),i=1,xg)
98        format(' ',20i4)
        end do
      end do
      do i=1,nbric
        write(33,105) i,(iv(j,i),j=1,27)
105     format(' ','   brick(',i4,')  ',27i4)
      end do
      do i=1,nol1,2
        write(33,115) i,(liv1(j,i),j=1,9),i+1,(liv1(j,i+1),j=1,9)
115     format(' ',2('   sur. ele.(',i4,') on c1  ',9i4))
      end do
      do i=1,nol2,2
        write(33,116) i,(liv2(j,i),j=1,9),i+1,(liv2(j,i+1),j=1,9)
116     format(' ',2('   sur. ele.(',i4,') on c2  ',9i4))
      end do
      close(33)
      endif
      return
      end
```

Appendix C:

Computer Program for the Mode Matching Method

```
C     Description:
C     ------------
C       This program solves a waveguide discontinuity problem.
C     The problem consists of a junction between two rectangular
C     waveguides. The input guide has dimensions a1 X b1, and the
C     output guide has dimensions a2 X b2 and is filled with a lossy
C     dielectric. The guides are coaxial and a capacitive iris of
C     zero thickness is symmetrically placed at the junction. The
C     problem is solved via the mode matching technique. A cross
C     sectionnal view in the plane of the discontinuity is shown below:
C     (looking from input side, i.e. smaller guide)
C
C       y
C       !
C       !
C     b3!-----------------------!
C       !                       !
C       !  !-----------------!  !     - input guide is the smaller.
C       !  !_________________!  !     - iris is symmetric about b2/2
C   eta_!  !_________________!  !
C       !  !                 !  !
C alpha-!  -------------------  !
C       !                       !
C       !--!--------------------!---------> x
C         zeta                 a3
C
C     The fields in the three regions, ( i.e. input guide, output guide
C    and aperture ), are expanded in LSEnm modes, and the tangential
C    components are equated on the aperture. This leads to a system of
C    equations in terms of the unknown modal amplitudes. Due to symmetry
C    only the LSEnm modes with n odd, and m even are considered.
C
C
C     Global variables:
C     -----------------
C     a1        - broad dimension of input guide. (guide 1) [cm]
C     b1        - narrow dimension of input guide. [cm]
C     a3        - broad dimension of output guide. (guide 3) [cm]
C     b3        - narrow dimension of output guide. [cm]
C     b2        - narrow dimension of aperture. (guide 2) [cm]
C     p1        - number of waveguide modes considered in guide 1. (max. 50)
C     p2        - number of waveguide modes considered in guide 2. (max. 50)
C     P3        - number of waveguide modes considered in guide 3.(max. 5000)
C     n1(i),m1(i) - the n, m indexes of mode i in input guide.
C     n2(r),m2(r) - the n, m indexes of mode r in aperture.
C     n3(s),m3(s) - the n, m indexes of mode s in output guide.
C     ko          - propogation constant of free space. [1/cm]
C     kx1(i)      - x-comp. of prop. const. of mode i (input guide)  [1/cm]
```

```
C     kx2(r)       -   "     "    "     "    "   "   r (aperture)      [1/cm]
C     kx3(s)       -   "     "    "     "    "   "   s (output guide)  [1/cm]
C     ky1(i)       - y-comp  of prop. const. of mode i (input guide)   [1/cm]
C     ky2(r)       -   "     "    "     "    "   "   r (aperture)      [1/cm]
C     ky3(s)       -   "     "    "     "    "   "   s (output guide)  [1/cm]
C     kz1(i),kz2(r),kz3(s) - you guessed it !
C     epsr         -relative permittivity of material in output guide.
C     Ar1(i)       -complex reflection coefficient of mode i in guide 1.
C     Ar3(s)       -complex transmission coefficient of mode s into guide 3.
C     B(r)         -coefficent of electric field in aperture.
C     R1(i,r)      -obtained by equating fields in aperture and guide 1.
C     R3(s,r)      -obtained by equating fields in aperture and guide 3.
C     S1(r,i)      -transpose of R1.
C     S3(r,s)      -transpose of R3.
C     Sys(r,r)     -coefficient matrix used to solve for b(r)
C
C     local variables:
C     ---------------
C      eta            - y-coordinate of lower edge of aperture.
C      zeta           - x-coordinate of left hand side of aperture.
C      alpha          - y-coordinate of lower edge of input guide.
C      e1,e2,e3       - number of distinct n idexes in guides 1,2,3.
C      f1,f2,f3       - number of distinct m indexes in guides 1,2,3.
C      nrow           - size of sys(r,r). (i.e. 50)
C      nn             - size of system to solve. (i.e. nn=p2)
C      work(nrow)     - work area for zgeco.
C      rcond          - matrix condition number. (should be large)
C      job            - flag for zgesl. ( job = 0 to solve Ax=b)
C      piv(nrow)      - integer array used by zgeco,zgesl
C      pi             - 3.14159.......
C      scale          - scale factor for guide 3.
C                       (i.e. a3=scale*a1, b3=scale*b1)
C      freq           - the frequency of operation [GHz]
C      omeg           - the radial frequency
C      sum      - temporary variable used in matrix multiplication.
C
C
C     Functions:
C     ---------
C      I1(x1,x2,xa,xb,xc,xd) :function used in calculation of R1, R2.
C                             calculates the integral from x1 to x2 of
C
C                               sin(xa*(x-xb))*sin(xc*(x-xd))dx
C
C      I2(y1,y2,ya,yb,yc,yd) :used in calculation of R1, R2.
C                             calculates integral from y1 to y2 of
C
C                               cos(ya*(y-yb))*cos(yc*(y-yd))dy
C
C      AA(i,r)     :calculates the multiplying factor in R1.
C      BB(s,r)    :calculates the multiplying factor in R2.
C
C     Declarations:
C     -------------
        IMPLICIT NONE
        PARAMETER pp1=50,pp2=50,pp3=5000
        REAL*8 a1,a3,b1,b3,b2,pi,ko,I1,zeta,eta,alpha
        REAL*8 I2,freq,omeg,rcond
```

```
      REAL*8 kx1(pp1),ky1(pp1)
      REAL*8 kx2(pp2),ky2(pp2)
      REAL*8 kx3(pp3),ky3(pp3)
      INTEGER*2 n1(pp1),m1(pp1),n2(pp2),m2(pp2),n3(pp3),m3(pp3)
      INTEGER*2 j,i,r,s,p1,p2,p3,e1,e2,e3,f1,f2,f3,scale
      INTEGER*4 job,nrow,nn,piv(pp2)
      COMPLEX*16 epsr,kz1(pp1),kz2(pp2),kz3(pp3),sum
      COMPLEX*16 Ar1(pp1),B(pp2),Ar3(pp3)
      COMPLEX*16 R1(pp1,pp2),R3(pp3,pp2),S1(pp2,pp1),S3(pp2,pp3)
      COMPLEX*16 AA,BB,sys(pp2,pp2),work(pp2),admit
       common/dim/a1,b1,b2,a3,b3,epsr
       common/index/n1,m1,n2,m2,n3,m3,p1,p2,p3
       common/k/ko,kx1,ky1,kz1,kx2,ky2,kz2,kx3,ky3,kz3
       common/amp/ar1,ar3,b
       common/matrix/r1,r3,s1,s3,sys
       open(99,file='iris.out',status='new')
C     initialize constants
      pi=dacos(-1.d0)
      nrow=pp2
      write(*,'(a$)') ' enter frequency [GHz] --->'
      read(*,*) freq
      write(*,'(a$)') ' enter permittivity (ereal,eimag)--->'
      read(*,*) epsr
      write(*,'(a$)') ' enter scale factor (a3/a1=b3/b1) --->'
      read(*,*) scale
      omeg=2.0d9*pi*freq
      ko=omeg/2.997925d10
      a1=2.286
      b1=1.016
      write(*,'(a$)') ' enter width of aperture [cm]--->'
      read(*,*) b2
      a3=scale*a1
      b3=scale*b1
      zeta=(a3-a1)/2.0d0
      eta=(b3-b2)/2.0d0
      alpha=(b3-b1)/2.0d0
C     enter modes to consider:
      write(*,'(a$)') ' enter e1 --->'
      read(*,*) e1
      write(*,'(a$)') ' enter f1 --->'
      read(*,*) f1
      p1=e1*f1
      write(*,'(a$)') ' enter e2 --->'
      read(*,*) e2
      write(*,'(a$)') ' enter f2 --->'
      read(*,*) f2
      p2=e2*f2
      write(*,'(a$)') ' enter e3 --->'
      read(*,*) e3
      write(*,'(a$)') ' enter f3 --->'
      read(*,*) f3
      p3=e3*f3
C     initialize n1(i),m1(i). Only n odd, m even considered
C     note: n1(1)=1, m1(1)=0 ie LSE10 is mode 1
```

```
      do j=0,f1-1
        do i=0,e1-1
          n1(i+1+j*e1)=2*i+1
          m1(i+1+j*e1)=2*j
        end do
      end do
C     initialize n2(r),m2(r)
      do j=0,f2-1
        do r=0,e2-1
          n2(r+1+j*e2)=2*r+1
          m2(r+1+j*e2)=2*j
        end do
      end do
C     initialize n3(s),m3(s)
      do j=0,f3-1
        do s=0,e3-1
          n3(s+1+j*e3)=2*s+1
          m3(s+1+j*e3)=2*j
        end do
      end do
C     initialize kx1(i),ky1(i),kz1(i)
      do i=1,p1
        kx1(i)=n1(i)*pi/a1
        ky1(i)=m1(i)*pi/b1
        kz1(i)=cdsqrt(dcmplx(kx1(i)**2+ky1(i)**2-ko**2))
      end do
C     initialize kx2(r),ky2(r),kz2(r)
      do r=1,p2
        kx2(r)=n2(r)*pi/a1
        ky2(r)=m2(r)*pi/b2
        kz2(r)=cdsqrt(dcmplx(kx2(r)**2+ky2(r)**2-ko**2))
      end do
C     initialize kx3(s),ky2(s),kz2(s)
      do s=1,p3
        kx3(s)=n3(s)*pi/a3
        ky3(s)=m3(s)*pi/b3
        kz3(s)=cdsqrt(kx3(s)**2+ky3(s)**2-epsr*ko**2)
      end do
C     output initial values:
      write(99,5) ' dimensions of input guide: ',a1,b1
5     format(' ',a,' a [cm]: ',f6.4,' b [cm]: 'f6.4)
      write(99,10) ' frequency of operation [GHz]:  ',freq
10    format(/,a,f8.5)
      write(99,11) epsr
11    format(' ','permittivity in guide 3: ',f8.4,1x,f8.4,'j')
      write(99,15) ' dimensions of iris: ',a1,b2
15    format(/,a,' a [cm]: ',f6.4,' b [cm]: 'f6.4)
      write(99,20) ' # OF MODES: ',e1,f1,p1
20    format(/,a,//,' input:  e1= ',i4,'  f1= ',i4,'  p1= ',i4)
      write(99,21) e2,f2,p2
21    format(' ','iris:  e2= ',i4,'  f2= ',i4,'  p2= ',i4)
      write(99,22) e3,f3,p3
22    format(' ','output:  e3= ',i4,'  f3= ',i4,'  p3= ',i4)
      write(99,25) ' ratios : ',b2/b1,dble(p2)/dble(p1)
25    format(/,a,' b2/b1 : ',f9.6,' p2/p1 : ',f9.6)
      write(*,'(a$)') ' output modes ? (1=y,0=n)-->'
      read(*,*) i
      if(i .eq. 1) then
```

```
      write(99,'(//,a,//)') '       MODES IN INPUT GUIDE'
      do i=1,p1
        write(99,30) i,n1(i),i,m1(i),i,kx1(i),i,ky1(i),i,kz1(i)
30      format('  n(',i4,'): ',i4,' m(',i4,'): ',i4,
     &          ' kx(',i4,'): ',f8.4,' ky(',i4,'): ',f8.4,
     &          ' kz(',i4,'): ',f9.4,2x,f9.4)
      end do
      write(99,'(//,a,//)') '       MODES IN IRIS'
      do r=1,p2
        write(99,35) r,n2(r),r,m2(r),r,kx2(r),r,ky2(r),r,kz2(r)
35      format('  n(',i4,'): ',i2,' m(',i4,'): ',i4,
     &          ' kx(',i4,'): ',f8.4,' ky(',i4,'): ',f8.4,
     &          ' kz(',i4,'): ',f9.4,2x,f9.4)
      end do
      write(99,'(//,a,//)') '       MODES IN OUTPUT GUIDE'
      do s=1,p3
        write(99,40) s,n3(s),s,m3(s),s,kx3(s),s,ky3(s),s,kz3(s)
40      format('  n(',i4,'): ',i5,' m(',i4,'): ',i5,
     &          ' kx(',i4,'): ',f8.4,' ky(',i4,'): ',f8.4,
     &          ' kz(',i4,'): ',f9.4,2x,f9.4)
      end do
      end if
C     initialize r1(i,r) and s1(r,i)
      do i=1,p1
        do r=1,p2
          r1(i,r)=dcmplx(i1(zeta,zeta+a1,kx2(r),zeta,kx1(i),zeta))
          r1(i,r)=r1(i,r)*dcmplx(i2(eta,eta+b2,ky2(r),eta,ky1(i),alpha))
          r1(i,r)=r1(i,r)*aa(i,r)
          s1(r,i)=r1(i,r)
        end do
      end do
C     initialize r3(s,r) and s3(r,s)
      do s=1,p3
        do r=1,p2
          r3(s,r)=dcmplx(i1(zeta,zeta+a1,kx2(r),zeta,kx3(s),0.0d0))
          r3(s,r)=r3(s,r)*dcmplx(i2(eta,eta+b2,ky2(r),eta,ky3(s),0.0d0))
          r3(s,r)=bb(s,r)*r3(s,r)
          s3(r,s)=r3(s,r)
        end do
      end do
C     now form matrix sys(r,r)=(s1(r,i)*r1(i,r)+s3(r,s)*r3(s,r)
C     note: sys is a symetric matrix.
      do r=1,p2
        do j=r,p2
          sum=(0.0d0,0.0d0)
          do i=1,p1
            sum=sum+s1(r,i)*r1(i,j)
          end do
          sys(r,j)=sum
        end do
      end do
      do r=1,p2
        do j=r,p2
          sum=(0.0d0,0.0d0)
          do s=1,p3
            sum=sum+s3(r,s)*r3(s,j)
          end do
          sys(r,j)=sys(r,j)+sum
```

```
        end do
      end do
      do r=1,p2
        do j=r,p2
          sys(j,r)=sys(r,j)
        end do
      end do
C     initialize RHS of system, only dominant mode in guide 1 incident
C     guide 3 is matched. (i.e. ai1(1)=1, ai1(i)=0 if i>1 ai3(s)=0)
      do r=1,p2
        b(r)=2.0d0*s1(r,1)
      end do
C     solve the system for b(r)
      nn=p2
      call zgeco(sys,nrow,nn,piv,rcond,work)
      write(*,*) ' condition # is: ',rcond
      write(99,*) ' condition # is: ',rcond
      job=0
      call zgesl(sys,nrow,nn,piv,b,job)
C     Finally, calculate reflection coefficients
      do i=1,p1
        sum=(0.0d0,0.0d0)
        do r=1,p2
          sum=sum+r1(i,r)*b(r)
        end do
        ar1(i)=sum
      end do
      ar1(1)=ar1(1)-(1.0d0,0.0d0)
      do s=1,p3
        sum=(0.0d0,0.0d0)
        do r=1,p2
          sum=sum+r3(s,r)*b(r)
        end do
        ar3(s)=sum
      end do
C     output reflection and transmission coefficients
      write(99,'(//,a,//)') '    REFLECTION COEFFICIENTS'
      do i=1,p1
        write(99,45) ' LSE',n1(i),m1(i),ar1(i),cdabs(ar1(i)),
     &               datan2(dimag(ar1(i)),dreal(ar1(i)))
45      format(' ',a,i3,i3,2x,4(2x,1pd12.5))
      end do
      write(99,'(//,a,//)') '    APERTURE ELECTRIC FIELD'
      do i=1,p2
        write(99,46) ' LSE',n2(i),m2(i),B(i),cdabs(b(i)),
     &               datan2(dimag(b(i)),dreal(b(i)))
46      format(' ',a,i3,i3,2x,4(2x,1pd12.5))
      end do
      write(*,'(a$)') ' output trans. coeff. (1=y)-->'
      read(*,*) s
      if(s .eq. 1) then
      write(99,'(//,a,//)') '    TRANSMISSION COEFFICIENTS'
      do s=1,p3
        write(99,50) ' LSE',n3(s),m3(s),ar3(s),cdabs(ar3(s)),
     &               datan2(dimag(ar3(s)),dreal(ar3(s)))
50      format(' ',a,i3,i3,2x,4(2x,1pd12.5))
      end do
      end if
```

```
C     finally calculate normalized dominant mode admittance
      admit=(1.0d0-ar1(1))/(1.0d0+ar1(1))
      write(99,55) admit
55    format('  normalized admittance : ',f9.5,2x,f9.5)
      close(99)
      stop
      end
C     Function definitions
C *********************************
      function i1(x1,x2,xa,xb,xc,xd)
C *********************************
C     Description:
C     ------------
C       Calculates the integral from x1 to x2 of :
C
C            sin(xa*(x-xb))*sin(xc*(x-xd))dx
C
C     Local variables:
C     ----------------
C        x1,x2     :lower and upper limits of integration in x.
C        Xa,xb,xc,xd: parameters for function I1.
C
C     declarations:
C     -------------
      IMPLICIT NONE
      REAL*8 i1,x1,x2,xa,xb,xc,xd

      if(xa .eq. 0.0d0 .and. xc .eq. 0.0d0) then
        i1=0.0d0
      else
        if(xa .eq. xc) then
          i1=(x2-x1)*dcos(xc*xd-xa*xb)
        else
          i1=dsin(x2*(xa-xc)-xa*xb+xc*xd)/(xa-xc)
          i1=i1-dsin(x1*(xa-xc)-xa*xb+xc*xd)/(xa-xc)
        endif
        i1=i1+dsin(x1*(xa+xc)-xa*xb-xc*xd)/(xa+xc)
        i1=i1-dsin(x2*(xa+xc)-xa*xb-xc*xd)/(xa+xc)
        i1=i1/2.0d0
      end if
      return
      end
C *********************************
      function i2(y1,y2,ya,yb,yc,yd)
C *********************************
C     description:
C     ------------
C       calculates the integral from y1 to y2 of:
C
C          cos(ya*(y-yb))*cos(yc*(y-yd))dy
C
C     local variables:
C     ----------------
C        y1,y2     :lower and upper limits of integration in y.
C        ya,yb,yc,yd: parameters for function I2.
C
C     declarations:
```

```
C     ------------
      implicit none
      real*8 i2,y1,y2,ya,yb,yc,yd
        if(ya .eq. 0.0d0 .and. yc .eq. 0.0d0) then
        i2=(y2-y1)
      else
        if(ya .eq. yc) then
          i2=(y2-y1)*dcos(yc*yd-ya*yb)
          else
          i2=dsin(y2*(ya-yc)-ya*yb+yc*yd)/(ya-yc)
          i2=i2-dsin(y1*(ya-yc)-ya*yb+yc*yd)/(ya-yc)
          endif
        i2=i2+dsin(y2*(ya+yc)-ya*yb-yc*yd)/(ya+yc)
        i2=i2-dsin(y1*(ya+yc)-ya*yb-yc*yd)/(ya+yc)
        i2=i2/2.0d0
      end if
      return
      end
C **********************
      function aa(i,r)
C **********************
C     description:
C     ------------
C       calculates the multiplying term in calculation of r1(i,r).
C     see notes for more details.
C
C     common variables:
C     -----------------
C       a1          :broad dimension of guide 1. (input guide) [cm]
C       b1          :narrow dimension of guide 1. [cm]
C       b2          :narrow dimension of aperture. (aperture is a1 X b2) [cm]
C       kx1(i)      :x-comp. of prop. const. of mode i in guide 1. [1/cm]
C       kz1(i)      :z-comp. of prop. const. of mode i in guide 1. [1/cm]
C       kx2(r)      :x-comp. of prop. const. of mode r in guide 2. [1/cm]
C       kz2(r)      :z-comp. of prop. const. of mode r in guide 2. [1/cm]
C       ko          :prop. const. of free space. [1/cm]
C       m1(i)       :m index of mode i in guide 1.
C       m2(r)       :m index of mode r in guide 2.
C
C     local variables:
C     ----------------
C        i       :mode index for input guide. (current row in r1(i,r))
C        r       :mode index for guide 2. (current column in r1(i,r))
C        temp    :temporary variable.
C
C     declarations:
C     -------------
      IMPLICIT NONE
      PARAMETER pp1=50,pp2=50,pp3=5000
      REAL*8 a1,b1,b2,kx1(pp1),kx2(pp1),ky1(pp2),ky2(pp2),ko
      REAL*8 a3,b3,kx3(pp3),ky3(pp3)
      INTEGER*2 n1(pp1),m1(pp1),n2(pp2),m2(pp2),i,r,p1,p2,p3
      INTEGER*2 n3(pp3),m3(pp3)
      COMPLEX*16 aa,kz1(pp1),kz2(pp2),kz3(pp3),epsr,temp
      common/dim/a1,b1,b2,a3,b3,epsr
      common/index/n1,m1,n2,m2,n3,m3,p1,p2,p3
      common/k/ko,kx1,ky1,kz1,kx2,ky2,kz2,kx3,ky3,kz3
```

```
      temp=dcmplx((kx1(i)**2-ko**2)/(kx2(r)**2-ko**2))
      temp=temp/dcmplx(a1**2*b1*b2)
      aa=2.0d0*cdsqrt(kz2(r)*temp/kz1(i))
      if(m1(i) .gt. 0) aa=dsqrt(2.0d0)*aa
      if(m2(r) .gt. 0) aa=dsqrt(2.0d0)*aa
      return
      end
C *********************
      function bb(s,r)
C *********************
C     description:
C     ------------
C       calculates the multiplying term in calculation of r3(s,r).
C     see notes for more details.
C
C     common variables:
C     -----------------
C       a3          :broad dimension of guide 3. (output guide) [cm]
C       b3          :narrow dimension of guide 3. [cm]
C       b2          :narrow dimension of aperture. (aperture is a1 X b2) [cm]
C       kx3(s)      :x-comp. of prop. const. of mode s in guide 3. [1/cm]
C       kz3(s)      :z-comp. of prop. const. of mode s in guide 3. [1/cm]
C       kx2(r)      :x-comp. of prop. const. of mode r in guide 2. [1/cm]
C       kz2(r)      :z-comp. of prop. const. of mode r in guide 2. [1/cm]
C       ko          :prop. const. of free space. [1/cm]
C       m3(s)       :m index of mode s in guide 3.
C       m2(r)       :m index of mode r in guide 2.
C       epsr        :relative permittivity of material filling guide 3.
C
C     local variables:
C     ----------------
C        s       :mode index for output guide. (current row in r3(s,r))
C        r       :mode index for guide 2. (current column in r3(s,r))
C        temp    :temporary variable.
C
C     declarations:
C     -------------
      IMPLICIT NONE
      PARAMETER pp1=50,pp2=50,pp3=5000
      REAL*8 a1,b1,b2,a3,b3,kx1(pp1),kx2(pp2),kx3(pp3)
      REAL*8 ky1(pp1),ky2(pp2),ky3(pp3),ko
      INTEGER*2 n1(pp1),m1(pp1),n2(pp2),m2(pp2),n3(pp3),m3(pp3),s,r
      INTEGER*2 p1,p2,p3
      COMPLEX*16 bb,kz1(pp1),kz2(pp2),kz3(pp3),epsr,temp
      common/dim/a1,b1,b2,a3,b3,epsr
      common/index/n1,m1,n2,m2,n3,m3,p1,p2,p3
      common/k/ko,kx1,ky1,kz1,kx2,ky2,kz2,kx3,ky3,kz3
      temp=dcmplx((kx3(s)**2-epsr*ko**2)/(kx2(r)**2-ko**2))
      temp=temp/dcmplx(a1*a3*b2*b3)
      bb=2.0d0*cdsqrt(kz2(r)*temp/kz3(s))
      if(m3(s) .gt. 0) bb=dsqrt(2.0d0)*bb
      if(m2(r) .gt. 0) bb=dsqrt(2.0d0)*bb
      return
      end
```

Appendix D:

Computer Program for the Method of Moments

```
C     DESCRIPTION:
C     ------------
C     This program solves the problem of transmission of electromagnetic
c     waves from a rectangular waveguide into half-space through a
c     rectangular aperture(s). The aperture(s) may cover all or part of
c     the waveguide cross section, but the sides of the aperture must be
c     parallel to those of the waveguide.
C     The solution uses the method of moments applied to an integral
c     equation for the equivalent magnetic current in the aperture. the
c     incident field in the waveguide is considered to the the dominant
c     TE10 mode and only the LSEmn are excited at the aperture, and
c     hence, the equivalent magnetic current has only an x-component.
c     The expansion functions are triangles in the x-direction and pulses
c     in the y-direction. Galerkin's method with subsectional basis is
c     employed. The quatities computed are the equivalent magnetic current,
c     the reflection coefficient and the aperture admittance seen by the
c     dominant mode.
c
c    Local variables:
c    ----------------
c     YA(i,j)   - the generalized admittance matrix of region A ( z < 0 )
c     YB(i,j)   - the generalized admittance matrix of region B ( z > 0 )
c     V(j)      - the generalized voltage matrix.
c     IA(i)     - the generalized current matrix. (sources in region A)
c     i         - index/loop counter associated with testing functions.
c     j         - index/loop counter associated with expansion functions.
c     IV(6,NS)  - global node numbers of each subsection.
c                 iv(L,j) global node number of node L of subsection j
c     NS        - total number of subsection used.
c     X(NN)     - x-coordinates of nodes.
c     Y(NN)     - y-coordinates of nodes.
c     NN        - total number of nodes.
c     m         - mode index of x variation of LSEmn modes.
c     n         - mode index of y variation of LSEmn modes.
c     LM        - number of m mode indexes. ( LSEmn  m=1,2,...,LM )
c     LN        - number of n mode indexes. ( LSEmn  n=0,1,...,LN-1 )
c     NM        - total number of waveguide modes considered. NM=LM*LN
c     k         - compressed mode index. k = m+n*LM --> LSEk
c     YO(k)     - wave admittance of waveguide mode k. ( k = m+n*LM )
c     AA(j,k)   - amplitude of kth mode due to jth expansion function.
c     REF(k)    - reflection coefficient of kth mode.
c     YAP       - aperture admittance seen by dominant mode.
c     PWG       - complex power flowing out of waveguide.
c     PHS       - complex power flowing into half space.
c     FREQ      - frequency of operation. [GHz]
c     PIV       - array used by zgeco
c     RCOND     - condition number of final system. (close to 1 is good)
c     WORK      - array used by zgeco
c     JOB       - flag for zgeco
c
```

```
      Common variables:
c     -----------------
c       A         - the broad dimension (x-dimension) of guide. [m]
c       B         - the narrow dimension (y-dimension) of guide. [m]
c       EPSO      - permittivity of free space [F/m]
c       MIUO      - permiability of free space. [H/m]
c       EPSR      - relative permittivity of half-space z>0
c       OMEG      - radian frequency of operation [rad/s]
c       PI        - 3.1415....
c       KO        - the free space wave number [rad/m]
c
c     Subroutines:
c     ------------
c     GRID(NNM,NSM,NN,NS,IV,X,Y)  - initializes the number of nodes,
c                    number of subsections, the global node numbers
c                    and the coordinates of each node.
c
c     YWG(NNM,NSM,NMM,LM,LN,NS,NN,IV,X,Y,AA,YO,YA,IA) - calculates the
c            admitance matrix for the waveguide, the wave impedance,
c            the amplitude matrix, and the current matrix.
c
c     YHS(NNM,NSM,NS,NN,IV,X,Y,YB)  - calculates the admittance matrix
c                                     for half-space.
c
c     ZGECO, ZGESL - solves the final system of equations.
c
c     Declarations:
c     -------------
      IMPLICIT NONE
      PARAMETER NNMAX=250
      PARAMETER NMMAX=100
      PARAMETER NSMAX=200
      REAL*8 X(NNMAX),Y(NNMAX),AA(NSMAX,NMMAX)
      REAL*8 A,B,EPSO,MIUO,FREQ,OMEG,PI,KO,RCOND
      COMPLEX*16 YA(NSMAX,NSMAX),YB(NSMAX,NSMAX),V(NSMAX),IA(NSMAX)
      COMPLEX*16 REF(NMMAX),YAP,YO(NMMAX),EPSR,WORK(NSMAX),PHS,PWG
      INTEGER*4 I,J,K,M,N,NN,NM,NS,IV(6,NSMAX),LM,LN,JOB,PIV(NSMAX)
      COMMON /CONST/A,B,EPSO,MIUO,EPSR,OMEG,PI,KO
C
C     INITIALIZE CONSTANTS
C
      PI=DACOS(-1.0D0)
      EPSO=8.8542D-12
      MIUO=4.0D-7*PI
      WRITE(*,'(A$)') ' ENTER BROAD DIMENSION OF GUIDE [m]--->'
      READ(*,*) A
      WRITE(*,'(A$)') ' ENTER NARROW DIMENSION OF GUIDE [m]--->'
      READ(*,*) B
1     WRITE(*,'(A$)') ' ENTER OPERATING FREQUENCY [GHz]-->'
      READ(*,*) FREQ
      OMEG=2.0d9*PI*FREQ
      KO=OMEG*DSQRT(EPSO*MIUO)
      IF(KO .LT. (PI/A)) THEN
      WRITE(*,'(A)') '  WAVEGUIDE BELOW CUTOFF'
c     GOTO 1
      ENDIF
2     WRITE(*,'(A$)') ' ENTER NUMBER OF M INDEXES (X VARIATION)-->'
      READ(*,*) LM
```

```
      WRITE(*,'(A$)') ' ENTER NUMBER OF N INDEXES (Y VARIATION)-->'
      READ(*,*) LN
      NM=LM*LN
      IF(NM  .GT. NMMAX) THEN
      WRITE(*,'(A)') ' TOO MANY MODES'
      GOTO 2
      END IF
      WRITE(*,'(A,A,$)') ' ENTER RELATIVE PERMITTIVITY OF HALF-SPACE ',
     &                   '(EREAL,EIMAG) -->'
      READ(*,*) EPSR
C
C     GET APERTURE GEOMETRY AND INITIALIZE NODE NUMBERS AND SUBSECTIONS
C
      CALL GRID(NNMAX,NSMAX,NN,NS,IV,X,Y)
C
C     INITIALIZE ADMITANCE MATRIX OF WAVEGUIDE AND EXCITATION MATRIX
C
      CALL YWG(NNMAX,NSMAX,NMMAX,LM,LN,NS,NN,IV,X,Y,AA,YO,YA,IA)
C
C     INITIALIZE ADMITANCE MATRIX OF HALF-SPACE
C
      CALL YHS(NNMAX,NSMAX,NS,NN,IV,X,Y,YB)
C
C     ADD THE TWO ADMITTANCE MATRICES.
C
      DO J=1,NS
        DO I=1,NS
          YA(I,J)=YA(I,J)+YB(I,J)
        END DO
      END DO
C
C     SOLVE THE SYSTEM
C
      CALL ZGECO(YA,NSMAX,NS,PIV,RCOND,WORK)
      WRITE(*,*) ' CONDITION # IS: ',RCOND
      JOB=0
      CALL ZGESL(YA,NSMAX,NS,PIV,IA,JOB)
      DO J=1,NS
        V(J)=IA(J)
      END DO
C
C     CALCULATE REFLECTION COEFFICIENTS.
C
      DO K=1,NM
        REF(K)=(0.0D0,0.0D0)
        DO J=1,NS
          REF(K)=REF(K)+AA(J,K)*V(J)
        END DO
      END DO
      REF(1)=REF(1)-1.0D0
C
C     CALCULATE APERTURE ADMITTANCE
C
      YAP=(1.0D0-REF(1))*YO(1)/(1.0D0+REF(1))
C
C     CALCULATE POWER TRANSMITTED TO HALF SPACE.
C
      PHS=(0.0D0,0.0D0)
```

```
      DO J=1,NS
        DO I=1,NS
          PHS=PHS+V(I)*CONJG(V(J))*CONJG(YB(I,J))
        END DO
      END DO
C
C     CALCULATE COMPLEX POWER FLOWING OUT OF WAVEGUIDE
C
      PWG=CONJG(YO(1))*(1.0D0+REF(1))*(1.0D0-CONJG(REF(1)))
      DO K=2,NM
        PWG=PWG-CONJG(YO(K))*CDABS(REF(K))**2
      END DO
C
C     NORMALIZE V(J) TO RMS INCIDENT E FIELD OVER GUIDE CROSS SECTION
C
      DO J=1,NS
        V(J)=DSQRT(A*B)*V(J)
      END DO
C
C     OUTPUT RESULTS
C
      OPEN(20,FILE='MOM.OUT',STATUS='NEW')
      WRITE(20,'(A,/)') ' OUPUT DATA'
      WRITE(20,10) A
10    FORMAT(' ',' BROAD DIMENSION OF GUIDE [m]: ',1PD10.3)
      WRITE(20,12) B
12    FORMAT(' ',' NARROW DIMENSION OF GUIDE [m]: ',1PD10.3)
      WRITE(20,14) FREQ
14    FORMAT(' ',' FREQUENCY OF OPERATION [GHz]',1PD10.3)
      WRITE(20,*) ' CONDITION NUMBER RCOND= ',RCOND
      WRITE(20,16) EPSR
16    FORMAT(' ',' RELATIVE PERMITTIVITY OF HALF SPACE: ',2(2X,1PD12.4))
      WRITE(20,'(//,A,/)') ' COEFFICIENTS V DIVIDED BY RMS E FIELD'
      WRITE(20,17) 'REAL          IMAG          MAG          PHASE'
17    FORMAT(' ',17X,A)
      DO J=1,NS
        WRITE(20,18) J,V(J),CDABS(V(J)),DATAN2D(DIMAG(V(J)),DREAL(V(J)))
18      FORMAT('  V(',I4,') = ',4(2X,1PD12.4))
      END DO
      WRITE(20,'(//,A,/)') ' AMPLITUDE OF REFLECTED WAVEGUIDE MODES'
      WRITE(20,17) 'REAL          IMAG          MAG          PHASE'
      DO N=0,LN-1,2
        DO M=1,LM
          K=M+N*LM
          WRITE(20,20) ' LSE',M,N,REF(K),CDABS(REF(K)),
     &                 DATAN2D(DIMAG(REF(K)),DREAL(REF(K)))
20        FORMAT(' ',A,I3,I3,2X,4(2X,1PD12.5))
        END DO
      END DO
      WRITE(20,22) YAP
22    FORMAT(/,' APERTURE ADMITTANCE SEEN BY DOMINANT MODE: ',
     &       2(2X,1PD12.5))
      WRITE(20,24) PWG
24    FORMAT(/,' COMPLEX WAVEGUIDE POWER: ',2(2X,1PD12.5))
      WRITE(20,26) PHS
26    FORMAT(/,' COMPLEX HALF-SPACE POWER: ',2(2X,1PD12.5))
```

```
      CLOSE(20)
      STOP
      END
c ************************************
      SUBROUTINE YHS(NNM,NSM,NS,NN,IV,X,Y,YB)
c ************************************
c
c     description:
c     ------------
c       This subroutine calculates the generalized admittance matrix of
c     a rectangular aperture(s) cut in perfectly conducting screen. The
c     screen covers the entire plane z = 0 except for the aperture(s).
c     The magnetic current has only an x-component and is expanded over
c     subsectional basis by triangle functions in the x-direction and
c     pulses in the y-direction.
c
c     Import parameters:
c     ------------------
c       NNM      - maximum number of nodes. (array dimension)
c       NSM      - maximum number of subsection. (array dimension)
c       NS       - total number of subsections.
c       NN       - total number of nodes.
c       IV(6,NSM)- global node numbers for each subsection.
c       X(NNM)   - the x-coordinates of nodes.
c       Y(NNM)   - the y-coordinates of nodes.
c
c      Export parameters:
c      ------------------
c        YB(NSM,NSM)  -the generalized admittance matrix of aperture.
c
c      Local variables:
c      ----------------
c        X1,X2,..,X6 - temporary variables. ( x limits of integration )
c        Y1,Y2       -     "          "      ( y   "    "      "       )
c        U           - sqrt(-1)
c        U1,U2,...U5 - constant in calculations of YB
c        i           - index associated with testing functions.
c        j           - index associated with expansion functions.
c        DXI         - half the x dimension of subsection i.
c        DXJ         -  "    "  "    "      "     "       j.
c        DYI      - the y-dimension of subsection i.
c        DYJ         - the y-dimension of subsection j.
c        K           - wave number in dielectric.
c
c     Common variables:
c     -----------------
c       A         - the broad dimension (x-dimension) of guide. [m]
c       B         - the narrow dimension (y-dimension) of guide. [m]
c       EPSO      - permittivity of free space [F/m]
c       MIUO      - permiability of free space. [H/m]
c       EPSR      - relative permittivity of half-space z>0
c       OMEG      - radian frequency of operation [rad/s]
c       PI        - 3.1415....
c       KO        - the free space wave number [rad/m]
c
c      Functions:
c      ----------
c       IXC(xl,xu,yl,yu,fac) integrates (k*(x-fac)*exp(-jkr)/(r*(xu-xl)) dx dy)
```

```
c
c       Declarations:
c       -------------
        Implicit none
        INTEGER*4 NNM,NSM,NS,NN,IV(6,NSM),I,J
        REAL*8 X(NNM),Y(NNM),DXI,DYI,DXJ,DYJ
        COMPLEX*16 YB(NSM,NSM),U,U1,U2,U3,U4,U5,EPSR,K,IXC
        REAL*8 X1,X2,X3,X4,X5,X6,Y1,Y2
        REAL*8 A,B,EPSO,MIUO,OMEG,PI,KO
        COMMON /CONST/A,B,EPSO,MIUO,EPSR,OMEG,PI,KO
c
c       Initialize constants
c
        U=(0.0d0,1.0d0)
        K=CDSQRT(EPSR)*KO
c
c       ASSEMBLE YB
c
        DO J=1,NS
          DXJ=X(IV(6,J))-X(IV(2,J))
          DYJ=Y(IV(6,J))-Y(IV(2,J))
          DO I=1,NS
            DXI=X(IV(6,I))-X(IV(2,I))
            DYI=Y(IV(6,I))-Y(IV(2,I))
            X1=X(IV(2,J))-X(IV(2,I))+DXI/2.0D0-DXJ
            X2=X1+DXJ
            X3=X2+DXJ
            X4=X(IV(2,J))-X(IV(2,I))-DXI/2.0D0-DXJ
            X5=X4+DXJ
            X6=X5+DXJ
            Y1=Y(IV(4,J))-Y(IV(4,I))+DYI/2.0D0-DYJ
            Y2=Y1+DYJ
            U1=U*OMEG*EPSO*EPSR*DXI*DYI/(4.0D0*PI*K)
            U2=X1+2.0D0/(K**2*DXI)
            U3=X3+2.0D0/(K**2*DXI)
            U4=X4-2.0D0/(K**2*DXI)
            U5=X6-2.0D0/(K**2*DXI)
            YB(I,J)=U1*(IXC(X1,X2,Y1,Y2,U2)-IXC(X2,X3,Y1,Y2,U3)+
     &                  IXC(X4,X5,Y1,Y2,U4)-IXC(X5,X6,Y1,Y2,U5))
          END DO
        END DO
        RETURN
        END
c ****************************************************
        COMPLEX*16 FUNCTION IXC(XL,XU,YL,YU,FAC)
C ****************************************************
C       Description:
c       ------------
          This program calculates the integral of:
c
c               (k*(x-fac))*exp(-jkr)/(r*(xu-xl)) dx dy
c
c         where:
c                 r=sqrt(x**2+y**2)
c
c       input parameters:
c       -----------------
c         XL    - lower x limit of integration
```

```
c       XU   - upper "   "   "      "
c       YL   - lower y limit of integration
c       YU   - upper "    "   "      "
c       FAC  - the constant term in integrand.
c
c     Local variables:
c     ----------------
c        U   - sqrt(-1)
c        S1,S2, . . . , S4  - temporary variables.
c        RO   - the center of Taylor expansion of exp(-jkr)
c        RUU  - temporary variable, sqrt(xu**2+yu**2)
c        RUL  - temporary variable, sqrt(xu**2+yl**2)
c        RLU  -     "         "    , sqrt(xl**2+yu**2)
c        RLL  -     "         "    , sqrt(xl**2+yl**2)
c        K    - complex wave number in dielectric
c        LNYUL-
c        LNYLU-  temporary variables
c        LNXUL-
c        LNXLU-
c        IR2  - the value of the integral of ( r**2 dx dy)
c        IR   - the value of the integral of ( r dx dy )
c        IR1  - the value of the integral of ( 1/r dx )
c        IXR2 - the value of the integral of ( x*r**2 dx dy)
c        IXR  - the value of the integral of ( x*r dx dy)
c        IXR1 - the value of the integral of ( x/r dx dy )
c        IC   - intermediate value. i.e. integral of (k*exp(-jkr)/(r*(xu-xl))
c       IX   - intermediate value. i.e. integral of (k*x*exp(-jkr)/(r*(xu-xl))
c
c     Common variables:
c     -----------------
c       A         - the broad dimension (x-dimension) of guide. [m]
c       B         - the narrow dimension (y-dimension) of guide. [m]
c       EPSO      - permittivity of free space [F/m]
c       MIUO      - permiability of free space. [H/m]
c       EPSR      - relative permittivity of half-space z>0
c       OMEG      - radian frequency of operation [rad/s]
c       PI        - 3.1415....
c       KO        - the free space wave number [rad/m]
c
c     Declarations:
c     -------------
      IMPLICIT NONE
      REAL*8 A,B,EPSO,MIUO,OMEG,PI,KO,XL,XU,YL,YU
      REAL*8 LNYUL,LNYLU,LNXUL,LNXLU
      REAL*8 RO,RUU,RUL,RLU,RLL,IR2,IR,IR1,IXR2,IXR,IXR1
      COMPLEX*16 EPSR,U,S1,S2,S3,S4,K,FAC,IX,IC
      COMMON /CONST/A,B,EPSO,MIUO,EPSR,OMEG,PI,KO
      U=(0.0D0,1.0D0)
      K=KO*CDSQRT(EPSR)
      RO=DSQRT((XL+XU)**2+(YL+YU)**2)/2.0D0
      RUU=DSQRT(XU**2+YU**2)
      RUL=DSQRT(XU**2+YL**2)
      RLU=DSQRT(XL**2+YU**2)
      RLL=DSQRT(XL**2+YL**2)
      S1=U*K**4/6.0D0
      S2=-K**3*(U*K*RO+1.0D0)/2.0D0
      S3=K**2*(U*(K*RO)**2/2.0D0+K*RO-U)
      S4=K*(1.0D0+U*K*RO-(K*RO)**2/2.0D0-U*(K*RO)**3/6.0D0)
```

```
      LNYUL=DLOG((YU+RUU)/(YL+RUL))
      LNYLU=DLOG((YL+RLL)/(YU+RLU))
      LNXUL=DLOG((XU+RUU)/(XL+RLU))
      LNXLU=DLOG((XL+RLL)/(XU+RUL))
      IXR2=(YU-YL)*(XU**4-XL**4)/4.0D0+(XU**2-XL**2)*(YU**3-YL**3)/6.0D0
      IXR=(XU**4*LNYUL+XL**4*LNYLU)/8.0D0+(YL*(RLL**3-RUL**3)+YU*(RUU**3
     &    -RLU**3))/12.0D0+(YL*(RLL*XL**2-RUL*XU**2)+YU*(RUU*XU**2-RLU*
     &    XL**2))/8.0D0
      IXR1=(YU*(RUU-RLU)+YL*(RLL-RUL)+XU**2*LNYUL+XL**2*LNYLU)/2.0D0
      IX=S1*IXR2+S2*IXR+S3*(XU**2-XL**2)*(YU-YL)/2.0D0+S4*IXR1
      IX=CDEXP(-U*K*RO)*IX/(XU-XL)
      IR2=(XU*YU*RUU**2+XL*YL*RLL**2-XU*YL*RUL**2-XL*YU*RLU**2)/3.0D0
      IR=(XU*YU*RUU+XL*YL*RLL-XU*YL*RUL-XL*YU*RLU)/3.0D0+
     &    (XU**3*LNYUL+XL**3*LNYLU+YU**3*LNXUL+YL**3*LNXLU)/6.0D0
      IR1=XU*LNYUL+XL*LNYLU+YU*LNXUL+YL*LNXLU
      IC=S1*IR2+S2*IR+S3*(XU-XL)*(YU-YL)+S4*IR1
      IC=CDEXP(-U*K*RO)*IC/(XU-XL)
      IXC=IX-FAC*IC
      RETURN
      END
c *****************************************************
      SUBROUTINE YWG(NNM,NSM,NMM,LM,LN,NS,NN,IV,X,Y,AA,YO,YA,IA)
c *****************************************************
c
c     Description:
c     ------------
c     This subroutine calculates the generalized admittance matrix of a
c     rectancular waveguide terminated in a conducting screen which
c     has one or more rectangular apertures cut in it. The aperture
c     is replaced by a perfect conductor on which flows an equivalent
c     magnetic current which has only an x component ( hence only
c     a y component of electric field ).
c     The magnetic current is expanded over rectangular subsections by
c     triangles in the x direction and pulses in the y-direction.
c
c     import parameters:
c     ------------------
c     NNM     - maximum number of nodes. (array dimension)
c     NSM     - maximum number of subsections.
c     NMM     - maximum number of waveguide modes
c     LM      - the number of m mode indexes. LSEmn m=1,2,...,LM
c     LN      - the number of n mode indexes used. LSEmn n=0,1,...,LN-1
c     NS      - the number of subsections.
c     NN      - the number of nodes.
c     IV(6,NSM)-the global node number of each node of subsection j.
c     X(NNM)  - the x coordinates of the nodes.
c     Y(NNM)  - the y coordinates of the nodes.
c
c     export parameters:
c     ------------------
c     AA(NSM,NMM)   - the "amplitude" matrix of mode k due to current j.
c     YO(NMM)       - the wave admittance of the kth mode.
c     YA(NSM,NSM)   - the generalized admittance matrix.
c     IA(NSM)       - the generalized current matrix due to incident mode.
c
c     local variables:
c     ----------------
c     I     -index associated with testing functions.
```

```
c     J     -index associated with expansion functions.
c     M     -x index of LSEmn modes.
c     N     -y index of LSEmn modes.
c     K     -index associated with wave guide mode. (K=M+N*LM)
c     NM    -total number of modes considered. (NM=LM*LN)
c     DXJ   -half the x dimension of subsection J. [m]
c     DYJ   -half the y dimension of subsection J. [m]
c     X1    -temporary variable ( x coordinate )
c     Y1    -    "          "     ( y coordinate )
c     GAM   -the propogation constant of a wave guide mode.
c     KC    -the cutoff wavenumber of a waveguide mode.
C     SX1,SX2,SY1,CY1 - temporary real variables.
C     SUM   - SUMMATION REGISTER
c
c     Common variables:
c     -----------------
c       A         - the broad dimension (x-dimension) of guide. [m]
c       B         - the narrow dimension (y-dimension) of guide. [m]
c       EPSO      - permittivity of free space [F/m]
c       MIUO      - permiability of free space. [H/m]
c       EPSR      - relative permittivity of half-space z>0
c       OMEG      - radian frequency of operation [rad/s]
c       PI        - 3.1415....
c       KO        - the free space wave number [rad/m]
c
c     Declarations:
c     -------------
      IMPLICIT NONE
      INTEGER*4 NNM,NSM,NMM,I,J,M,N,K,LM,LN,NM,NN,NS,IV(6,NSM)
      REAL*8 A,B,EPSO,MIUO,OMEG,PI,KO,X(NNM),Y(NNM),AA(NSM,NMM)
      REAL*8 DXJ,DYJ,XJ,YJ,SX1,SX2,SY1,CY1,KC
      COMPLEX*16 YO(NMM),YA(NSM,NSM),IA(NSM),U,SUM,GAM,EPSR
      COMMON /CONST/A,B,EPSO,MIUO,EPSR,OMEG,PI,KO
      NM=LM*LN
      U=(0.0D0,1.0D0)
C
C     First calculate aa(j,k) and yo(k)
c
      DO N=0,LN-1
        DO M=1,LM
          K=M+N*LM
          KC=PI*DSQRT((M/A)**2+(N/B)**2)
          IF(KC .GT. KO) THEN
            GAM=DCMPLX(DSQRT(KC**2-KO**2))
          ELSE
            GAM=U*DCMPLX(DSQRT(KO**2-KC**2))
          END IF
          YO(K)=((M*PI/A)**2-KO**2)/(U*GAM*OMEG*MIUO)
          DO J=1,NS
            XJ=X(IV(2,J))
            YJ=Y(IV(4,J))
            DXJ=XJ-X(IV(1,J))
            DYJ=YJ-Y(IV(1,J))
            SX1=DSIN(M*PI*XJ/A)
            SX2=(2.0D0*A*DSIN(M*PI*DXJ/2.0D0/A)/(M*PI*DXJ))**2
            IF(N .EQ. 0) THEN
              SY1=1.0D0
            ELSE
```

```
              SY1=2.0D0*B*DSIN(N*PI*DYJ/2.0D0/B)/(N*PI*DYJ)
            END IF
            CY1=DCOS(N*PI*(YJ-DYJ/2.0D0)/B)
            AA(J,K)=-DSQRT(4.0D0/A/B)*DXJ*DYJ*SY1*SX2*SX1*CY1
            IF(N .EQ. 0) AA(J,K)=AA(J,K)/DSQRT(2.0D0)
          END DO
        END DO
      END DO
c
c     now calculate yb(i,j) and ia(i)
c
      DO J=1,NS
        IA(J)=2.0D0*YO(1)*AA(J,1)
        DO I=1,NS
          SUM=(0.0D0,0.0D0)
          DO K=1,NM
            SUM=SUM+AA(J,K)*AA(I,K)*YO(K)
          END DO
          YA(I,J)=SUM
        END DO
      END DO
      RETURN
      END
C *********************************
      SUBROUTINE GRID(NNM,NSM,NN,NS,IV,X,Y)
C *********************************
C
C     description:
C     ------------
C     This subroutine initializes the node coordinates and node numbering
C     for the rectangular subsections used in the moment method solution of
C     the problem of electromagnetic transmission through one or more
C     apertures in a perfectly conducting plane. The aperture(s) are made
C     up of rectangular patches. The user enters the number of patches
C     and the lower left and upper right coordinates of each patch as
C     well as the number of x and y sub-divisions in each patch (i.e.
C     subsections/patch). Patches may touch.
C
C    import variable:
C    ----------------
C     NNM      - the maximum number of nodes allowed.
C     NSM      - the maximum number of subsections allowed.
C
C    export variables:
C    -----------------
C     NN       - the total number of nodes on aperture.
C     NS       - the total number of subsections on aperture.
C     IV(6,NS) - the global node number of nodes for subsection NS.
C     X(NN)    - the x coordinate of nodes.
C     Y(NN)    - the y coordinates of nodes.
C
C    local variables:
C    ----------------
C     NP     - number of patches forming aperture.
C     I      - index/loop counter associated with x variations.
C     J      - index/loop counter associated with y variations.
C     K      - index/loop counter associated with patch variations.
C     P,Q    - loop counters.
```

```
c     DX      - the x increment between nodes in patch K. [m]
c     DY      - the y increment between node in patch K. [m]
c     (X1,Y1)- the lower left coordinate of patch K.
c     (X2,X2)- the upper right coordinate of patch K.
c     TX(I)   - temporary storage of x coordinates.
c     TY(J)   - temporary storage of y coordinates.
c     NODE(I,J,K) -array of global node numbers.
c     LNO     - index associated with local node numbers.
c     NX      - the number of x intervals in patch K.
c     NY      - the number of y intervals in patch K.
c
c     Common variables:
c     -----------------
c       A         - the broad dimension (x-dimension) of guide. [m]
c       B         - the narrow dimension (y-dimension) of guide. [m]
c       EPSO      - permittivity of free space [F/m]
c       MIUO      - permiability of free space. [H/m]
c       EPSR      - relative permittivity of half-space z>0
c       OMEG      - radian frequency of operation [rad/s]
c       PI        - 3.1415....
c       KO        - the free space wave number [rad/m]
c
c     declarations:
c     -------------
      IMPLICIT NONE
      PARAMETER NPMAX=2
      INTEGER*4 NNM,NSM,NN,NS,IV(6,NSM),I,J,K,P,Q
      INTEGER*4 LNO,NP,NX(NPMAX),NY(NPMAX)
      INTEGER*4 NODE(50,50,NPMAX)
      REAL*8 A,B,EPSO,MIUO,OMEG,PI,KO
      COMPLEX*16 EPSR
      REAL*8 X(NNM),Y(NNM),X1(NPMAX),X2(NPMAX),Y1(NPMAX)
      REAL*8 Y2(NPMAX),DX(NPMAX),DY(NPMAX),TX(50),TY(50)
      CHARACTER*1 ANS
      COMMON /CONST/A,B,EPSO,MIUO,EPSR,OMEG,PI,KO
      WRITE(*,'(A,A,I1,A$)') ' NUMBER OF PATCHES FORMING APERTURE?',
     &    '  (MAXIMUM OF ',NPMAX,' )--->'
      READ(*,*) NP
      NN=0
      NS=0
      DO K=1,NP
C       GET PATCH GEOMETRY FOR PATCH K
        WRITE(*,'(A,I2,A$)') ' ENTER LOWER LEFT CORNER OF PATCH ',K,
     &        ' (XL,YL) [m] --->'
        READ(*,*) X1(K),Y1(K)
        WRITE(*,'(A,I2,A$)') ' ENTER UPPER RIGHT CORNER OF PATCH ',K,
     &        ' (XU,YU) [m] --->'
        READ(*,*) X2(K),Y2(K)
        WRITE(*,'(A$)') ' NUMBER OF X INTERVALS BETWEEN XL AND XU ? ->'
        READ(*,*) NX(K)
        WRITE(*,'(A$)') ' NUMBER OF Y INTERVALS BETWEEN YL AND YU ? ->'
        READ(*,*) NY(K)
        NN=NN+(NX(K)+1)*(NY(K)+1)
        NS=NS+NY(K)*(NX(K)-1)
      END DO
      IF(NN .GT. NNM) THEN
        WRITE(*,'(A)') ' TOO MANY NODES!!'
        STOP
```

```
      END IF
      IF(NS .GT. NSM) THEN
        WRITE(*,'(A)') ' TOO MANY SUBSECTIONS!!'
        STOP
      END IF
      NN=0
      NS=0
      DO K=1,NP
C     CALCULATE X AND Y COORDINATES OF NODES OF PATCH K
        DX(K)=(X2(K)-X1(K))/NX(K)
        DY(K)=(Y2(K)-Y1(K))/NY(K)
        DO I=1,NX(K)+1
          TX(I)=(I-1)*DX(K)+X1(K)
        END DO
        DO J=1,NY(K)+1
          TY(J)=(J-1)*DY(K)+Y1(K)
        END DO

C     NUMBER NODES OF PATCH K
        DO J=1,NY(K)+1
          DO I=1,NX(K)+1
            NN=NN+1
            NODE(I,J,K)=NN
            X(NN)=TX(I)
            Y(NN)=TY(J)
          END DO
        END DO
C     FORM SUBSECTIONS AND ASSIGN GLOBAL NODE NUMBERS.
        DO J=1,NY(K)
          DO I=1,NX(K)-1
            LNO=0
            NS=NS+1
            DO Q=0,1
              DO P=0,2
                LNO=LNO+1
                IV(LNO,NS)=NODE(I+P,J+Q,K)
              END DO
            END DO
          END DO
        END DO
      END DO
      WRITE(*,'(A$)') ' CREATE GRIDING OUTPUT FILE? (y/n) -->'
      READ(*,'(A)') ANS
      IF(ANS .EQ. 'Y' .OR. ANS .EQ. 'y') THEN
        OPEN(33,FILE='SUBSEC.MAP',STATUS='NEW')
        WRITE(33,80) NN,NS,NP
80      FORMAT(' NUMBER OF NODES: ',I4,' TOTAL NUMBER OF SUBSECTIONS: ',
     &   I4,' NUMBER OF PATCHES: ',I4)
        WRITE(33,82) ' BROAD DIMENSION OF GUIDE [CM]:',A*1.D2
        WRITE(33,82) ' NARROW DIMENSION OF GUIDE [CM]:',B*1.D2
        WRITE(33,82) ' FREQUENCY OF OPERATION [GHz]:', OMEG/(2.0D9*PI)
        WRITE(33,88) ' RELATIVE PERMITTIVITY OF HALF SPACE:',EPSR
82      FORMAT(' ',A,F8.4)
88      FORMAT(' ',A,2(2X,1PD10.3))
        DO K=1,NP
          IF(K .EQ. 1) THEN
            P=0
            Q=0
```

```
        ELSE
          P=(NX(K-1)+1)*(NY(K-1)+1)     !  # OF NODES IN PATCH (K-1)
          Q=NY(K-1)*(NX(K-1)-1)         !  # OF SUBSECTIONS IN PATCH (K-1)
        END IF
        WRITE(33,'(//,A,I2,A,/)') ' PATCH ',K,' DATA:'
        WRITE(33,'(A,/)') ' NODE COORDINATES:'
        DO I=P+1,P+(NX(K)+1)*(NY(K)+1)
          WRITE(33,95) I,X(I),Y(I)
95        FORMAT(' NODE(',I3,')  X',1PD12.4,'  Y',1PD12.4)
        END DO
        WRITE(33,'(//,A,/)') ' NODE MAP'
        DO J=NY(K)+1,1,-1
          WRITE(33,97) (NODE(I,J,K), I=1,NX(K)+1)
97        FORMAT(' ',20I4)
        END DO
        WRITE(33,'(//,A,/)') ' SUBSECTIONS MAP'
        DO I=Q+1,Q+NY(K)*(NX(K)-1)
          WRITE(33,99) I,(IV(J,I), J=1,6)
99        FORMAT('  SUBSECTION(',I4,'): ',6I5)
        END DO .
      END DO
      CLOSE(33)
    END IF
    RETURN
    END
```

Index of Principal Symbols and Abbreviations

All complex quatities are underlined. An exception is the complex relative permittivity which carries a ^ .

Vector quatities are denoted by an arrow above the variable.

Square brackets are used to identify matrices.

$\hat{\varepsilon}_r$ the relative permittivity, $\hat{\varepsilon}_r = \varepsilon' - j\varepsilon''$.

ε' the relative dielctric constant, real part of the complex relative permittivity.

ε'' the loss factor, imaginary part of the complex relative permittivity.

$\underline{\vec{e}}_i, \underline{\vec{h}}_i$ the transverse mode functions of the ith mode for the electric and magnetic fields, respectively, in a rectangular guide.

$\underline{\vec{F}}$ the electric vector potential.

FEM the Finite-Element Method

$\underline{\Gamma}_1$ the reflection coefficient of the dominant TE_{10} mode.

$\underline{\gamma}_i$ the propagation constant of the ith mode in a rectangular guide.

$[\underline{I}]$ the excitation vector in the Method of Moments.

$L_l(x), L_m(y), L_n(z)$ Lagrange polynomials.

$\underline{\vec{M}}$ the magnetic current density.

$\vec{M}_j$ the set of expansion functions used in the Method of Moments to approximate the magnetic current density.

$\underline{m}_j$ the magnetic charge density.

MM the Mode Matching Method

MOM the Method of Moments

N_{ib} the set of 2nd order interpolatory functions used in the Finite-Element analysis.

$\vec{n}$ unit external normal

$\underline{\vec{\Pi}}_m$ the magnetic Hertzian potential.

$\underline{\phi}_{ib}$ node potentials for the Finite-Element mesh.

$\underline{\Psi}$ the x-component of the magnetic Hertzian potential (Chapter 2) or the scalar magnetic potential (Chapter 4)

$\underline{\tilde{\Psi}}$ approximate solution for the magnetic Hertzian potential obtained by the Finite-Element method.

$\underline{V}_j$ the amplitude coefficients of the magnetic current, solution obtained by the Method of Moments.

W weighting function used in Galerkin's method.(FEM and MOM)

$\underline{Y}_i$ the z-directed wave admittance of the ith mode in a rectangular guide.

$[\underline{Y}^1], [\underline{Y}^2]$ the generalized admittance matrices for the waveguide region and the half-space region, respectively in the Method of Moments.

Bibliography

1. D. A. Christensen and C. H. Durney, "Hyperthermia Production for Cancer Therapy: A Review of Fundamentals and Methods," J. Microwave Power, Vol. 16, No. 2, pp. 89-105, June 1981.
2. F. Sterzer, R. Paglione, M. Nowogrodzki, E. Beck, J. Mandecki, E. Friedenthal and C. Botstein, "Microwave Apparatus for the Treatment of Cancer," Microwave Journal, Vol. 23, No. 1, pp. 39-44, January 1980.
3. J. Edrich, "Centimeter- and Millimeter-Wave Thermography: A Survey of Tumor Detection," J. Microwave Power, Vol. 14, No. 2, pp. 95-104, 1979.
4. I. J. Bahl, A. Thansandote and S. S. Stuchly, "Open-Ended Rectangular Waveguides as Antennas for Medical Diagnostics," J. Microwave Power, Vol. 15, No. 2, pp. 81-86, 1980.
5. N. E. Hill *et al, Dielectric Properties and Molecular Behavior*, New York:Van Norstrand Reinhold, 1969.
6. M. A. Stuchly, S. S. Stuchly, R. P. Liburdy and D. A. Russeau, "Dielectric Properties of Liposome Vesicles at the Membrane Phase Transition," presented at the Tenth Annual Meeting of the Bioelectromagnetics Society, Stamford, Connecticut, June 1988 (unpublished).
7. A. Kraszewski, "Microwave Aquametry - A Review," J. Microwave Power, Vol. 15, No. 4, pp. 209-220, 1980.
8. C. H. Durney, "Electromagnetic Dosimetry for Models of Humans and Animals: A Review of Theoretical and Numerical Techniques," Proc. IEEE, Vol. 68, No. 1, January 1980.
9. T. W. Athey, M. A. Stuchly and S. S. Stuchly, "Measurement of Radio Frequency Permittivity of Biological Tissues with an Open-Ended Coaxial Line: Parts I and II," IEEE Trans. Microwave Theory and Tech., Vol. MTT-30, No. 1, pp. 82-92, January 1982.
10. G. B. Gajda, M.A.Sc. Thesis, University of Ottawa, Ottawa, 1982.
11. T. Sphicopoulos, V. Teodoridis and F. Gardiol, "Simple Nondestructive Method for the Measurement of Material Permittivity," J. Microwave Power, 1985.
12. S. S. Stuchly, G. Gajda, L. Anderson and A. Kraszewski, "A New Sensor for Dielectric Measurements," IEEE Trans. Instum. Meas., Vol. IM-35, No. 2, pp. 138-141, June 1986.
13. S. S. Stuchly, A. Kraszewski and M. A. Stuchly, "Uncertainties in Radiofrequency Dielectric Measurements of Biological Substances," IEEE Trans. Instrum. Meas., Vol. IM-36, No. 1, pp. 67-70, March 1987.
14. M. C. Decreton and F. Gardiol, "Simple Nondestructive Method for the Measurement of Complex Permittivity," IEEE Tran. Instrum. Meas., Vol. IM-23, No. 4, pp. 434-438, December 1974.
15. F. Gardiol, "Open-Ended Waveguides: Principles and Applications," in *Advances in Electronics and Electron Physics*, P. Hawkes editor, Vol. 63, pp. 139-187. Academic Press, New York.
16. L. J. Chu, J. Appl. Phys., Vol. 11, pp. 603- ,1940.
17. L. Lewin, *Advanced Theory of Waveguides*, Iliffe, London, 1951.

18. J. R. Mautz and R. F. Harrington, "Transmission from a Rectangular Waveguide into Half Space through a Rectangular Aperture," Rep. TR-76-5, Dept. of Electrical and Computer Engineering, Syracuse University, New York.

19. A. R. Jamieson and T. E. Rozzi, "Rigorous Analysis of Cross-Polarization in Flange-Mounted Rectangular Waveguide Radiators," Electron. Lett., Vol. 13, pp. 742-744, November 1977.

20. R. H. MacPhie and A. I. Zaghloul, "Radiation from a Rectangular Waveguide with Infinite Flange - Exact Solution by the Correlation Matrix Method," IEEE Tran. Antennas and Propagation, Vol. AP-28, No. 4, pp. 497-503, July 1980.

21. R. T. Compton, Ph.D. Thesis, Ohio State University, Columbus, 1964.

22. A. T. Villeneuve, "Admittance of Waveguide Radiating into Plasma Environment," IEEE Trans. Antennas and Propagation, Vol. AP-13, No. 1, pp. 115-121, January 1965.

23. J. Galejs, "Admittance of a Waveguide Radiating into Stratified Plasma," IEEE Trans. Antennas and Propagation, Vol. AP-13, No. 1, pp. 64-70, January 1965.

24. W. F. Croswell, W. C. Taylor, C. T. Swift and C. R. Cockrell, "Input Admitance of a Rectangular Waveguide-Fed Aperture Under an Inhomogeneous Plasma: Theory and Experiment," IEEE Trans. Antennas and Propagation, Vol. AP-16, No. 4, pp. 475-487, July 1968.

25. J. Audet, J. C. Bolomey, C. Pichot, D. D. Nguyen, M. Robillard, M. Chive and Y. Leroy, "Electrical Characteristics of Waveguide Apertures for Medical Applications," J. Microwave Power, Vol. 15, No. 3, pp. 177-186, 1980.

26. J. A. Encinar and J. M. Rebollar, "Convergence of Numerical Solutions of Open-Ended Waveguide by Modal Analysis and Hybrid Modal-Spectral Techniques," IEEE Trans. Microwave Theory Tech., Vol. MTT-34, No. 7, pp. 809-814, July 1986.

27. T. B. A. Senior, "Impedance Boundary Condition for Imperfectly Conducting Surfaces," Appl. Sci. Res., Section B, Vol. 8, pp. 418-436, 1960.

28. Dau-Sing Wang, "Limits and Validity of the Impedance Boundary Condition on Penetrable Surfaces," IEEE Trans. Antennas Propogat., Vol. AP-35, No. 4, pp. 453-457, April 1987.

29. M. A. Leontovich, *Investigation of Propagation of Radiowaves, Part II*. Moscow, 1948

30. N. K. Deshmukh and K. C. Mukherji, "Finite-element Analysis of Three-Dimensional Eddy Currents in Attractive Electromagnetic Levitation," Proc. IEE, Vol. 134 A, No. 8, pp. 651-662, September 1987

31. J. J. Dongarra, C. B. Moler, J. R. Bunch and G. W. Stewart, "LINPACK Users' Guide," SIAM, U.S.A., 1979

32. G. Jeng and A. Wexler, "Self-Adjoint Variational Formulation of Problems Having Non-Self-Adjoint Operators," IEEE Trans. Microwave Theory Tech., Vol. MTT-26, No. 2, pp. 91-94, February 1978

33. R. E. Collin, *Field Theory of Guided Waves*, New York: McGraw Hill, p. 230, 1960.

34. R. Mittra, T. Itoh, and T. S. Li, "Analytical and Numerical Studies of the Relative Convergence Phenomenon Arising in the Solution of an Integral Equation by the Moment Method," IEEE Trans.Microwave Theory Tech., Vol. MTT-20, pp. 96-104, February 1972.

35. S. W. Lee, W. R. Jones, and J. J. Campbell, "Convergence of Numerical Solutions of Iris-Type Discontinuity Problems," IEEE Trans. Microwave Theory Tech., Vol. MTT-19, pp. 528-536, June 1971.

36. Y. C. Shih, and K. G. Gray, "Convergence of Numerical Solutions of Step-Type Waveguide Discontinuity Problems by Modal Analysis," IEEE Trans. Microwave Theory Tech. Symp., pp. 233-235, 1983.

37. R. F. Harrington, *Time-Harmonic Electromagnetic Fields*, M°Graw-Hill, New York, 1961.

38. J. Hasted, *Aqueous Dielectrics*, Chapman-Hall, London, 1973.

39. C. Malmberg and A. Maryott, "Dielectric Constant of Water from 0° to 100°C," J. Res. NBS. Vol. 56 (1), pp. 1-8, 1956.

40. H. P. Schwan, R. J. Sheppard, and E. Grant, "Complex Permittivity of Water at 25°C", J. Chem. Phys., Vol. 64 (5), pp. 2257-2258, 1976.

41. B. P. Jordan, R. J. Sheppard, and S. Szwarnowski, "The Dielectric Properties of Formamide, Ethanediol and Methanol," J. Phys. D: Appl. Phys., Vol. 11, pp. 695-701, 1978.

42. Hewlett-Packard Application Note 221A, "Automating the HP8410B Network Analyzer," June 1980.

43. Hewlett-Packard seminar, "Vector Measurements of High Frequency Networks",1988.